THERMAL ACTIVITY OF BASE COURSE MATERIAL RELATED TO PAVEMENT CRACKING

by

Samuel H. Carpenter
Robert L. Lytton

Research Report Number 18-2

Environmental Deterioration of Pavement
Research Project 2-8-73-18

Conducted for the
State Department of Highways
and Public Transportation

in cooperation with the
U.S. Department of Transportation
Federal Highway Administration

by the

Texas Transportation Institute
Texas A&M Univeristy
College station, Texas

December, 1975

TECHNICAL REPORT STANDARD TITLE PAGE

1. Report No.	2. Government Accession No.	3. Recipient's Catalog No.

4. Title and Subtitle	5. Report Date
Thermal Activity of Base Course Material Related to Pavement Cracking	December, 1975
	6. Performing Organization Code
7. Author(s)	8. Performing Organization Report No.
Samuel H. Carpenter and Robert L. Lytton	Research Report No. 18-2
9. Performing Organization Name and Address	10. Work Unit No.
Texas Transportation Institute Texas A&M University College Station, Texas 77843	11. Contract or Grant No. Study No. 2-8-73-18
	13. Type of Report and Period Covered
12. Sponsoring Agency Name and Address Texas State Department of Highways and Public Transportation; Transportation Planning Division P. O. Box 5051 Austin, Texas 78763	Interim - September, 1972 December, 1975
	14. Sponsoring Agency Code

15. Supplementary Notes

Research performed in cooperation with DOT, FHWA.
Study Title: "Environmental Deterioration of Pavement"

16. Abstract

Preliminary studies into environmental deterioration of pavements indicated that low-temperature cracking of the asphalt concrete surface was not likely for the west Texas area. Likewise, shrinkage cracking due to moisture loss in the base course was not a likely mechanism. An initial computer study using a heat transfer program showed that freeze-thaw activity during a winter, for Perryton, Texas, was centered mainly in the base course for a typical pavement.

Comprehensive freeze-thaw testing showed the base course to be more active, thermally, than asphaltic concrete. The thermal activity is composed of a freeze deformation and a residual deformation. Both quantities are related to the soil moisture suction of the material. The soil moisture suction which develops in a sample is a function of the grain size, moisture, pore structure and clay mineralogy. Clay mineralogy determinations were done using x-ray diffraction to obtain the relative percentages of the clay minerals present. A direct relationship is established between the freeze deformation and clay mineralogy of the material tested.

The data collected indicate a mechanism of particle reorientation may be causing the measured volume changes and be responsible for observed loss of strength in roadbed material after undergoing several freeze-thaw cycles. The data also demonstrate the validity of using clay mineralogy properties as a design quantity for base course material.

17. Key Words	18. Distribution Statement
Low-temperature cracking, weather, thermal fatigue cracking, suction, clay mineralogy.	

19. Security Classif. (of this report)	20. Security Classif. (of this page)	21. No. of Pages	22. Price
Unclassified	Unclassified	125	

Form DOT F 1700.7 (8-69)

TABLE OF CONTENTS

TABLE OF CONTENTS (CONT'D)

PREFACE

This report details the testing done on several representative base course materials from the west Texas area. The major area of study was narrowed to the thermal activity in the base course material. The data presented have not been previously considered as a mechanism in the environmental deterioration of pavements. This is one of a series of reports from the study entitled "Environmental Deterioration of Pavement." The study, sponsored by the State Department of Highways and Public Transportation in cooperation with the Federal Highway Administration is a comprehensive program to verify environmental cracking mechanisms and recommend maintenance and construction measures to alleviate this problem.

DISCLAIMER

LIST OF REPORTS

Report No. 18-1, "Environmental Factors Relevant to Pavement Cracking in West Texas," by Samuel H. Carpenter, Robert L. Lytton, Jon A. Epps, describes the environment existing in west Texas and relates it to other studies to determine its severity.

Report No. 18-2, "Thermal Activity of Base Course Material Related to Pavement Cracking," by Samuel H. Carpenter, and Robert L. Lytton describes the development of a pavement cracking mechanism emanating from thermal activity of the base course layer in the pavement.

ABSTRACT

Preliminary studies into environmental deterioration of pavements indicated that low-temperature cracking of the asphalt concrete surface was not likely for the west Texas area. Likewise, shrinkage cracking due to moisture loss in the base course was not a likely mechanism. An initial computer study using a heat transfer program showed that freeze-thaw activity during a winter, for Perryton, Texas, was centered mainly in the base course for a typical pavement.

Comprehensive freeze-thaw testing showed the base course to be more active, thermally, than asphaltic concrete. The thermal activity is composed of a freeze deformation and a residual deformation. Both quantities are related to the soil moisture suction of the material. The soil moisture suction which develops in a sample is a function of the grain size, moisture, pore structure and clay mineralogy. Clay mineralogy determinations were done using x-ray diffraction to obtain the relative percentages of the clay minerals present. A direct relationship is established between the freeze deformation and clay mineralogy of the material tested.

The data collected indicate a mechanism of particle reorientation may be causing the measured volume changes and be responsible for observed loss of strength in roadbed material after undergoing several freeze-thaw cycles. The data also demonstrate the validity of using clay mineralogy properties as a design quantity for base course material.

IMPLEMENTATION STATEMENT

The State of Texas, and in particular the west Texas area, currently has an extensive mileage of roads experiencing an enormous amount of unexplained transverse cracking. Currently proposed mechanisms do not accurately predict pavement cracking for this area.

The data presented herein show that the base course material should be considered as the prime factor in initiating transverse pavement cracking in the west Texas area. This same mechanism is responsible for accelerated deterioration of cracked pavements throughout the northern half of the state. Recognition of this thermal activity, which appears to occur in all untreated base course materials with a nominal ten percent clay content, emphasizes the need for a moisture proofing layer to be placed above the base course to prevent water entry once the pavement has cracked. The data in this report also show the need for a reevaluation of the basic material properties currently used in the design process to predict pavement behavior since it appears that more appropriate relations are available. The data presented in this study form the basis for a series of studies which will predict the amount of cracking caused by this mechanism and which will evaluate methods to alleviate the problem.

CHAPTER 1

INTRODUCTION

A growing concern over the environmental cracking of pavements has been realized in the last decade. This concern has been brought about by the increasing mileage of roads experiencing transverse cracking. Ample evidence of these forms of cracking exists in the colder regions of the Northern United States and Canada. Transverse cracking of this form is also found in the arid regions of the western United States.

Recent qualitative surveys of roads in Texas indicate that non-traffic load associated cracking may be a major cause of pavement distress. The area of west Texas, in particular, shows extensive transverse cracking commonly associated with environmental distress. In particular Districts 4, Amarillo; 5, Lubbock; 6, Odessa; 7, San Angelo; 8, Abilene; 24, El Paso, and 25, Childress, shown in Fig. 1 demonstrate similar cracking patterns which may or may not be the result of similar mechanism.

There are a variety of mechanisms that have been studied to account for this extensive cracking problem in flexible pavements. These mechanisms all show some dependence on environmental factors. Low temperature cracking is the most environmentally controlled mechanism in the formation of transverse cracks and has been studied extensively (13, 14, 23). This mechanism has been used in the colder regions of Canada and the Northern United States in predicting cracking during the life of a pavement. The concept of this mechanism involves the thermal contraction of the asphaltic concrete due to low temperatures. As the temperature drops, tensile stresses are

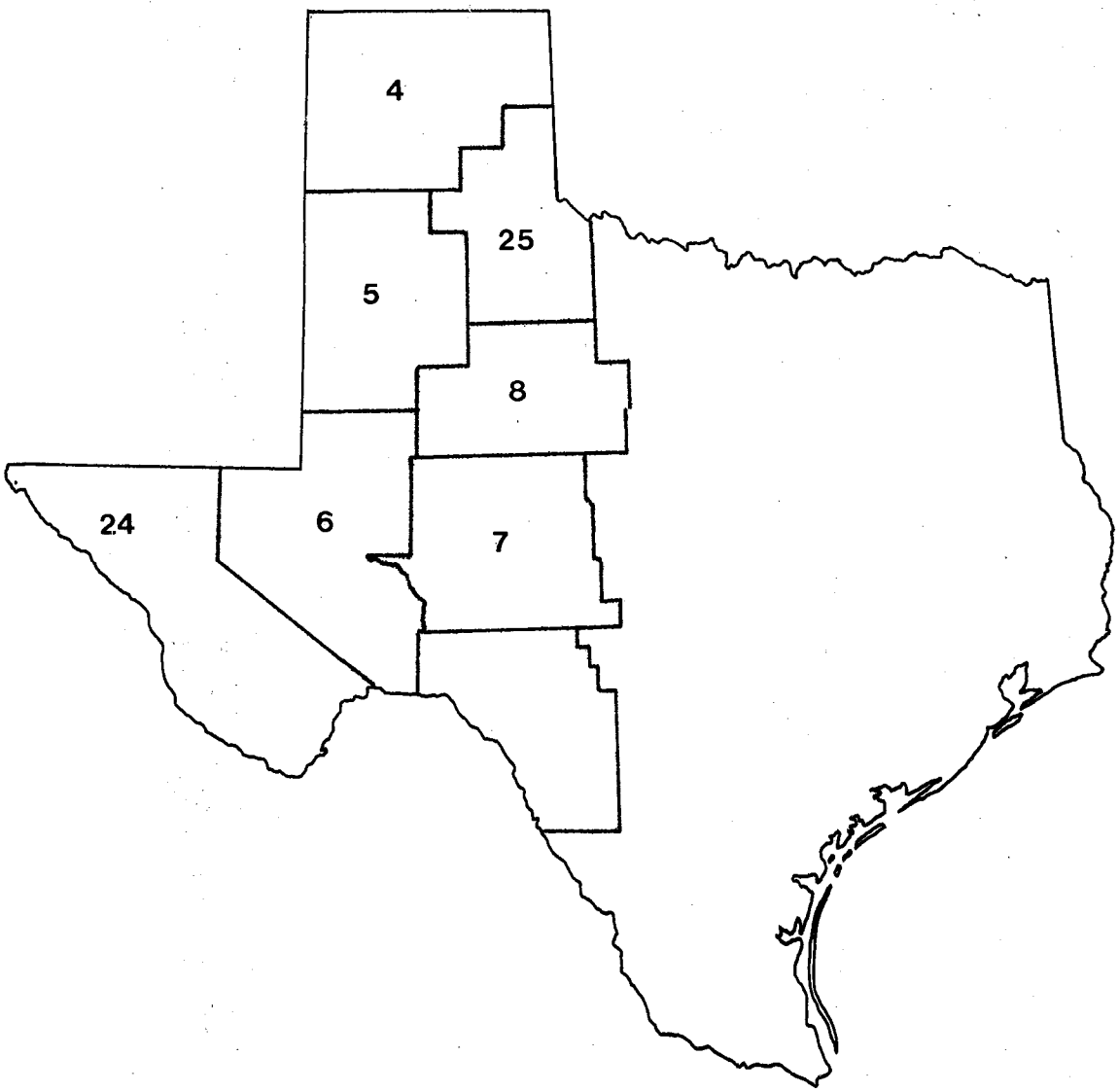

FIG. 1 - HIGHWAY DISTRICTS IN WEST TEXAS EXHIBITING EXTENSIVE TRANSVERSE CRACKING

induced due to the contraction. When these induced stresses exceed the tensile strength of the asphalt the material will crack. The extreme cold temperatures necessary to produce this form of cracking occur only rarely in Texas and thus this mechanism of cracking is not likely to occur in west Texas, as stated by McLeod (23).

Thermal fatigue cracking has been proposed to account for the discrepancy between observed and predicted cracking. This mechanism involves the fatiguing of the asphaltic concrete under the action of freeze-thaw cycling in much the same manner as repeated loading produces fatigue in metals. Previous studies have not applied fracture mechanics; but have assumed a fatigue law and obtained the constants necessary by forcing the result to match actual data. The constants thus determined were then used to predict cracking for various other pavements. The results of this procedure are not wholly satifactory and do not provide any insight into the mechanism itself. For these reasons it is felt that another mechanism may be acting in conjunction.

Transverse cracking is extremely common in asphaltic concrete surfaces placed over material that has been lime or cement stabilized. George (11) has shown that drying shrinkage of stabilized material cracks the asphaltic surface primarily through reflection cracking which begins only after the base course or subgrade has cracked. It is thus seen that the initiation of cracks in the subgrade or base course is an important factor as the asphaltic concrete will certainly crack once the granular materials have cracked.

Transverse cracking in stabilized material is due mainly to shrinkage brought about by a loss of moisture due to hydration of the admixture. This hydration of the lime or cement serves to remove moisture from the soil structure. This increases the soil

moisture suction in the material. The magnitude and distribution of the suction is extremely important in determing the magnitude of the induced tensile stress as is shown in Fig. 2 which was taken from George's paper. The figure shows that a distribution of relative humidity (related to suction) similar to what could be expected to occur in a natural pavement system produces the most severe stress distribution for crack initiation. The statement by George that this phenomenon may be more severe in untreated pavement systems opens the possibility that this mechanism should be considered for inclusion in any transverse cracking prediction scheme.

Research report 18-1, which dealt with environmental factors relevant to pavement cracking, presented data which indicated that this form of shrinkage cracking could be expected in west Texas in an untreated pavement system. Figure 3 shows the predicted suction that will develop in a subgrade after a pavement has been constructed. These suction levels are extremely high in west Texas and as such they could easily set up suction differentials which would dry out the base course from the bottom. This one-directional drying would set up a suction gradient similar to, but inverted from, that shown in Fig. 2 which could very easily crack the base course if the as-compacted suction level in the base course was sufficiently low to allow adequate moisture transfer.

Seven samples of base course material were collected from west Texas. Table 1 gives the location of the pits and general soil information commonly available (28). These materials were selected to represent typical base courses being constructed in west Texas. Material passing the 3/8" screen was used in the construction of samples at two compaction levels, Modified AASHTO, and Harvard

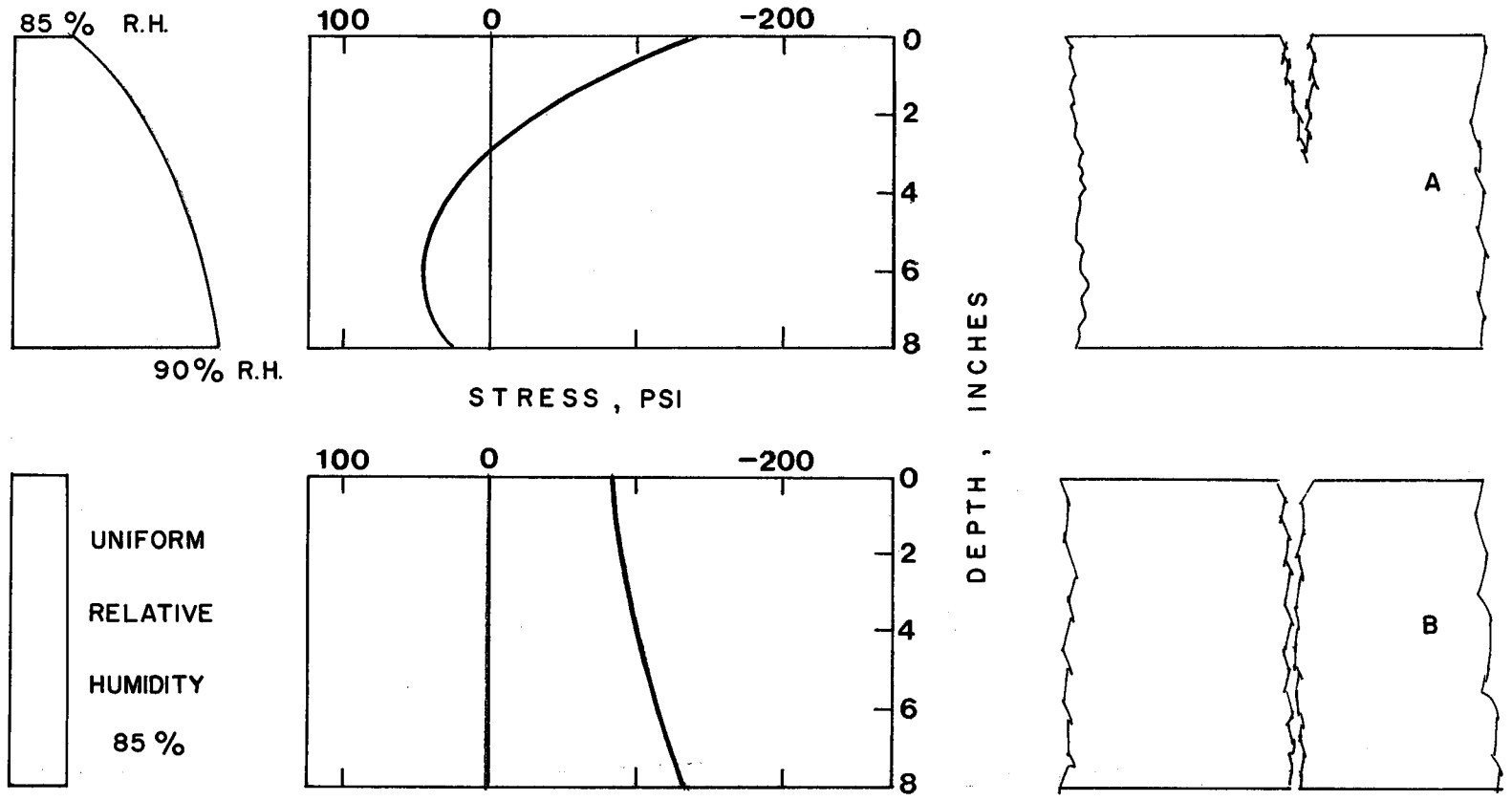

FIG. 2 - (A) CRACK INITIATED DUE TO LOCALIZED SURFACE (TENSION) STRESS
(B) CRACK PROPAGATES THROUGH, DUE TO CONTINUED SHRINKAGE (I)

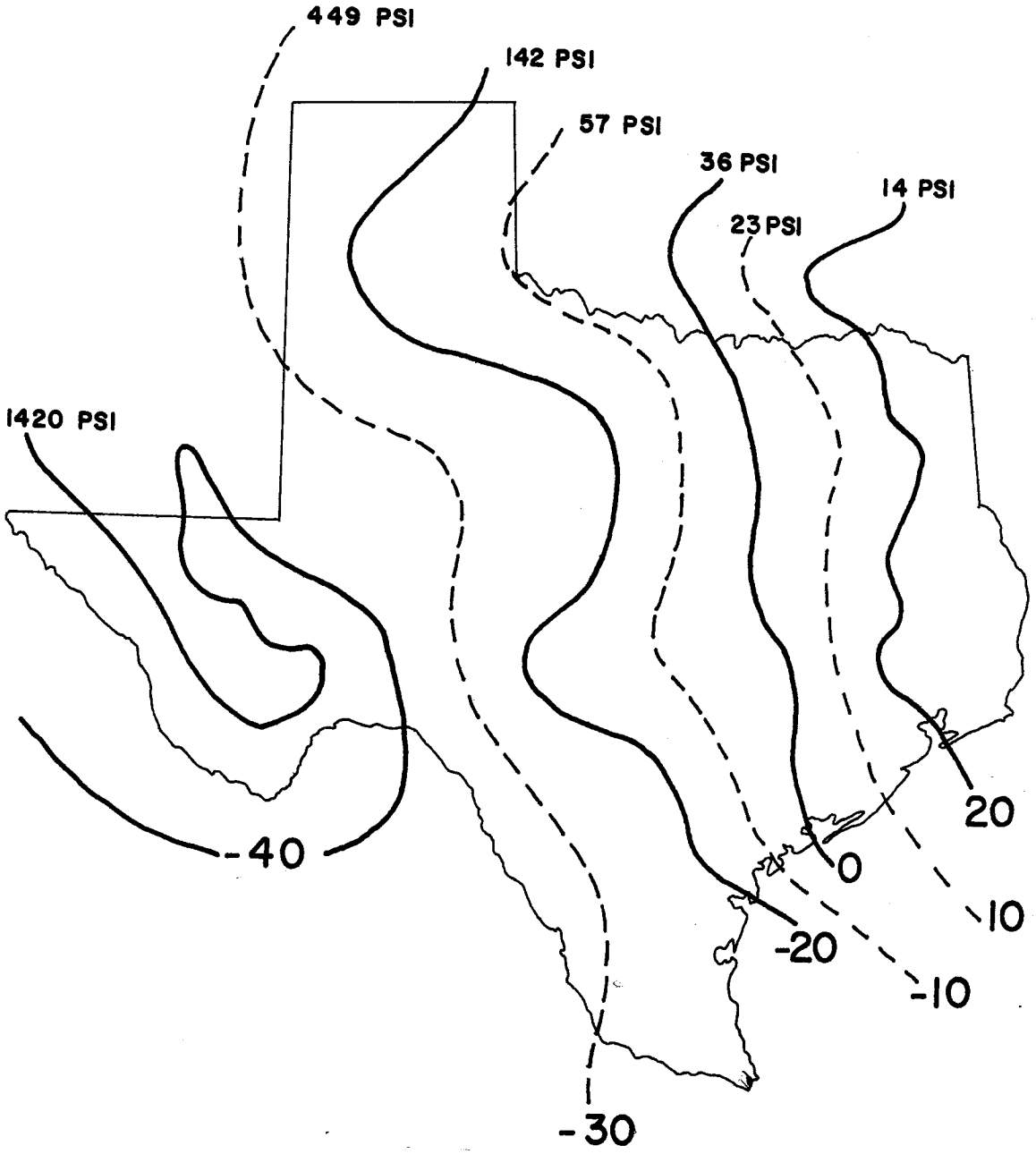

FIG. 3 - EXPECTED SUCTION IN SUBGRADE BENEATH PAVEMENT DERIVED FROM THORNTHWAITE MOISTURE INDEX RELATIONSHIPS, LOWER VALUES

TABLE I. LOCATION AND SOILS DESCRIPTION OF SAMPLES

Sample No.	Location	Soil Description
4	Ochiltree County 13 miles S.E. of Perryton on US 83, District 4	mixed montmorillonitic
5	Lynn County, District 5 1 mile So. of Lubbock-Lynn Co. line, 1 mile W. of US 87	mixed, carbonitic
6B	Reeves County Weenacht Pit #2 Balhmorea, Texas	Carbonitic, mixed gypsic
6JD	Martin County 2 miles East of Stanton on IH 20	mixed carbonitic
6FS	Pecos County Road cut material IH 20, Station, 840 to 0	carbonitic, mixed gypsic
7SA	Runnels County Storage pit on FM 2111	mixed, appreciable montmorillonite
6BAR	Barrow Pit Midland Co, 1/2 mile West of Tower Road	mixed, carbonitic

Miniature calibrated to produce 95% of modified compaction. The equilibrium suction was measured in all samples. Figure 4 shows the resulting suction contours for one material. These are similar to contours obtained by previous investigators. The suction levels near optimum moisture are considerably lower than the values expected to develop in the subgrade. Shrinkage cracking, thus, could be expected to develop.

To validate this concept and to substantiate any laboratory data which would be developed, three field installations of psychrometers to measure the suction were made beneath newly constructed pavements. These installations, which will be detailed in a later report when the data are complete, consist of a set of six psychrometers. One psychrometer is buried in the virgin material off the shoulder. The remaining five are buried beneath the centerline of the pavement to a depth of five feet, the topmost psychrometer being embedded in the base course.

The initial data collected from these psychrometers indicated that shrinkage cracking of the nature proposed was highly unlikely. Suction profiles for two of the installations are shown in Fig. 5. These clearly show the base course to possess a suction level well above that of the subgrade. This was typical of all measurements taken, regardless of soil types and pavement configuration. These data indicate that the base course, although initially placed at or slightly wet of optimum, dries out considerably before the asphaltic concrete surface is placed. This drying could typically amount to seven to 10 percent dry of optimum moisture which would produce the suction levels measured. Thus it may be inferred that due to construction practice the pavement as constructed is not at the same suction level as

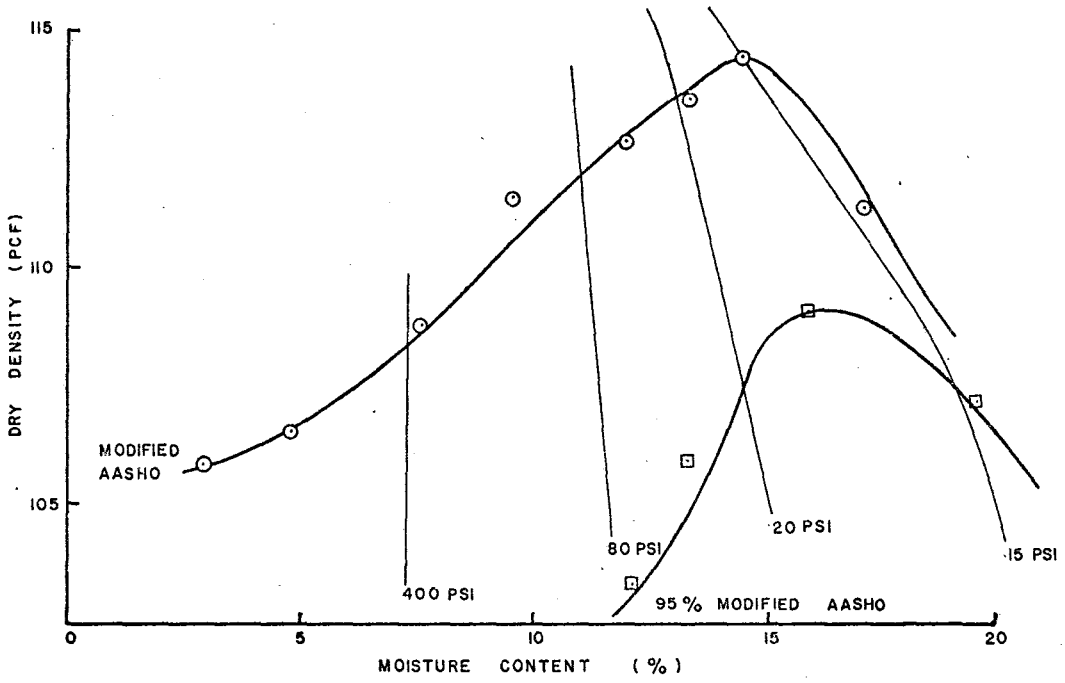

FIG. 4 – COMPACTION CURVE FOR DISTRICT 4 BASE MATERIAL WITH SOIL MOISTURE SUCTION VALUES

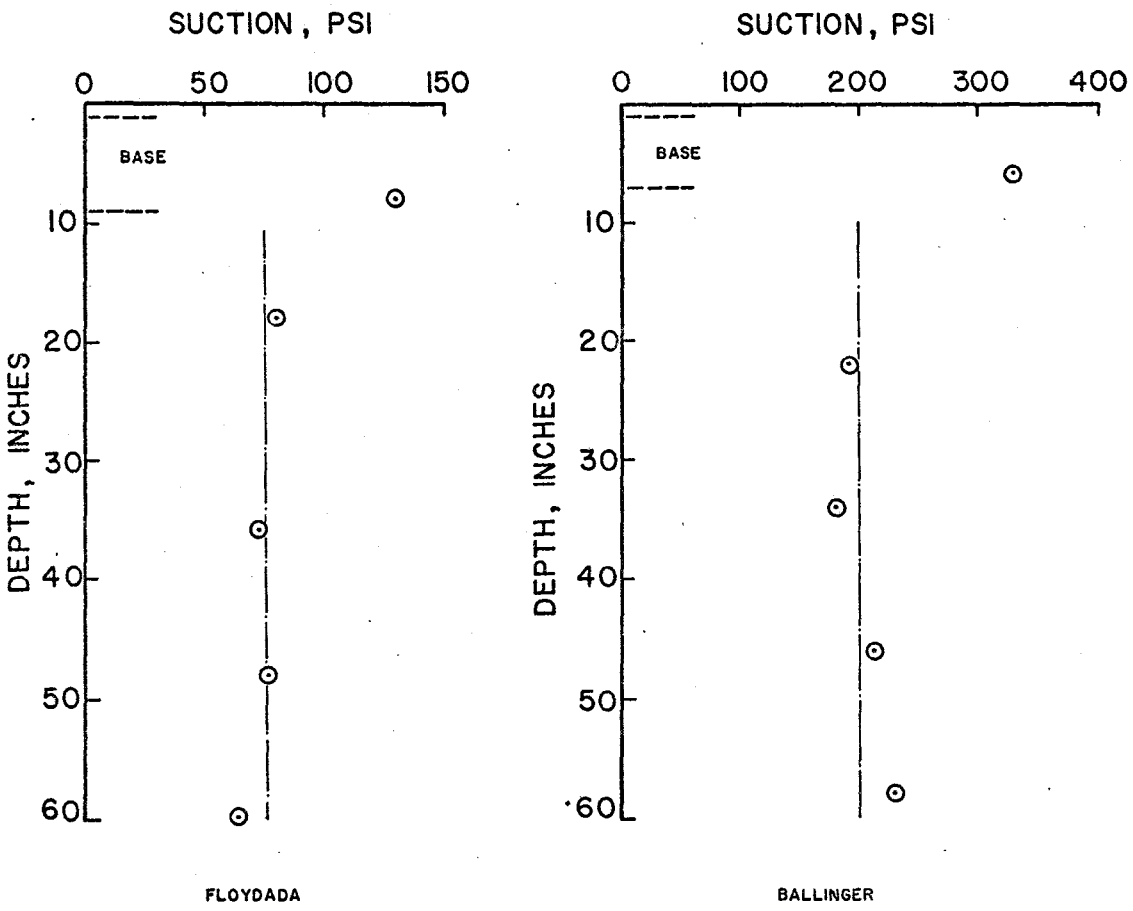

FIG. 5 - MEASURED SUCTION VALUES BENEATH TWO PAVEMENTS IN WEST TEXAS

it was when it was compacted. This concept will be discussed later in the report where it will take on added significance.

At this time a set of freeze-thaw susceptibility tests and a series of initial calculations of pavement temperature distributions combined to provide insight into a cracking mechanism for the base course. The temperature distributions were calculated from weather data for Perryton, Texas for one year. They showed that the freeze line penetrated part way through the base course and not into the subgrade. The freeze-thaw activity was centered in the base course.

A report by H.P. Carothers (6) involved the study of freeze damage to pavements across the entire state of Texas. His conclusions were that the freeze damage in Texas was centered in the base course. The majority of the damage involved soft material which barely passed durability testing and often produced excessive fines during compaction. Although frostheave, or "boils" were not noted as causing the deterioration, the progressive damage of the pavement clearly involved excessive moisture reaching the base course. Shortly after this study the Texas Highway Department began implementing more stringent controls on the base course materials used. The tighter controls only altered the mechanism acting. The fact that freeze damage will initiate mainly in the base course cannot be changed.

In the study reported here freeze-thaw susceptibility tests were initially set up to determine if there would be appreciable strength loss due to the freeze-thaw cycling, as was indicated in previous studies (2). Volume measurements on the samples indicated that they were undergoing continual volume change during a series of freeze-thaw cycles in such a manner that a

form of cracking similar to shrinkage cracking might develop. Because of this, a series of comprehensive freeze-thaw tests and property measurements was established to determine if the noted behavior could be considered typical of base course in use in west Texas, and whether the behavior could be predicted from material properties.

As will be shown later in this report the measured thermal activity of the base course is quite large. This raises the problem of thermal cracking in the base course due to excessive tensile stresses. The tensile stress in an initially uncracked pavement, for any layer, is given as follows:

$$\sigma_T = E\,\alpha\{\Delta T\} \text{----------(1)}$$

σ_T = Tensile Stress

E = Young's Modulus

α = Coefficient of Thermal Expansion

ΔT = Temperature Change

The measured α values for the base course were 10 times larger than those for asphalt. The temperature change is similar for both materials and E for the base course is about one-fifth of the asphalt. The tensile strength of the base course is typically one-third that of the asphalt. Thus the base course could be expected to crack first, due mainly to the size of the thermal coefficient, α.

The remaining chapters of this report will detail the test procedures, data, analysis, material property investigations, and the conclusions regarding a freeze-thaw mechanism in the base course capable of producing environmental pavement cracking.

CHAPTER II

TEST PROCEDURES AND DATA ACQUISITION

Freeze-Thaw.--There are several methods available for conducting freeze-thaw testing of granular material. The open system allows the sample free access to water during the freeze-thaw process usually by inserting one end of the sample in a pail of water. The closed system maintains a constant moisture content in the sample. The biaxial method of freezing of a sample exposes the sample to an all-around uniform temperature. The uniaxial method of freezing involves slowly advancing the freeze line through a sample; which better models the in-situ freezing process. The method of freezing finally selected combined the closed system with the biaxial method of freezing.

The closed system more closely approximates the conditions for a base course in west Texas where the water table will have negligible direct influence on the pavement. Uniaxial freezing in test samples is of prime importance mainly when investigating ice lensing and frost heave which require a freezing front to advance through the sample. This phenomenon usually requires a fine-grained saturated material with access to capillary water and a close water table. This situation does not apply to a base course in west Texas and previous studies have not found any significant structure change (moisture migraton or loss, ice lensing, etc.) in samples of similar material frozen in the closed system mode. For these reasons it was felt that the simpler method of biaxial freezing would be sufficient.

To examine material behavior it is necessary to test the material to a greater limit than it would experience in actual use. A study

by Hamilton (15) has shown that 90 percent of the total volume change due to freezing will occur between $0^{o}C$ and $-6.8^{o}C$ with the other ten percent occurring from ambient down to $0^{o}C$. Only very slight and erratic volume change was noted to occur below $-6.8^{o}C$. This is illustrated in Fig. 6 which is taken from Hamilton's study. Figure 7 shows data for two freeze-thaw cycles. The noted temperature dependence is evident but the more important feature is the volume change noted after the the first cycle. If this behavior is prevalent in base course material, with considerably less clay content than the subgrade material tested by Hamilton, the implications for pavement deterioration are apparent.

From this study a low temperature of $-6.8^{o}C$ was chosen. This allowed the use of a standard environmental chamber. The samples were placed in the chamber and removed when frozen. The thermocouple in the larger modified AASHO samples allowed monitoring of the temperature in the samples. These samples were frozen for a twenty-four-hour period and thawed for a similar period. The smaller Harvard miniature samples were frozen over night (16 hours) and thawed for eight hours.

Sample Preparation.--Each material was received in sample sacks as taken from the storage pit. The material was sieved and all material passing the 3/8 inch sieve was used to construct samples, although the AASHTO specifications for compaction call for the use of material passing the 1/4 inch sieve. The use of the larger aggregate was an attempt to better model the actual behavior of the material in-situ. The use of an excessive percentage of fines in the samples would tend to accentuate their behavior and give data not directly applicable to solution of field problems.

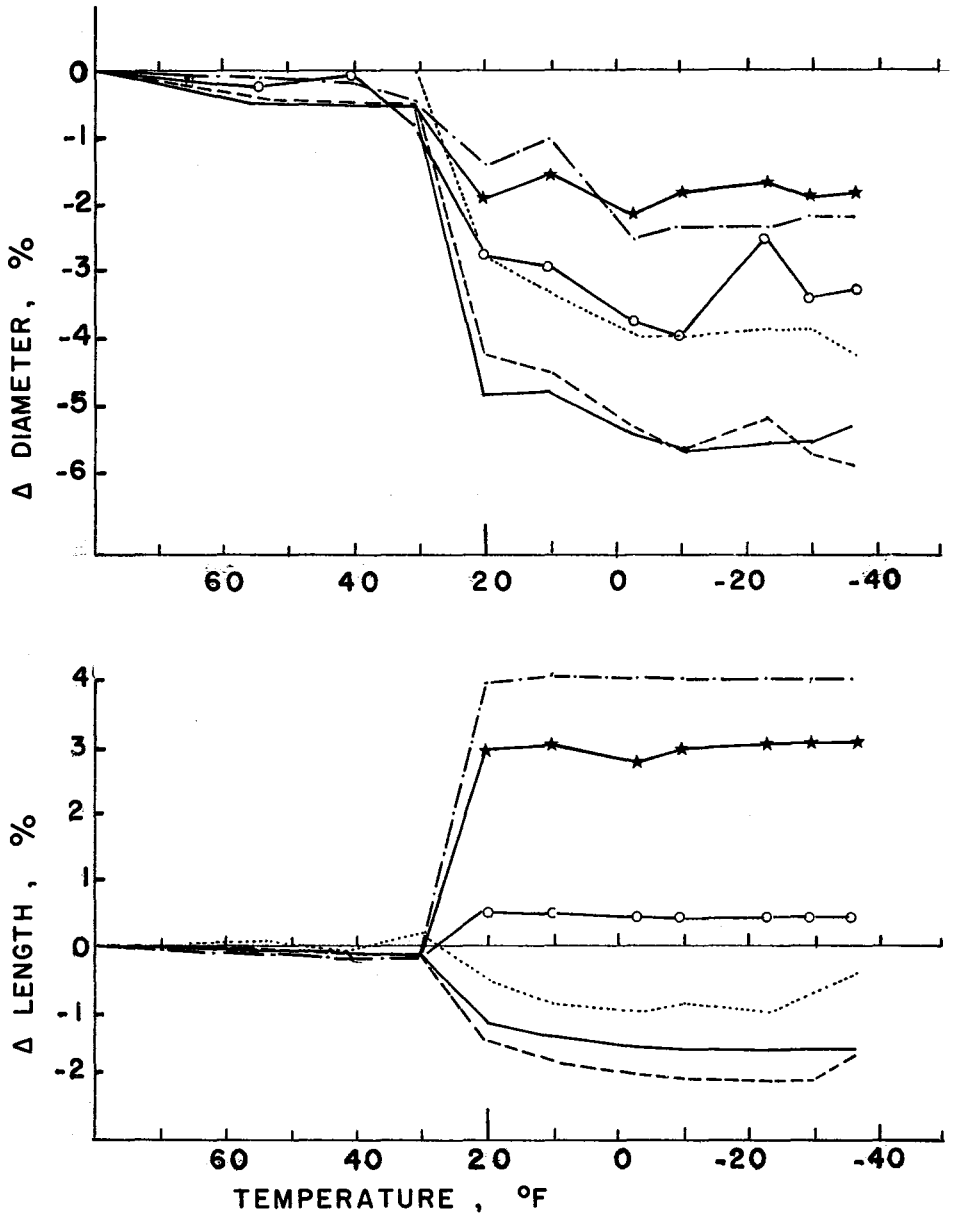

FIG. 6 - CHANGE IN LENGTH AND DIAMETER FOR SIX SAMPLES AS FUNCTION OF TEMPERATURE (15)

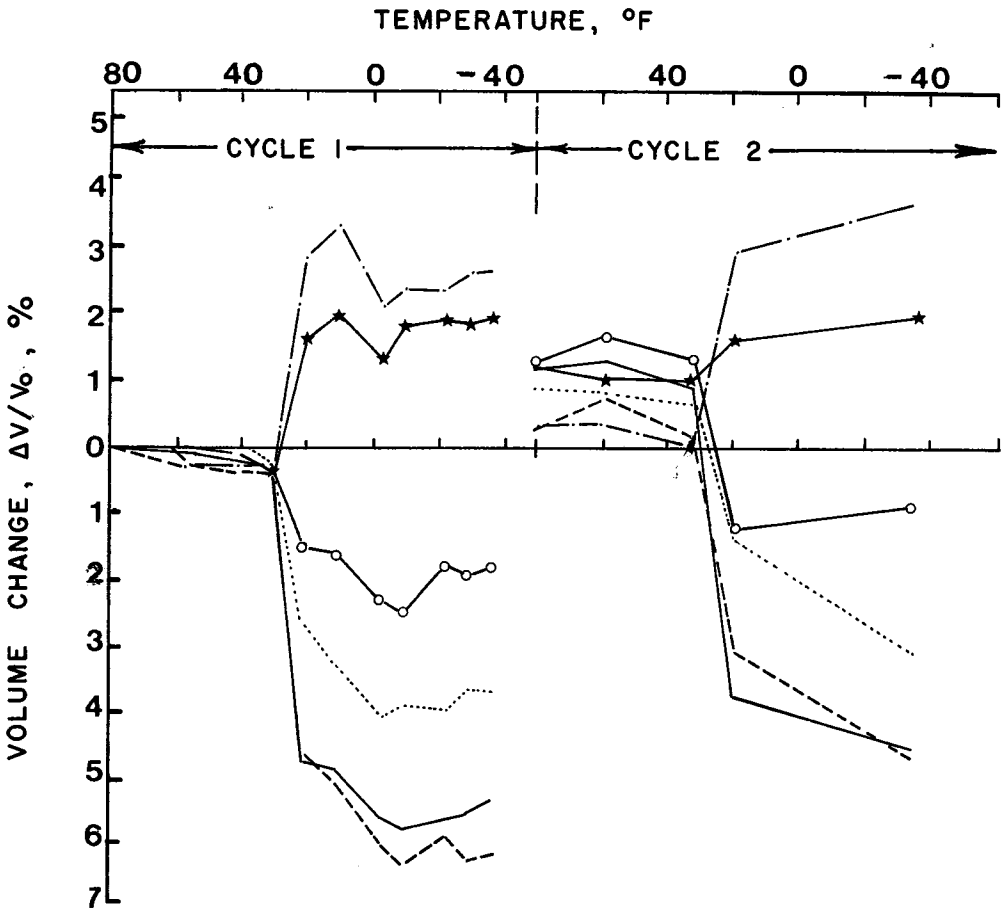

FIG. 7 - VOLUME CHANGE AS A FUNCTION OF TEMPERATURE FOR TWO FREEZE-THAW CYCLES(15)

Each material was compacted at two energy levels. The first level being Modified AASHTO using standard equipment and the second level being 95% of Modified using Harvard Miniature samples with a spring loaded tamper. These compactive levels produced two distinct curves for each material which allow the effects of compaction to be studied. The material was hand mixed at a given moisture content and stored overnight before compacting.

Variables to be measured.-- The freezing of a soil sample produces an extremely large volume change as the most obvious influence. The height and diameter of the samples were measured after every freeze and thaw. This procedure allows the complete history of the sample to be recorded for analysis.

The soil moisture suction, measured in samples of subgrade material, before and after freezing has shown a direct relationship with the load carrying ability of the material. Monismith and Bergan (2) have shown that there is a decrease in the load carrying ability of a subgrade after a winter that corresponds to a decrease in the suction potential. Additionally, Yong (27), has shown that the as-compacted soil moisture suction is related to the amount of moisture remaining unfrozen in the material at any sub-freezing temperature. From these previous studies it can be seen that suction can be used to describe the behavior of a sample undergoing freezing. The use of suction is complicated because total soil moisture suction is composed of two separate forms of suction. These are:

1. Osmotic suction which is the suction potential due to salts in the water portion of the three phase soil system.
2. Matric suction which is the suction due to the matrix, the soil particles themselves, which form capillaries.

These two components, added together, give the total soil moisture suction (1). To date the studies mentioned have reported values for the matrix suction as their suction measurement. It is extremely difficult to obtain in-situ measurements of matrix suction using equipment capable of being used in the laboratory on the same material. Psychrometers represent the best device for both laboratory and in-situ work. Their main disadvantage is that they measure total soil moisture suction only and cannot differentiate between matrix and solute forms of suction. During a freeze both forms of suction will change due to a decrease in the amount of free water. This causes a larger osmotic suction by increasing the concentration of ions in the remaining free water as well as a larger matric suction by decreasing the free water which decreases the capillary size. Both these mechanisms can contribute to a volumetric change. The contribution of each will be discussed later in detail. The main point to be made here is that since both components of the total suction contribute to the deformation both should be measured. Thus the total suction can be measured without any loss in understanding the mechanisms which will occur in freeze-thaw cycling. See Appendix A for the methods used.

Measurement of the Variables.-- When the modified AASHTO samples were compacted a small metallic rod was compacted in the middle layer. This rod was located, after extrusion from the mold, with a magnet and removed with a minimum of disturbance to the surrounding sample. A psychrometer, the same size as the rod, was then inserted into the void. The psychrometer, shown in Fig. 8, measures the relative humidity of the soil moisture by obtaining the wet bulb and dry bulb temperatures much the same as the hand held sling psychrometer

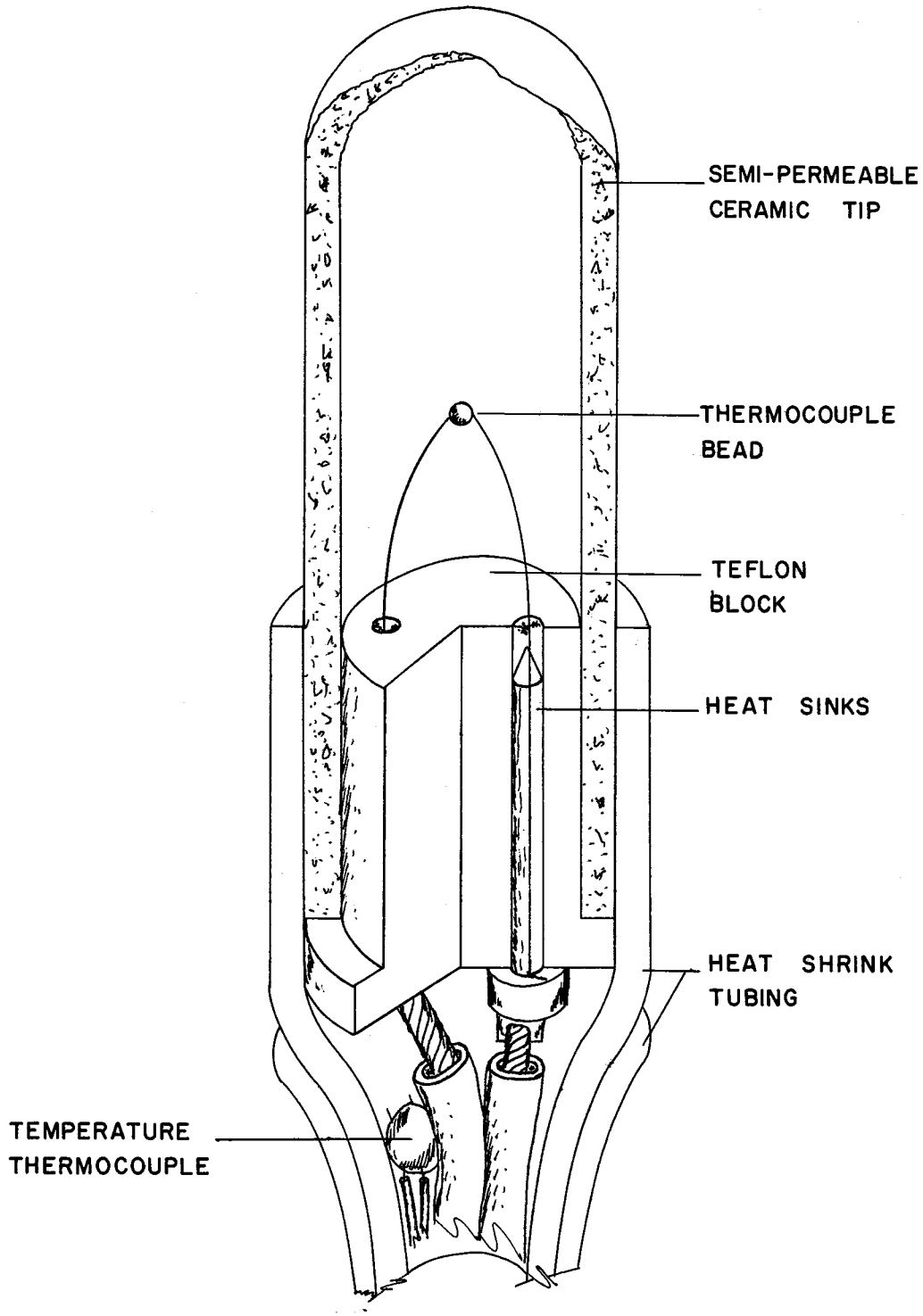

FIG. 8 - CROSS-SECTION VIEW OF A PSYCHROMETER

hence the name. The thermocouple psychrometer utilizes a very fine thermocouple bead to measure the temperatures. The soil moisture suction may then be obtained from the relationship:

$$h = \frac{RT}{gM} \log_e H \quad \text{----------(2)}$$

where

h = total soil water potential, in bars, a negative quantity,

R = 8.31 x 10^7 ergs/^oC, mol.,

T = absolute temperature,

g = 981 cm/sec^2,

M = molecular weight of water = 18.02, and

H = relative humidity.

Suction, a negative quantity, is considered in the absolute value sense as a positive quantity in this report for ease of discussion.

The modified AASHO samples (4 inch diameter, 4.6 inch height) were wrapped in foil and sealed in wax. The psychrometers were read continuously until the moisture had become evenly distributed and an equilibrium suction value was obtained. This typically involved three to four weeks after the sample was compacted before equilibrium was attained. Once equilibrium was attained the samples were ready for freeze-thaw testing. The psychrometers were left in the samples to monitor suction during freeze-thaw testing. This involved the removal of the wax and tin foil from small areas on the top, bottom, and sides. These openings were sealed by a thin plastic wrap with silicon grease around the edges. This is shown in Fig. 9 for both types of samples tested. This arrangement allows measurements to be made without opening the seals, thus maintaining a constant moisture content with a minimum amount of manipulation of the sample. The

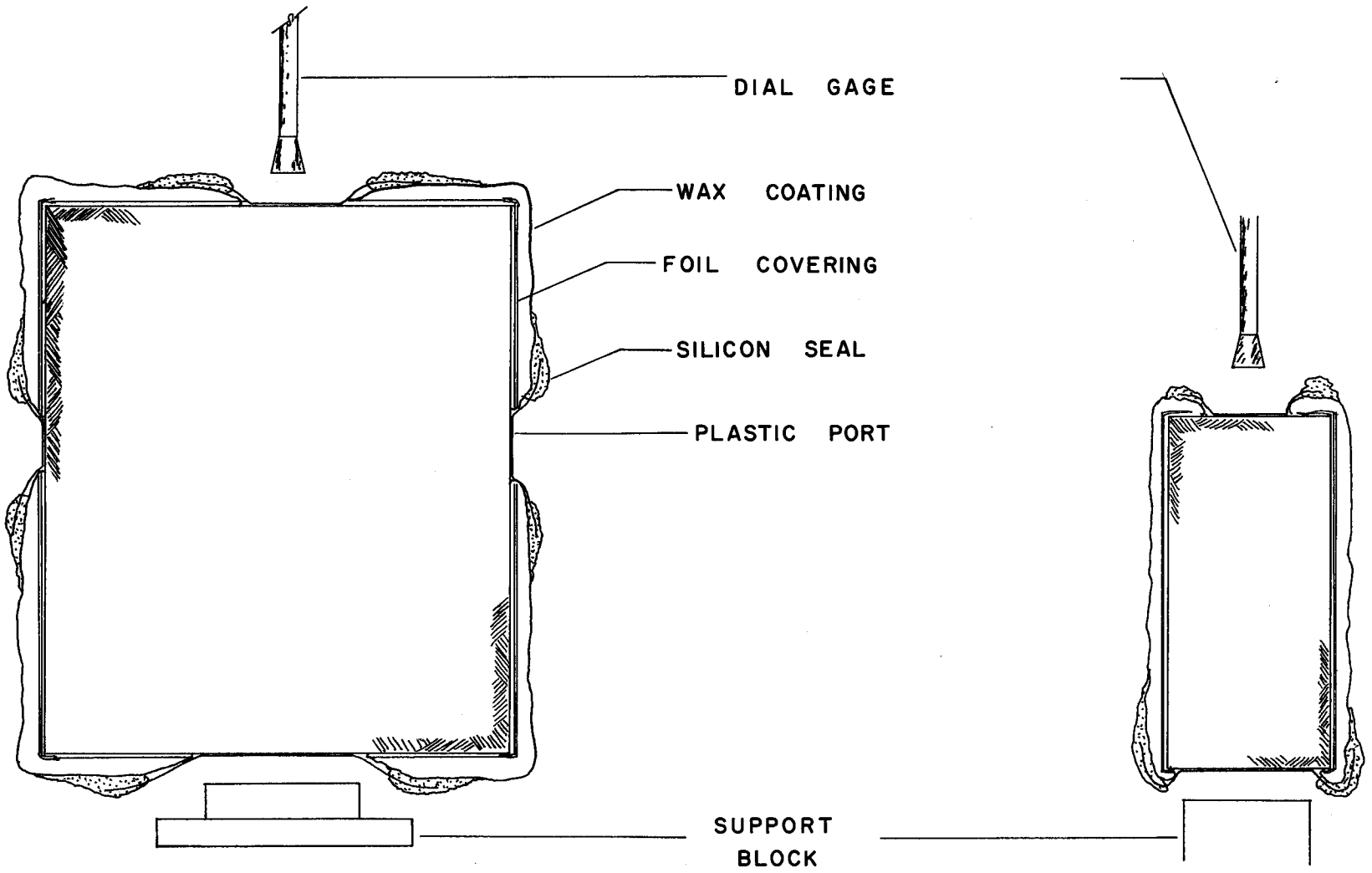

FIG. 9 - ILLUSTRATION OF SAMPLE PREPARATION TO ALLOW MEASUREMENT OF LENGTH AND DIAMETER WITHOUT OPENING SAMPLE

Harvard miniature samples were prepared in the same manner. The psychrometers were not embedded in these samples due to the small size but were sealed with the sample under the tin foil and wax to obtain equilibrium suction values. The volume measurements were made using a dial gage mounted on a tripod assembly and a micrometer.

CHAPTER III

DATA OBTAINED

General Description.--The data collected from the freeze-thaw portion of the investigation of the base course material may be presented in three separate categories. The categories are as follows:

1. Freeze Deformation. This deformation is that caused by the freeze portion of the cycle, part of which is typically recovered during the thaw portion of the overall freeze-thaw cycle.
2. Residual Deformation. This is the deformation that is not recovered during the thaw portion of a freeze-thaw cycle. This is a permanent deformation.
3. Suction Variations. These values represent the utilization of the moisture during the freeze-thaw cycle and give an indication of the physical process occuring in the material.

These areas are discussed more fully in the following sections.

Freeze Deformation.--Figure 10 shows the thermal behavior for two samples of the same material compacted at different moisture contents. The two samples demonstrate drastically different, although predictable, behavior. The freeze deformation is shown as the change in height from a thawed condition to a frozen condition. The two samples pictured demonstrate that this deformation may be either expansion or contraction.

As this deformation represents the total change in height due to a temperature drop from ambient to below freezing it is necessary to consider the deformation in two parts, one above freezing and the other below

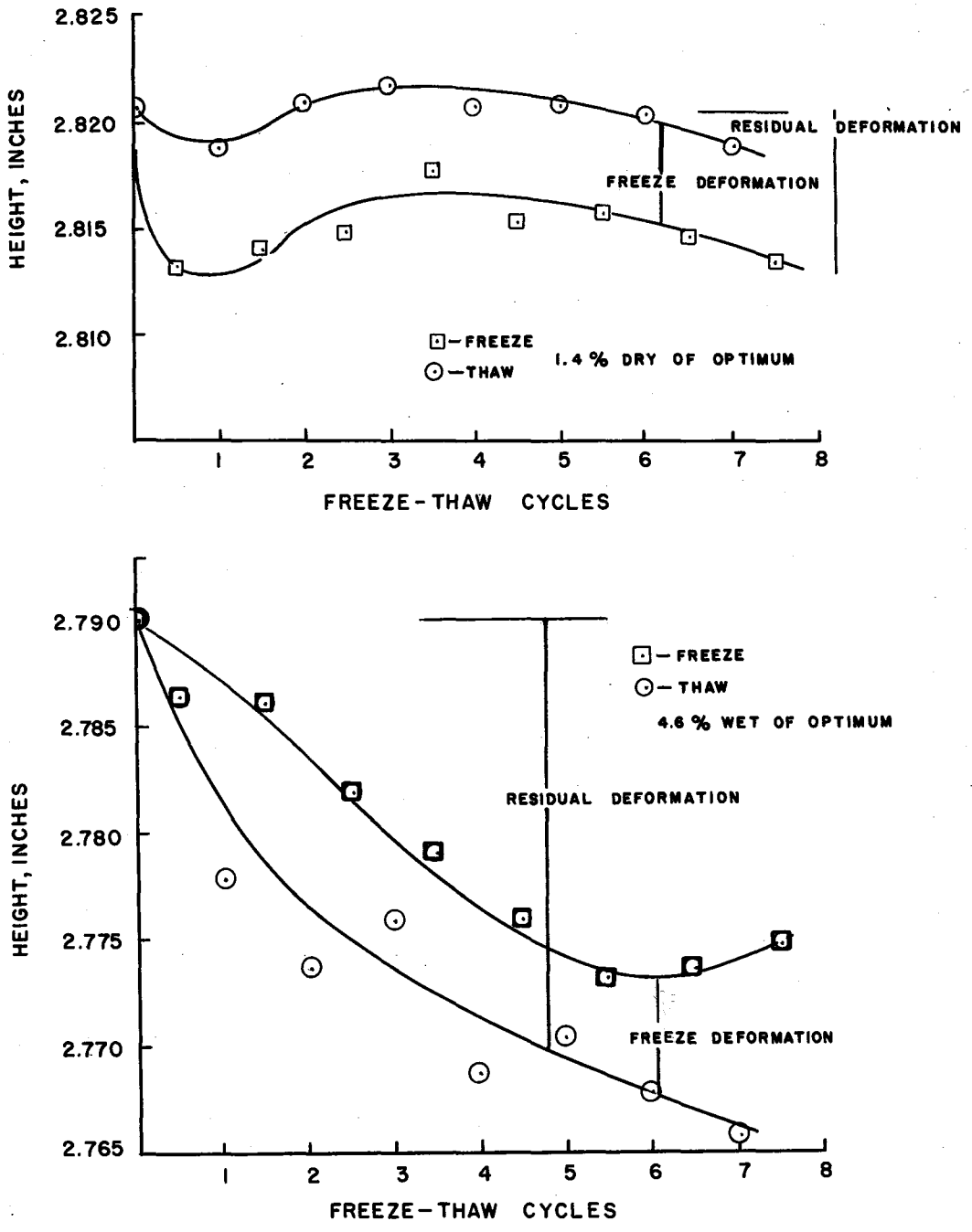

FIG. 10 -SAMPLE HEIGHT AS A FUNCTION OF FREEZE-THAW CYCLES

freezing, as indicated in the last chapter. The first coefficient represents the 10 percent change that occurs from ambient down to freezing. It may be expressed as follows:

$$TC = \left(\frac{\frac{\Delta H}{H_o}}{\Delta T} \right) \times 0.1 \quad \text{----------(3)}$$

where

TC is the thermal coefficient in percent strain per ^{o}C,

ΔH is the change in height

H_o is the initial height, and

ΔT is the change in temperature from ambient down to freezing, in ^{o}C.

The second, and more important, coefficient is termed the freeze coefficient. It represents the change in dimensions from $0^{o}C$ to $-6.8^{o}C$ and is expressed as follows:

$$FC = \left(\frac{(0.9)(\Delta H/H_o)}{6.8^{o}C} \right) \quad \text{----------(4)}$$

where the variables are as previously defined.

As was previously mentioned in reference to Fig. 10 the freeze behavior may be expansion or contraction. The relationship is illustrated in Fig. 11 which shows the freeze coefficients plotted over the moisture density curves. This relationship is similar to that obtained by Hamilton for a clay subgrade. There is an influence due to compaction as well as moisture which is brought out in this figure.

Residual Deformation.--Referring again to Fig. 10 the two samples yield different residual deformation patterns. The residual deformation is the total deformation from the original value, that is never recovered. This deformation, similar to the freeze deformation, may be either expansion or contraction.

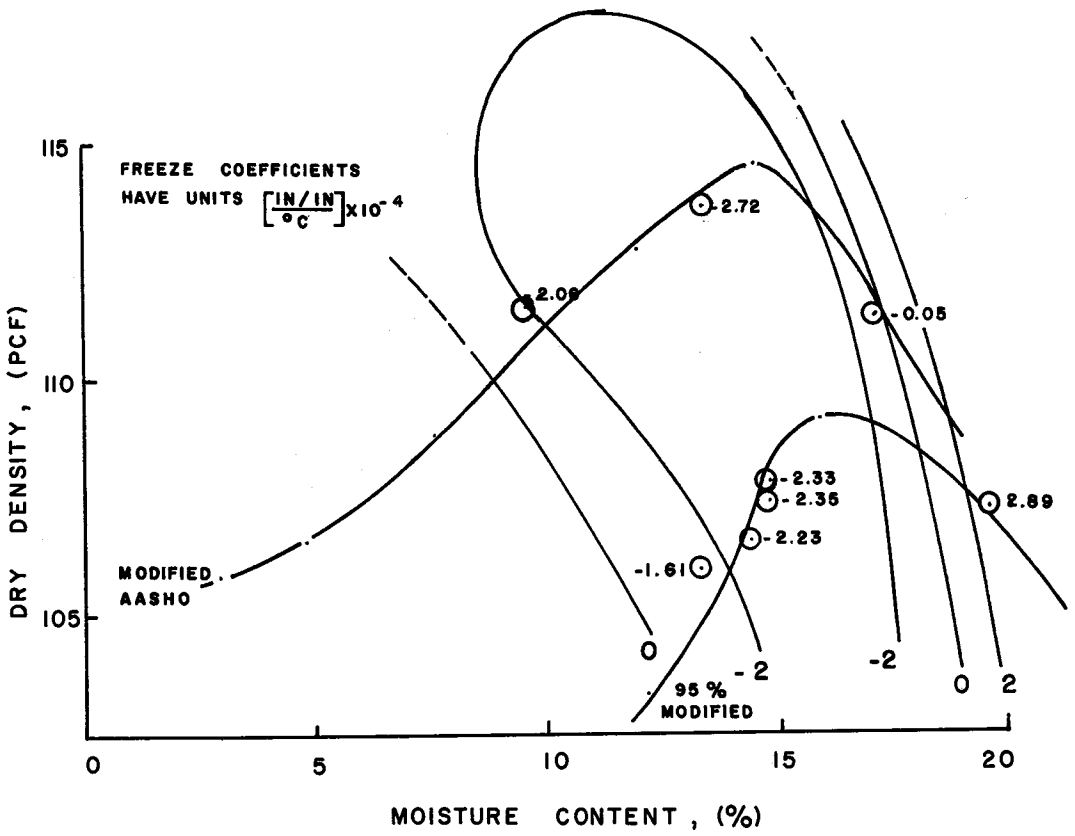

FIG. 11 - FREEZE COEFFICIENTS PLOTTED ON THE MOISTURE DENSITY CURVES FOR MATERIAL 4, -SIGN = CONTRACTION

Unlike the freeze deformation the residual deformation cannot be used to calculate a coefficient of contraction or expansion since the residual deformation changes constantly with additional loadings in much the same manner as shown in repetitive triaxial loading tests. This similarity provides the initial relationship in the analysis of the data. The plot of residual strain ($\Delta H/H_0$) as a function of the logarithm of the number of freeze-thaw cycles is shown in Fig. 12. This relationship produced a straight line relationship for all material tested.

From these straight line relationships the slope could be calculated from the best fit line by standard linear regression techniques. This value, B_1, is a measure of the permanent deformation that will occur per freeze-thaw cycle. These values are plotted on the moisture density curves in Fig. 13. Again there is a noticeable influence due to moisture and compaction effort although not necessarily the same influence as was noted for the freeze behavior.

Suction.--The equilbrium , or as-compacted, suction was determined over the entire range of the two moisture density curves by the techniques previously discussed. Figure 4 showed the values determined for material 4 plotted on the moisture density curves. This relationship is typical of values determined by other investigators for a wide range of soil materials (1, 2, 24). The major feature of this information is that compaction effort has a minimal effect on the suction within the range of compaction levels normally used. The major influencing factor is moisture.

The fact that moisture plays such an important role in both the thermal activity and the development of the as-compacted suction provides a relationship in which suction may be used to predict the thermal

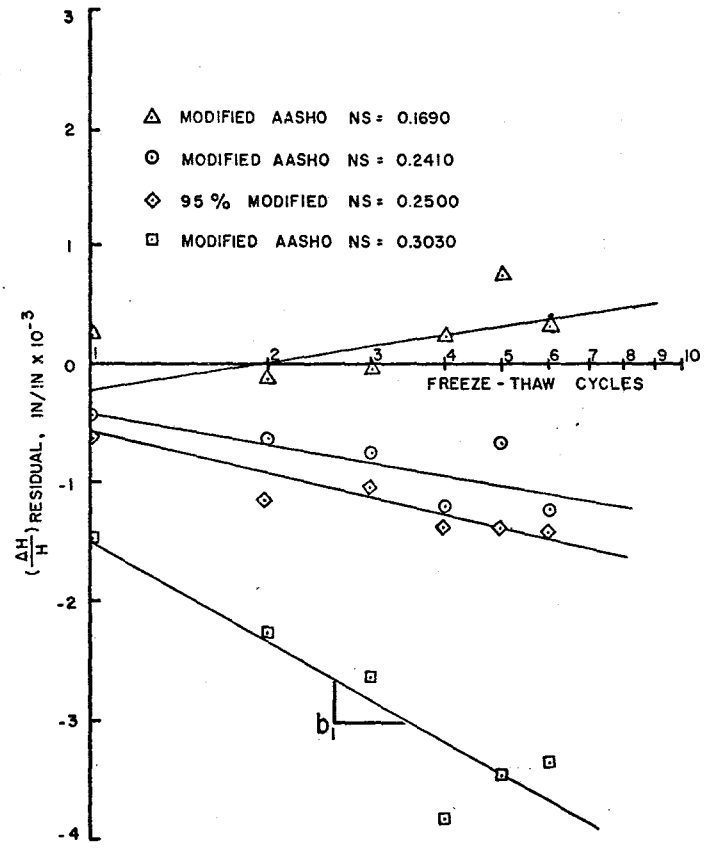

FIG. 12 – RESIDUAL STRAIN PLOTTED AGAINST LOG_{10} NUMBER OF FREEZE-THAW CYCLES, MATERIAL 4

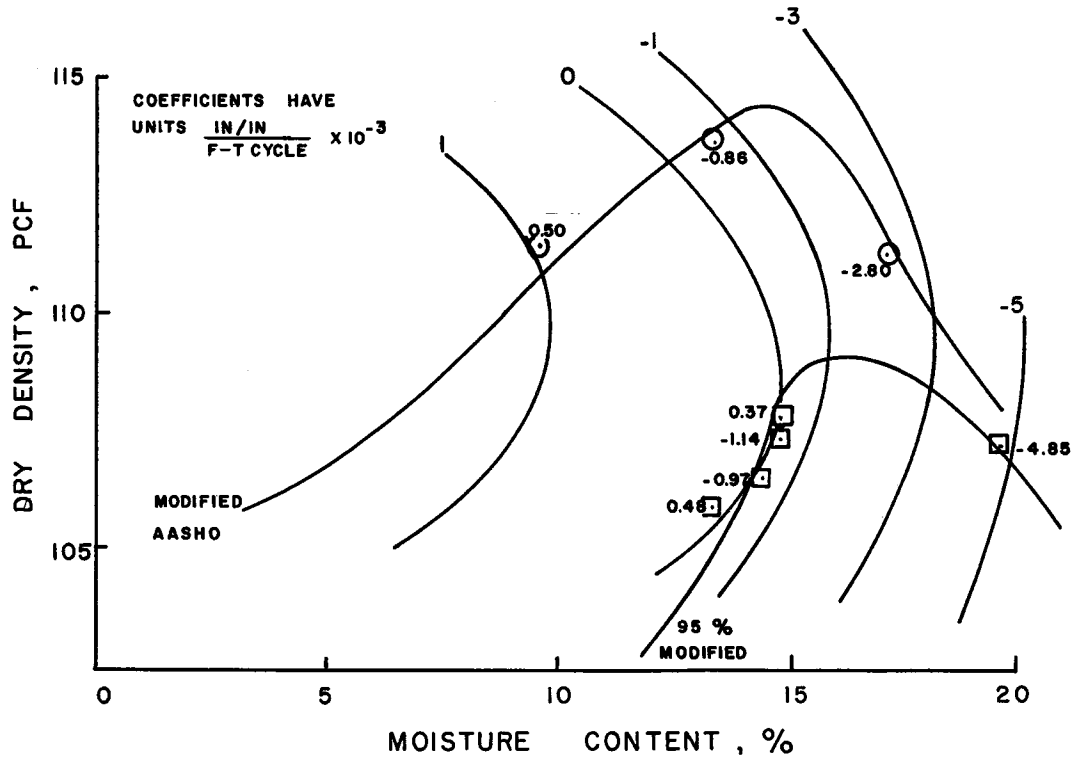

FIG. 13 - RESIDUAL STRAIN COEFFICIENTS PLOTTED ON MOISTURE DENSITY CURVES FOR MATERIAL 4, - SIGN = CONTRACTION

activity of a base course. This relationship will be described further later in this chapter.

The suction was monitored in the modified AASHTO samples during the freeze-thaw cycling as mentioned previously. The data collected show that the suction increased drastically when the sample was frozen. Upon thawing the suction returned to a level slightly below the original as-compacted value, indicating an internal change in the sample. Typical data in Fig. 14 show this trend for two samples compacted at different moisture content. These data are very important when interpreting the proposed mechanism.

Basic Properties.--For each material there were several standard tests run to determine some basic properties. These tests include:

1. Specific gravity, G_s,
2. Liquid limit, W_l,
3. Plastic limit, W_p, and
4. Grain size distribution.

For each sample compacted several sample properties could be calculated. These include:

1. Void ratio, e,
2. Porosity, n,
3. Degree of saturation, S, and
4. Volumetric water content (nS)

These basic properties are shown in Table 2. There was very little difference in the grain size distribution of the material tested. As suction is influenced by the grain sizes, especially in the finer fractions, the type of clay mineral present could be expected to be influencing the behavior of the material. A clay mineralogy study was conducted to obtain this information. This investigation

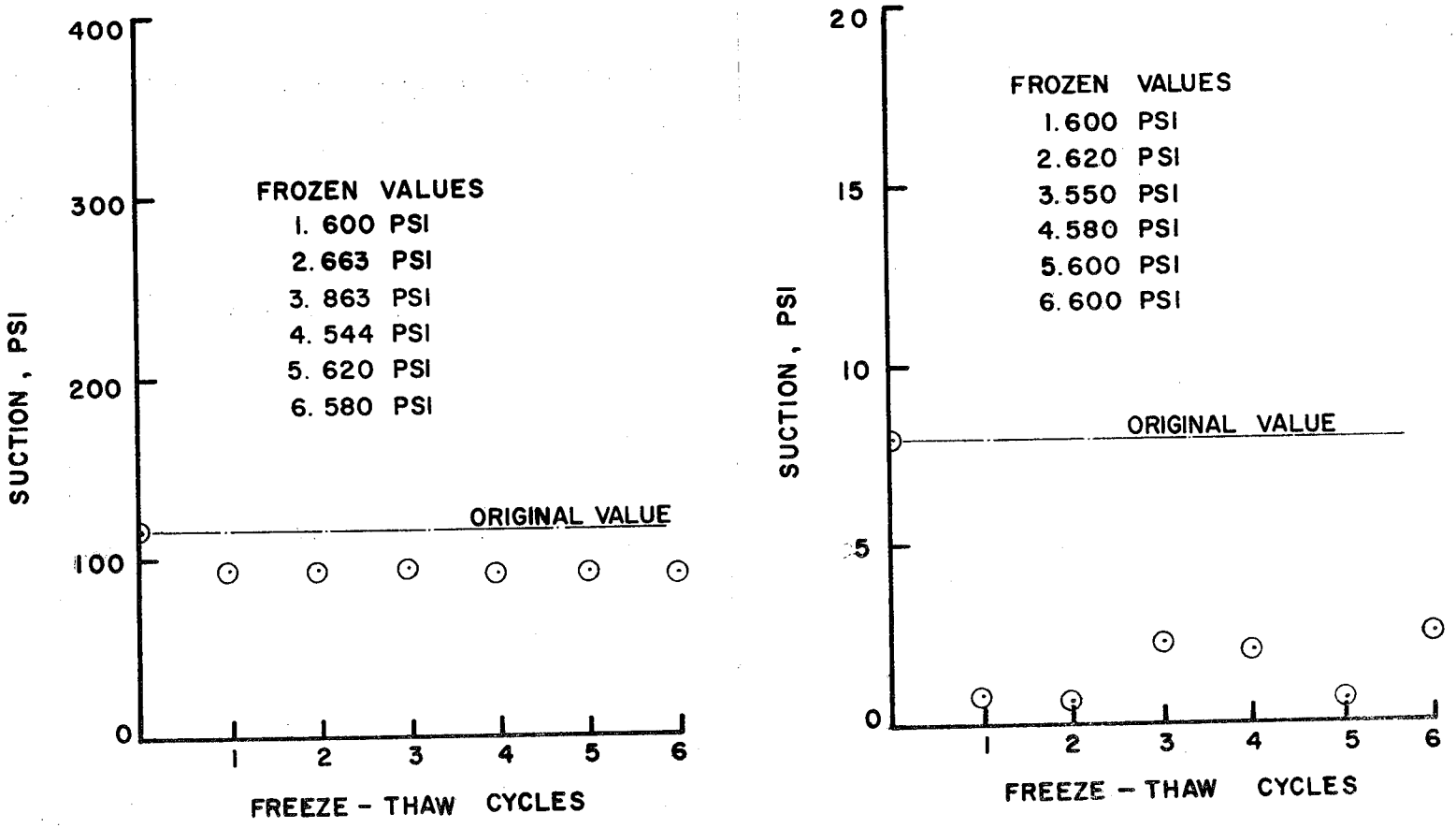

FIG. 14 - SUCTION VALUES DURING THAW CYCLE FOR TWO SAMPLES WITH FROZEN VALUES INDICATED

TABLE 2. PROPERTIES OF BASE COURSE MATERIAL TESTED

Material Number	Specific Gravity	Percent Fines (-#200 sieve)	Liquid Limit (%)	Plastic Limit (%)	Percent Clay (-2μ)	Maximum Freeze Coefficient ($\frac{in/in}{^oC}$)
4	2.65	10	30	21	9.0	-2.7×10^{-4}
5	2.68	9	32	21	7.7	-2.5×10^{-4}
6B	2.67	10	27	17	6.2	-1.3×10^{-4}
6JD	2.69	10	22	18	4.3	-4.0×10^{-4}
6FS	2.66	9	17	16	1.6	-0.5×10^{-4}
7SA	2.68	10	22	12	6.5	-1.85×10^{-4}

is discussed in detail in the next chapter as these data prove to be very important.

Predictive Relationships.--As mentioned, the moisture in the sample appeared to be most influential in determining sample behavior. The suction which is greatly influenced by the moisture gives a much more comprehensive picture of how the moisture is utilized in the sample. Suction is influenced by the grain size, pore structure, and the type of clay minerals present. Any change in suction must be accompanied by a change in one of the above variables. Suction is readily measured in-situ and in the laboratory, as stated, and as such provides a common quantity to relate observed behavior with a measurable value.

Typically suction has been predicted in terms of moisture content. Such regression equations took the form of:

$$h = a + b \log_{10} w \text{----------} (5)$$

where,

h = suction, psi

a,b = regression constants, and

w = gravimetric moisture

This type of regression equation will typically give correlation coefficients, R^2, of 0.85. A better approximation was obtained using the following equation:

$$\log h = a + b \log w \text{----------} (6)$$

where,

h = suction, in psi,

a,b = regression constants, and

w = gravimetric moisture content.

This equation typically give correlation coefficients, R^2, of 0.91

and above, dependent upon number of samples included in the regression. The equations developed for the base course materials are given in Table 3 for the Modified AASHTO samples.

Koopmans and Miller (20) have shown that the soil water characteristic, which is a curve relating moisture content to suction for wetting and drying of a soil specimen is essentially the same as a freeze characteristic which relates unfrozen moisture content to the suction during freezing and thawing. This relationship for a sodium montmorillonite clay is shown in Fig. 15. If the suction levels produced by compacting at different moisture contents may be considered analagous to the suction produced by drying out a sample, or wetting a sample, the regression equations developed should yield values approximating the soil water characteristic over the range of compacted moisture contents. Thus the regression equations may be used directly to study the relation of moisture and suction during freeze-thaw cycling.

Dillon and Andersland (9) developed a relationship for calculating the amount of water remaining unfrozen in a soil material at a temperature below freezing. The equation is as follows:

$$W_u = \frac{ST}{T_o} \cdot \frac{1}{A_c} \cdot \ell \cdot k \cdot 100 \text{----------} (7)$$

where

W_u is the unfrozen moisture content, in percent,

S is the average specific surface area, M^2/gm, from laboratory tests,

T is the temperature in ^oK,

T_o is the temperature of the initial freezing of soil pore water in ^oK,

A_c is the activity ratio = Plasticity index/percent clay,

ℓ is 1 for non expandable clays,

2 for expandable clays, and

K is a constant, 2.8×10^{-4} (gmH_2O/M^2).

TABLE 3. REGRESSION EQUATIONS TO PREDICT AS COMPACTED SUCTION (h) AS A FUNCTION OF GRAVIMETRIC MOISTURE (W)

Material No.	Equation	R^2
4	log h = 5.596 - 3.638 log w	0.91
5	log h = 4.761 - 3.066 log W	0.93
6B	log h = 6.132 - 4.402 log W	0.88
6JD	log h = 3.561 - 2.130 log W	0.97
6FS	log h = 2.574 - 1.560 log W	0.99
7SA	log h = 4.545 - 3.389 log W	0.86

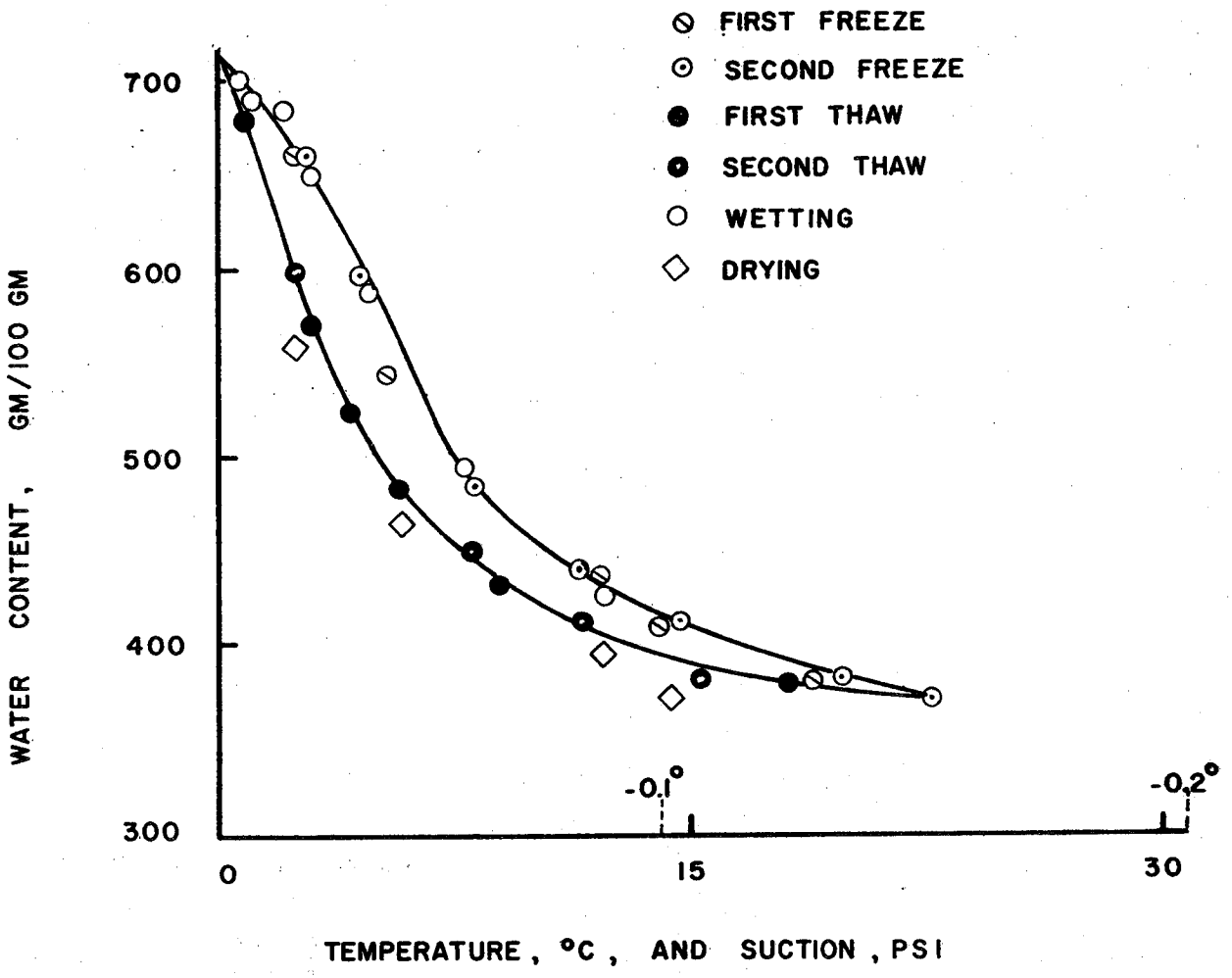

FIG. 15 - RELATIONSHIP BETWEEN WATER CONTENT AND SUCTION FOR FREEZING AND DRYING, THAWING AND WETTING (17)

This relationship was used to calculate the unfrozen moisture content for the base course materials tested. These moisture contents are shown in Table 4 with values obtained using the regression equations. The measured suction values during a freeze cycle were used in these regression equations to calculate a value of moisture content remaining unfrozen in the sample. The results of these calculations indicate a similarity between the two methods. Values obtained by Yong (27) show a better agreement with the regression values. Neither of the previous studies contained sufficient information to allow calculations, (for the low clay content base course materials) with the resolution provided by the regression equations. Since there appears to be a close correspondence between freeze-thaw and wet-dry activity, the mechanism involved in freeze-thaw may allow the problem to be studied under wetting and drying conditions, which are more easily controlled in the lab. This mechanism has been studied extensively and it may provide more insight into the freeze-thaw behavior of a granular material.

Utilizing suction as the measured quantity to predict thermal behavior this activity becomes quite predictable. When the freeze coefficient is plotted as a function of the as-compacted suction, Fig. 16 is the result. The shape of the curve is typical for all the materials tested. There is a maximum negative freeze coefficient which falls off to a lesser value for drier samples. The relative position of the curves for each compactive effort are inconclusive in predicting which compactive effort would produce the largest freeze coefficient. However, the effect of compactive effort on the relative position of the sample representing optimum moisture was quite conclusive.

TABLE 4. UNFROZEN MOISTURE CONTENTS

Sample No.	Yong (27)	Dillon & Andersland(9)	Regression
4		2.5	5.5
5		2.4	6.2
6B	3.8 to 5.8	2.2	5.2
6FS		1.6	0.6
6JD		2.7	2.1
7SA		2.2	2.9

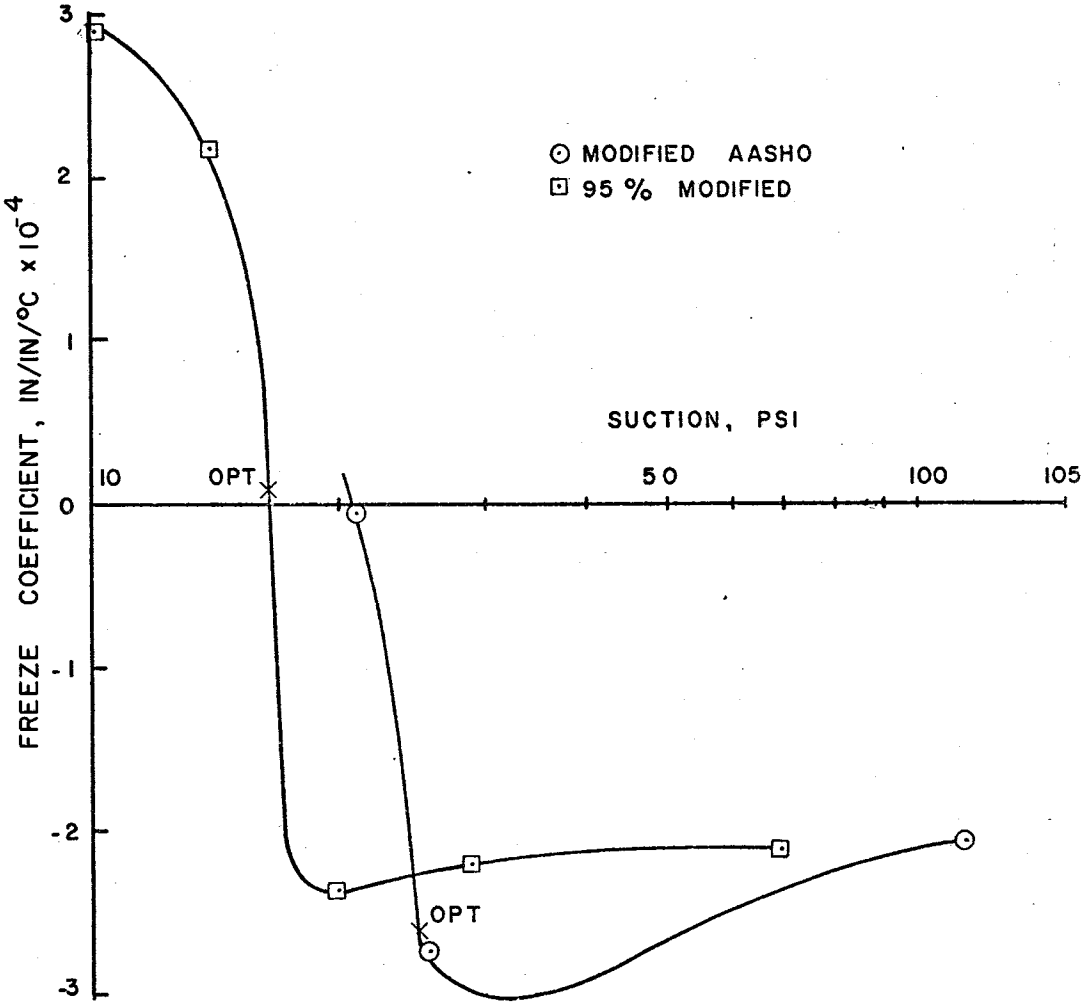

FIG. 16 - FREEZE COEFFICIENT AS A FUNCTION OF SUCTION FOR MATERIAL 4

The positions of optimum moisture content are indicated on Fig. 16 for material 4. For the larger compactive effort, modified AASHO, the optimum position was typically very near the point of maximum thermal activity and often on the dry side (higher suction). For the lower compaction effort, 95 percent of modified, the position of the optimum was shifted away from the area of maximum thermal activity, often into the area of freeze expansion. The suction at this point of maximum thermal activity is important when considered in light of the data collected from the field psychrometer installations mentioned earlier in chapter 1 (Fig. 5). Namely, that a typical base course ends up quite a bit dry of optimum moisture. Thus for the heavier compactive effort this drying will tend to have little effect on the thermal activity and may tend to decrease it as the sample is moved to the dry side of the maximum coefficient. For the lower compactive effort this drying will change the thermal activity causing it to assume a value very near the maximum. For most base courses then, the thermal activity will be a contraction upon freezing and will probably be near the maximum value for that material.

Suction can also predict the residual strain coefficient, B_1, which is shown in Fig. 17. The data shown here are typical of the data obtained for all materials. It is evident that increased compaction will produce less residual contraction for a given suction, and that in general, a difference in compaction effort does produce a different behavior in the residual strain.

The effect of suction on the residual strain is the opposite of its relationship with freeze strain. As the sample becomes drier the residual strain becomes less and eventually becomes an expansion.

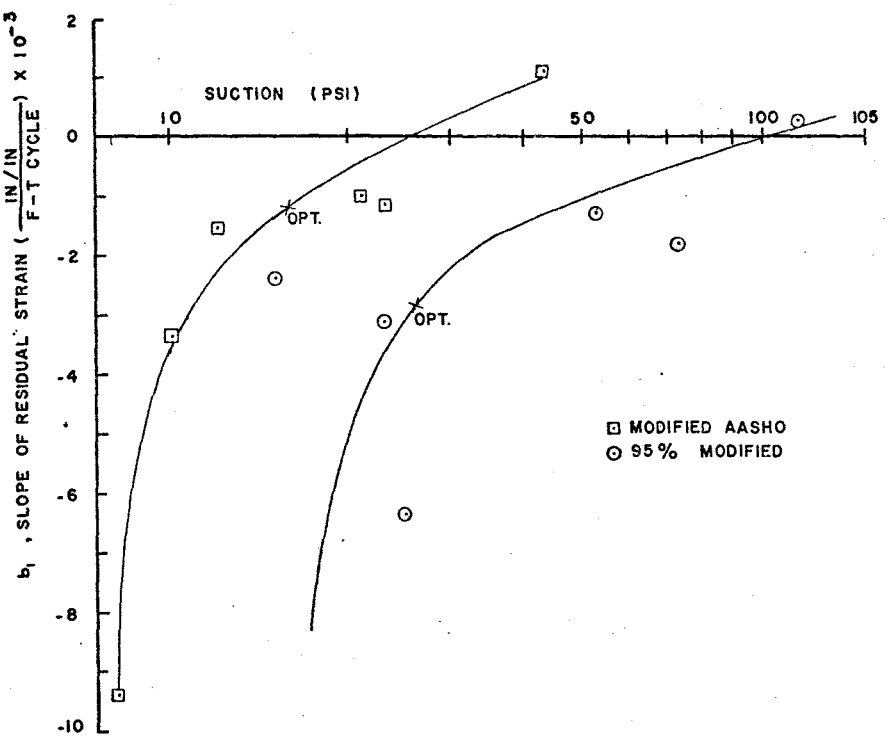

FIG. 17 - SLOPE OF RESIDUAL STRAIN VS. FREEZE-THAW CYCLES PLOTTED AGAINST SUCTION, MATERIAL 4

For the freeze strain the behavior became greater as the sample became drier. Thus, suction restrains residual behavior while enhancing freeze behavior, up to a point.

The data collected demonstrate that thermal activity can be predicted by knowing the suction of the material. Suction, in addition to providing the relationships just discussed, also provides insight into the physical process or the mechanism of the freeze-thaw activity of the material. Assuming the clay mineralogy and the moisture content do not change during a freeze-thaw cycle only the grain size, pore structure and distribution of ions are changeable to account for the noted variations in volume and in the suction during the freeze-thaw cycling.

The as-compacted suction can be utilized to predict an area of thermal activity although the maximum freeze coeffieient for any one type material cannot be inferred from the suction level. The compaction effort is extrememly important and combines with construction practices in influencing the thermal activity. The next chapter details the determination of a material property to allow a maximum value of freeze coefficient to be predicted while the suction freeze-relations established in this chapter provide a predictive capability over a range of suction extending from this point of maximum. As the grain size for the materials tested are nearly identical, the main variable between materials will be the clay mineralogy. This is the material property examined in the next chapter and related to the thermal activity.

CHAPTER IV

CLAY MINERALOGY INVESTIGATION

The moisture condition in a soil-aggregate system is a complex mechanism which is not yet fully understood. As such the connection and relationship with engineering phenomona has not been pursued. As stated, the nature of the problem of freezing soil dictates the necessity to examine the clay-water system as the basis for a mechanism of freeze-thaw damage in base course material.

A typical soil aggregate system is shown in Fig. 18. The three basic components are the soil, water and air. The soil must be considered as being composed of aggregate, silt, and clay with the clay being composed of different clay minerals. The water is composed of free water and adsorbed water which will depend on the type and amount of clay minerals. During freezing it is the interaction of the free and adsorbed water with the pore structure, formed mainly by the clay minerals, that is important.

The adsorbed water possesses a structure very different from that of the free water (12, 21). The structure of the clay particle surface and the water molecule are such that the water molecules are pulled into a preferred orientation. Hendricks and Jefferson (16) have suggested a concept that has found widespread acceptance. Water molecules are attracted to the surface of the clay mineral by a hydrogen-oxygen bond. This rotation of water molecule brings the remaining hydrogen atom into the plane of the oxygen atoms. This hydrogen atom is attracted to the oxygen atom of the next water molecule in that layer forming an hexagonal net of water molecules bonded to the clay surface. This net of water molecules would

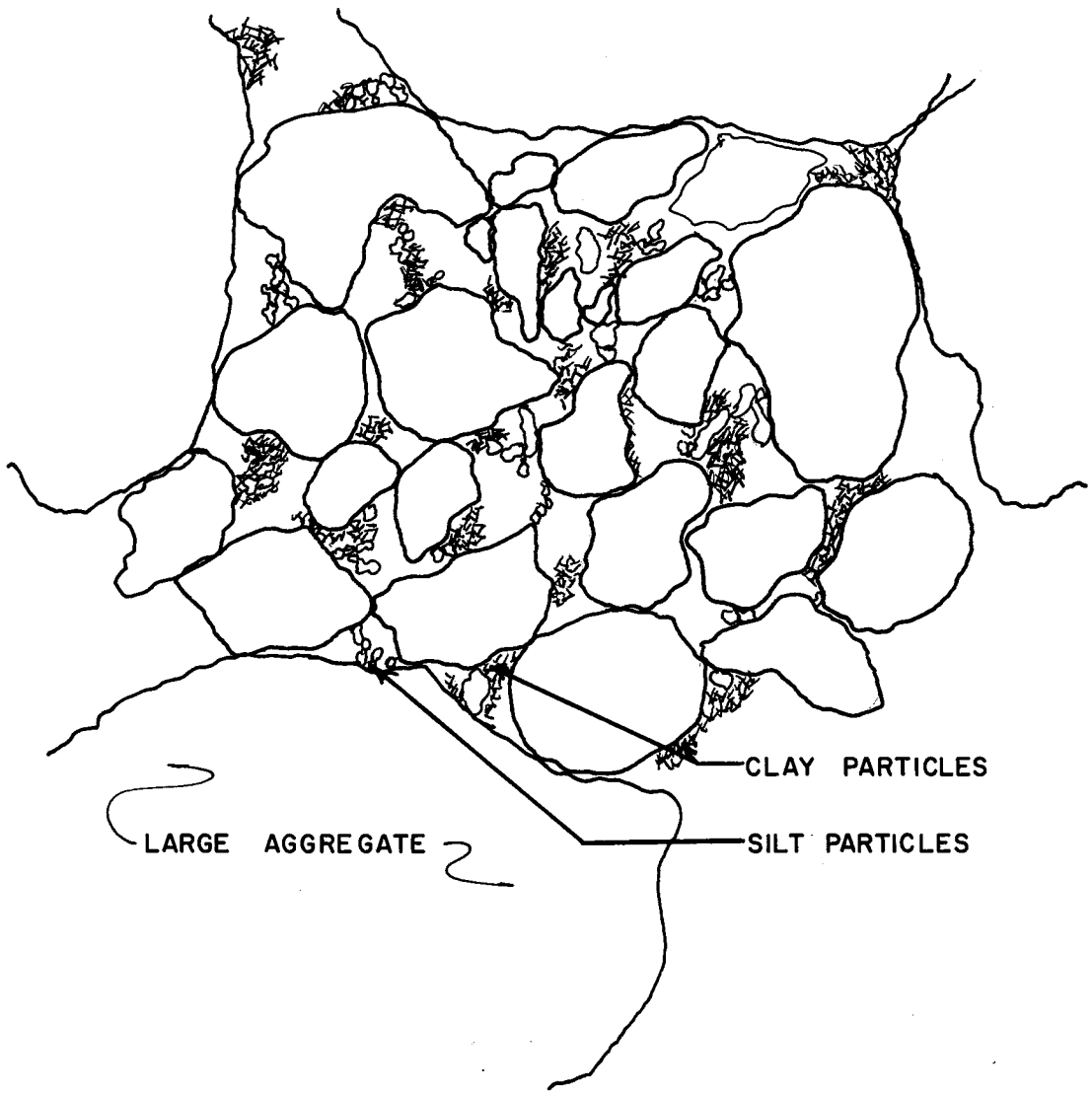

FIG. 18 - TYPICAL SOIL AGGREGATE SYSTEM

propagate itself away from the clay mineral with a structure that is essentially that of ice. A paper by Low and Lovell (21) discuss the nature of adsorbed water in more detail. However, this general idea of structured water is sufficient for this study.

When a soil-water system freezes the adsorbed water does not readily freeze and some free water held in very small pore spaces also does not freeze. As both the amount of adsorbed water and the pore structure are a function of the type and amount of clay minerals present the clay mineralogy may help relate unfrozen moisture to the thermal activity.

Clay Mineralogy.--The universally accepted method for determining what minerals are present is x-ray diffraction analysis. The seven base course samples were prepared according to a procedure established by Jackson and modified by Dixon (17) as shown in Appendix B. This procedure involves the removal of carbonates and organics by treatment with acid and hydrogen peroxide. The remaining particles are composed of the clay minerals and the sand and silt sized particles with all the carbonate material removed. This material is then separated into different size fractions to concentrate the clay minerals. The procedure for material preparation is included in this report since the procedure is critical to the analysis of the clay minerals prepared.

The amount of material in each size fraction is shown in Table 5. The amount of carbonate for these base course materials is quite high since the major constituent is limestone, a calcium carbonate. Very little organic matter was noted in any of the material examined. The amount of carbonates lost is equivalent for all of the base course materials except for material 6FS. This difference will be

TABLE 5. FRACTIONATION DATA

Material / Size fraction	4	5	6B	6JD	6FS	6BAR	7SA	F	B
75 µm *	8.7036	6.9051	7.8042	6.7461	0.3408	5.7269	9.0468	7.4454	3.3636
50-20 µm	0.7899	1.0462	1.8322	0.7869	0.3033	0.7515	1.5484	3.4939	6.0135
20-5 µm	0.5573	0.5259	1.1974	2.952	0.1643	0.7355	0.6161	2.3920	4.3128
5-2 µm	0.2363	0.3016	0.2413	0.2666	0.1005	0.1853	0.1766	0.6040	0.7937
2-0.2 µm	0.6450	0.5460	0.8440	0.3690	0.0542	1.3950	0.6710	1.3110	1.9830
<0.2 µm	0.5188	1.942	1.1260	1.0710	0.5340	1.0324	1.3110	6.0270	6.077
Total	11.4501	14.2698	13.0451	9.5348	1.4971	9.8266	13.3699	21.2603	22.5526
Original Amount	19.3792	25.5445	23.9225	24.7697	25.9052	23.5997	23.7316	22.5374	23.0866
% Recovery	58.10	44.12	54.53	38.49	5.78	41.64	56.34	94.30	97.73
% Clay #	10.0	22.0	15.2	15.0	39.2	24.7	14,8	34.6	35.6

*µm is the accepted symbology for a micrometer, 1 x 10^{-6} meters, approximately 3.94 x 10^{-5} inches

based on percent recovered, not on original amount of material used which contained large sizes, see Table 2.

discussed when the results for the material are presented subsequently.

Material 4 underwent more tests than the subsequent samples; and the data obtained for material 4 serve to show that the quantities obtained for the remaining materials are reasonably correct.

Material 4 underwent the following tests:

1. X-Ray Diffraction
   - A. 50-20 μm fraction
   - B. 20-5 μm fraction
   - C. 5-2 μm fraction
   - D. 2-0.2 μm fraction } CLAY SIZE FRACTIONS
   - E. <0.2 μm fraction }
2. Differential Thermal Analysis,
3. Cation Exchange Capacity Determination, and
4. Electron Microscope investigation

X-Ray Diffraction.--50 milligram samples of the two clay fractions were saturated separately with Potassium and Magnesium ions as set forth in Appendix B. Each sample was then treated with a 10 percent glycerin-water solution to expand clay minerals with expansible layers such as montmorillonite. These solutions were poured onto slides and allowed to dry. This gave them a preferred orientation which enhances the x-ray diffraction technique. The potassium saturated samples were dried on special Vikor slides. These slides are heat resistant as they will be heated to 500°C to collapse the montmorillonite.

The <0.2μm fraction is shown in Fig. 19. This series of x-ray diffraction patterns clearly show the collapse of montmorillonite into a 10 Å mineral spacing. The minerals present in these patterns include montmorillonite, mica, attapulgite, kaolinite, and possibly some quartz.

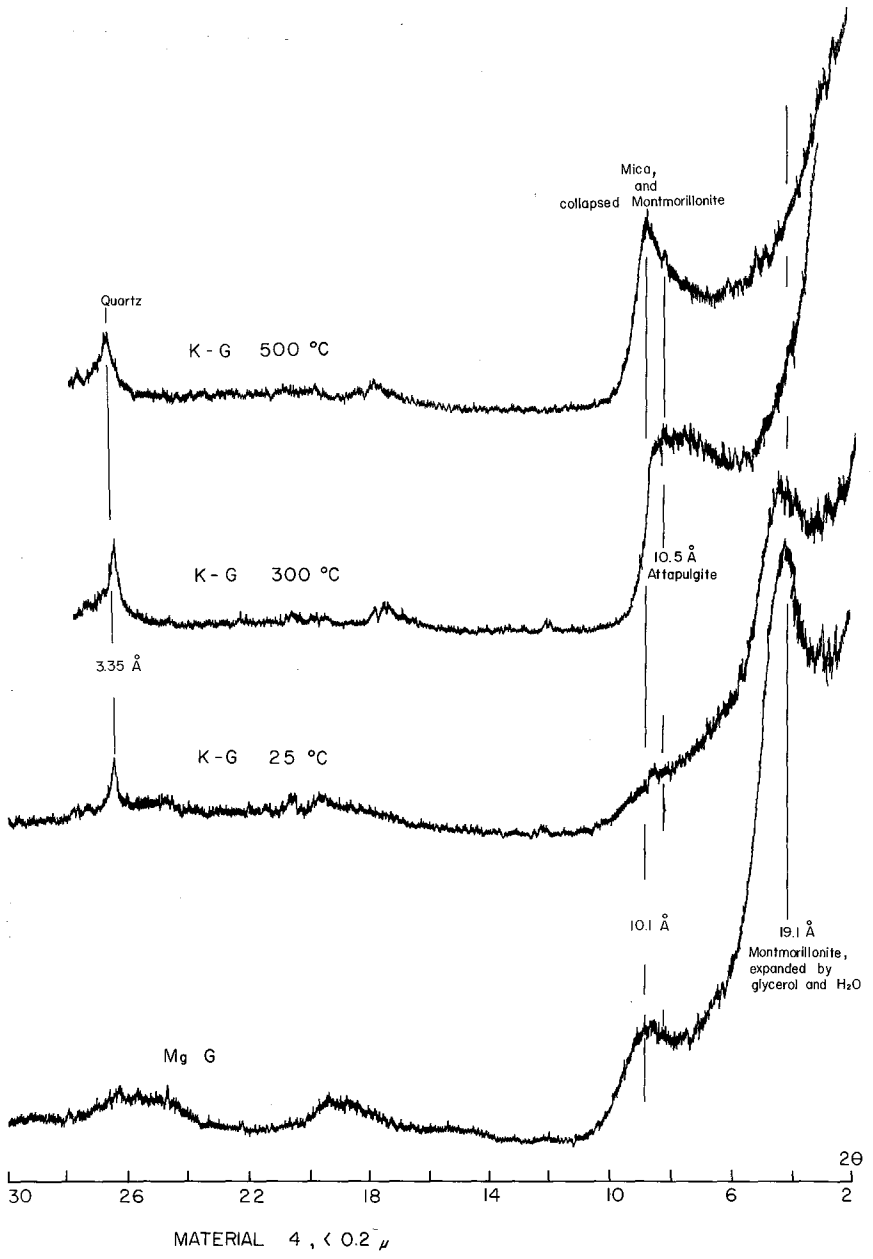

FIG. 19 - X-RAY DIFFRACTION PATTERN, < 0.2μm
FRACTION MATERIAL 4

The 2-0.2μ fraction is shown in Fig. 20. This series of x-ray diffraction patterns shows the same mineralogy as the finer <0.2μ fraction. It is felt that the fractionation procedure did not adequately separate the particle sizes. Montmorillonite is extremely fine sized and in all probability should not have shown up in the 2-0.2μ and larger fraction.

The 5-2μ fraction shown in Fig. 21 contains montmorillonite, quartz and some kaolinite as indicated. The 20-5μ fraction shows an increase in the quartz peak and an indication of feldspar. This is to be expected as these sizes are now into the sand and silt ranges. The 50-20μ fraction clearly indicates an extensive amount of quartz. Feldspars are indicated by the triplet of peaks near $28^{o}2\theta$. The study of the coarse sand sizes helps to show what minerals make up the entire structure of the material and give an insight into the weathering history of the material.

Differential Thermal Analysis.--The size fractions used in the differential thermal analysis (DTA) were prepared as indicated in Appendix B. They are magnesium saturated, dried, and ground to pass a #70 mesh sieve. DTA analysis involves heating a sample and an inert reference material in a furnace and comparing the temperature difference between the sample and the reference. The clay mineral sample will exhibit exothermic peaks, representing higher temperatures, and endothermic troughs, representing lower temperatures, which will be characteristic of each mineral, representing phase changes and moisture losses of varying energies.

The DTA curves for materials 4 are shown in Fig. 22. These curves present five major features which are:

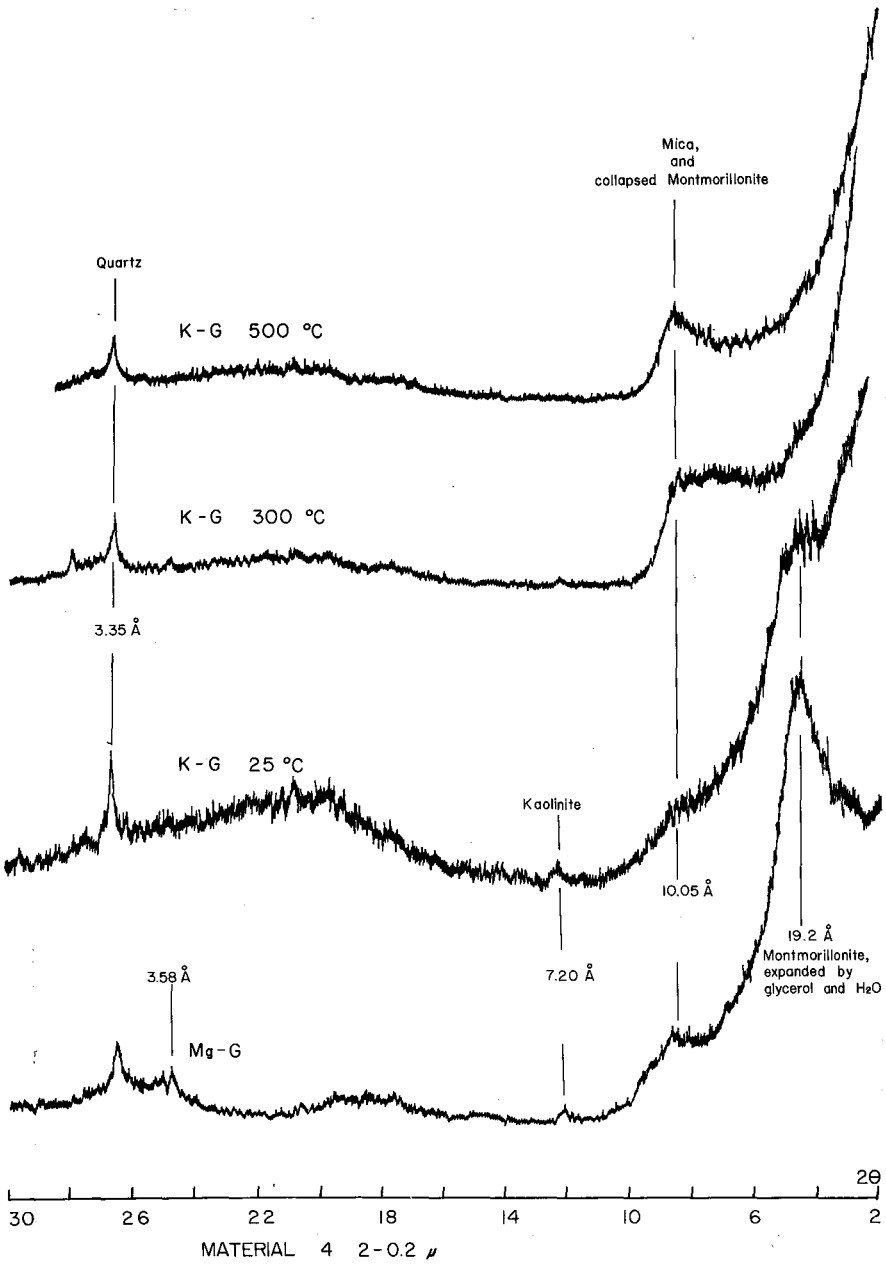

FIG. 20 - X-RAY DIFFRACTION PATTERNS, 2-0.2μm FRACTION MATERIAL 4

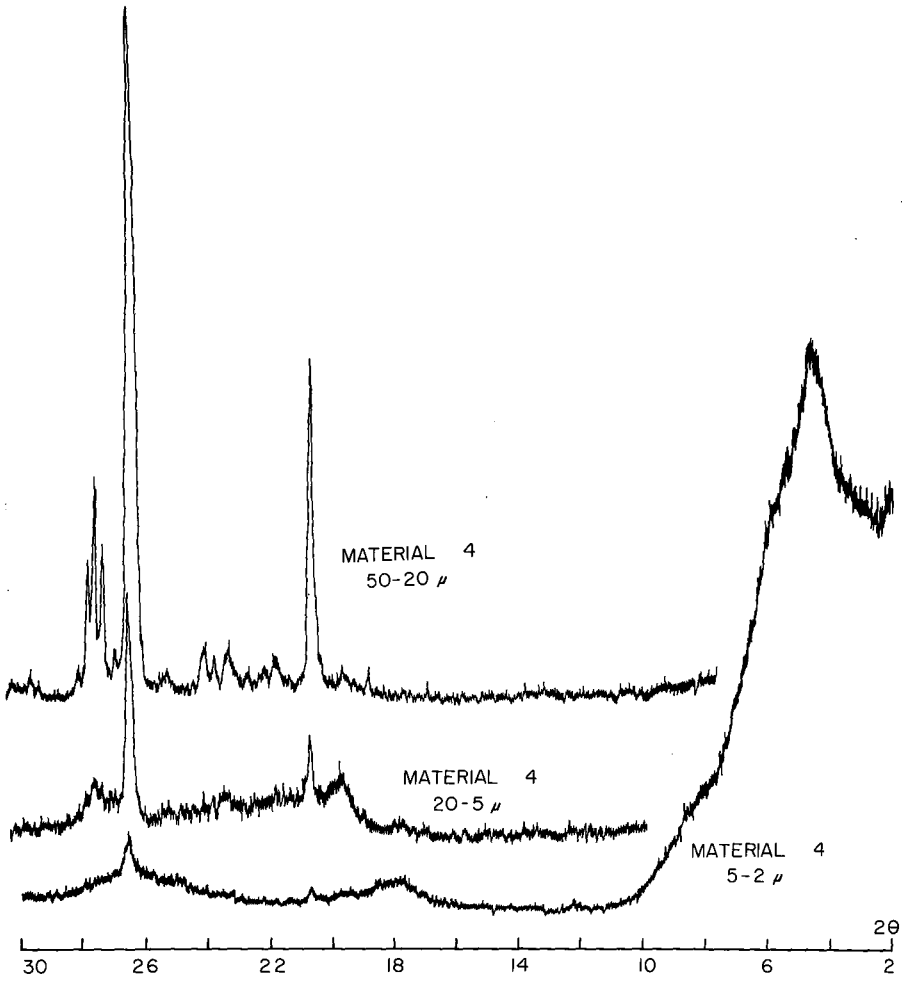

FIG. 21 - X-RAY DIFFRACTION PATTERNS FOR THE SILT AND SAND FRACTIONS, MATERIAL 4

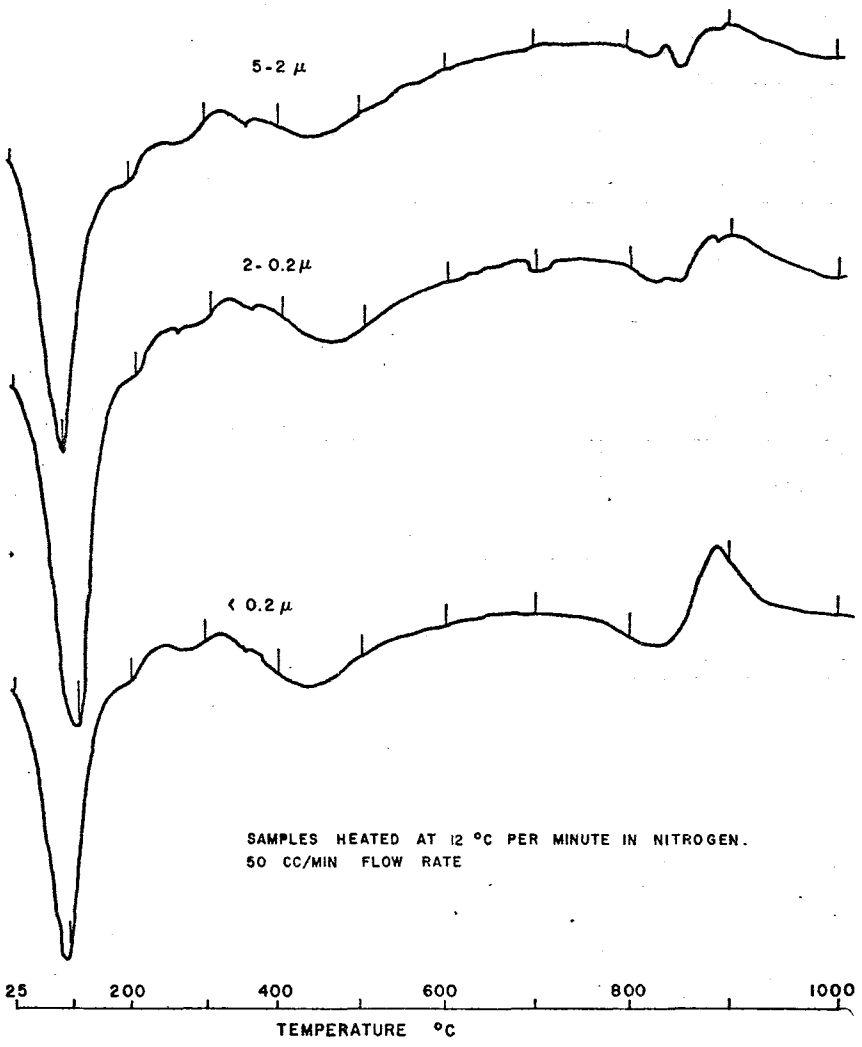

FIG. 22 - DTA CURVES FOR MATERIAL 4

1. Large endothermic trough below 100°C,
2. Endothermic trough around 450°C,
3. Slight endothermic trough near 840°C,
4. Exothermic peak just below 900°C, and
5. Indications of several slight sharp endothermic trough between 200°C and 350°C.

The large endothermic trough near 100°C is typical of montmorillonites and represents the loss of interlayer water. The loss of hydroxyl water is indicated by the trough between 450°C and 500°C. The difference in the temperature necessary to drive off the water is indicative of how tightly the water is being held. A standard DTA curve for montmorillonite is shown in Fig. 23.

Kaolinite exhibits only a sharp endothermic peak near 500°C. This peak influences the montmorillonite peak at 600°C by broadening it. This can be used as a quantitative tool as will be shown later.

Vermiculite gives a characteristic double or triple endo-thermic trough near 150°C to 200°C. The slight shoulder near 200°C could be indicative of vermiculite although no vermiculite was noted in the x-ray diffraction analysis. Mica will loose hydroxyl from 450°C to 650°C. This is usually all that will indicate the presence of Mica.

Attapulgite will demonstrate the feature listed as number 5 above. According to Bradley (3) water molecules in channel like interstices are lost below 100°C which indicates this water is rather loosely held, although held tighter than free water. There are additional endothermic reactions at about 225°C to 350°C and at 400°C to 525°C. Typical DTA curves for this mineral are shown in Fig. 24. They show similarities to the curves for material 4.

FIG. 23 - STANDARD DTA CURVE FOR MONTMORILLONITE

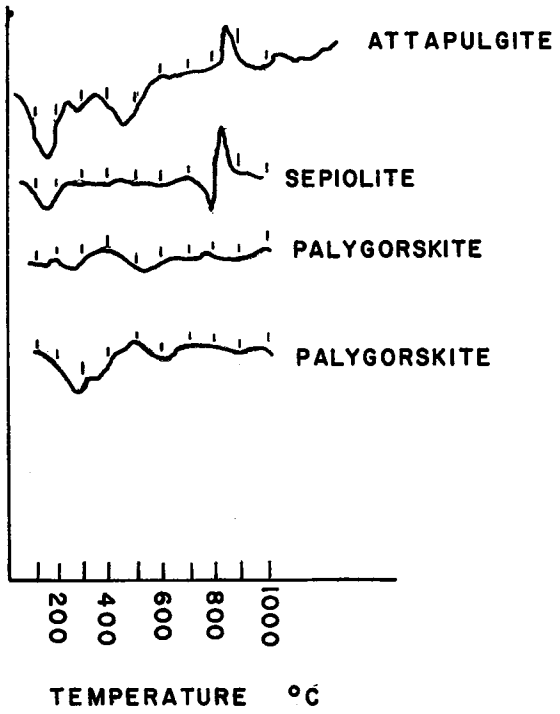

FIG. 24 - DTA CURVES FOR PALYGORSKITE-ATTAPULGITE (12)

Table II

Determination of K_m and V_{max}

Tube	Enz. (ml)	PO_4 Buffer (ml)	Substrate ONPG .0025M	Results: Absorbance 420 nm	Results: Total μ Moles NP/min	Results: $\frac{1}{V_o}$
1			0.0			
2	Selected by Students		0.2			
3			0.4			
4			0.6			
5			0.8			
6			1.0			

Table III

Determination of K_i for Lactose

Tube	Enz.	PO_4 Buffer (ml)	Substrate ONPG .0025M	Lactose (0.1 M)	Absorbance 420 nm	Total μ Moles NP/min	$\frac{1}{V_o}$
1	Selected by Students		0.0	0.5			
2			0.2	0.5			
3			0.4	0.5			
4			0.6	0.5			
5			0.8	0.5			
6			1.0	0.5			

1. Final volume in each tube must be 6.0 ml. Adjust enzyme and phosphate buffer volumes accordingly.

The percent of Kaolinite and montmorillinite in a sample may be very roughly estimated by comparing the area of the endothermic trough of the sample with the areas obtained by analyzing binary mixtures of kaolin and montmorillonite of known percentages. A standard curve is shown in Fig. 25. The ordinate represents the area under the endothermic curve from 350°C to 650°C. The areas for material 4 are given in Table 6. These data indicate the same information as the x-ray diffraction did, that is, montmorillonite is abundant compared to kaolinite. The actual percentages shown in Table 6 cannot be applied directly to the base course sample since they are composed of many minerals.

Table 6. Values Calculated From DTA Analysis for Percentages of Montmorillonite and Kaolinite.

Size Fraction μ	Area (mm^2)	% Kaolinite	% Montmorillonite
5-2	167	13	87
2-0.2	226	15	85
<0.2	390	0	100

Cation Exchange Capacity.--The different clay minerals each possess a rather well defined ability to sorb certain cations (or anions) and hold them in an exchangeable state. These cations will be replaced (exchanged) when the clay minerals are treated with solutions containing other cations. Typical values are listed in Table 7.

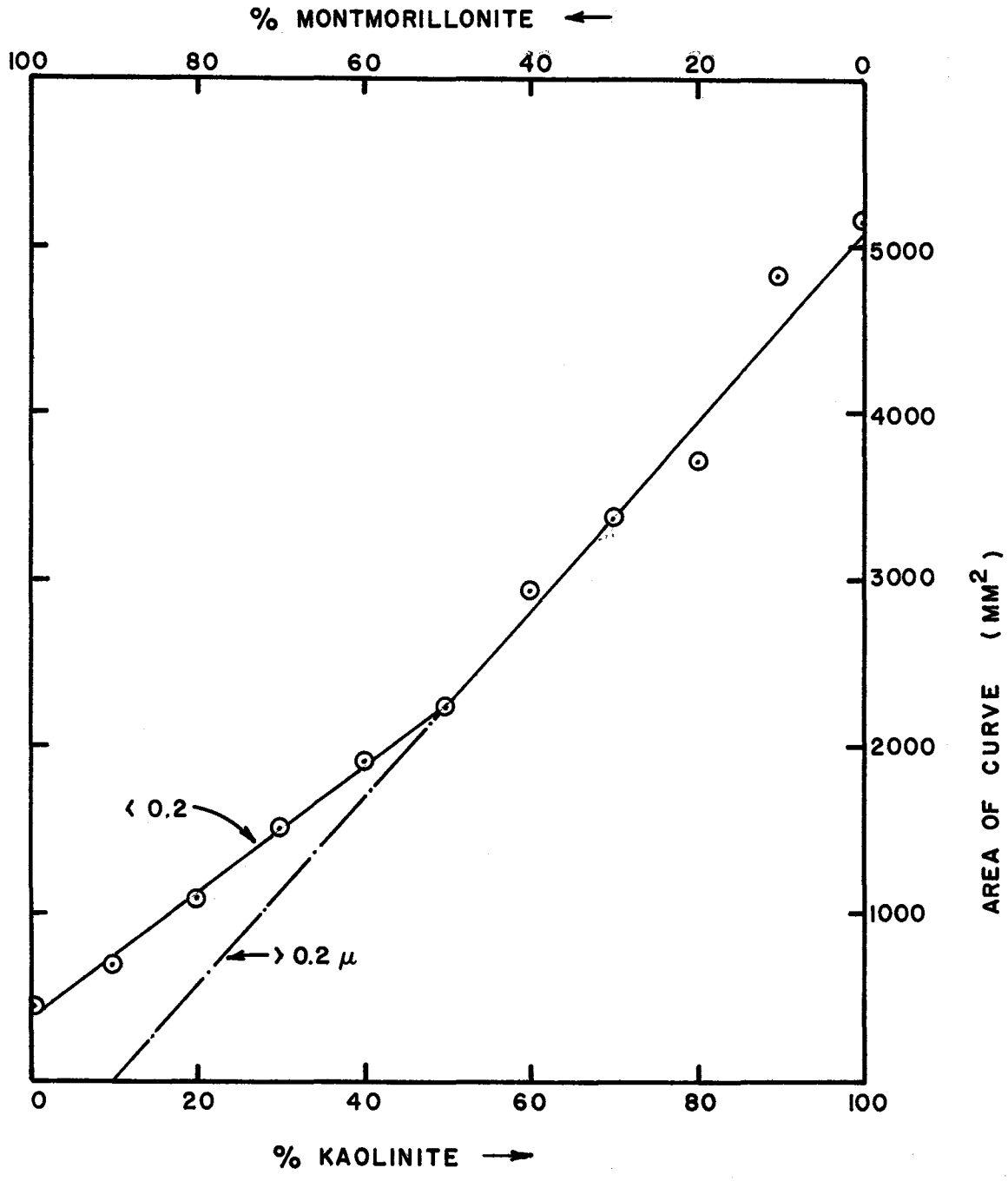

FIG. 25 - CURVES RELATING AMOUNTS OF KAOLINITE AND MONTMORILLONITE TO THE AREA IN THE DTA CURVE FOR THE ENDOTHERMIC PEAK AT 500°C

Table 7. Typical Values of Cation Exchange Capacity

	Meq/100gm
Kaolinite	5-10
Montmorillonite	110
Mica (Illite)	20
Vermiculite	15
Chlorite	10-46
Sepiolite	3-15
Attapulagite	3-15
Palygorskite	3-15

Knowing which minerals are present in the sample and a rough estimate of the percentage of several of them, the remaining minerals may be estimated when the Cation Exchange Capacity of the sample is known. The CEC determination was conducted on the two clay size fractions according to the procedure given in Appendix B. The data for material 4 are given in Table 8.

Table 8. Cation Exchange Capacity Data, Material 4

Size μm	Atomic Absorption Reading	CEC (meq/100gm)	Average
2-0.2	7.8 8.1	29.1 26.8	28.0
<0.2	11.9 12.6	76.6 78.2	77.4

From these data mineral estimates for montmorillonite and kaloinite may be obtained. Mica and attapulgite may be estimated together as they have essentially the same CEC. The estimates obtained from this analysis are presented in Table 9.

Table 9. Mineral Estimates From Cation Exchange Capacity Determination

Mineral	Size Fraction (μm)	Percentage	Total	
Quartz	2-0.2	10	5.5	
	<0.2	0		
Kaolinte	2-0.2	15	12.8	
	<0.2	10		
Montmorillonite	2-0.2	14	38.5	
	<0.2	69		
Mica	2-0.2	61	43.2	11.0
Attapulgite	<0.2	21		32.2

The estimates for montmorillonite and kaolinite are in general agreement with the values obtained from the DTA analysis.

Quantative Data From X-ray Diffraction Data.--Jackson, et al.,(19). have shown that reasonable estimates of mineral percentages may be obtained from x-ray diffraction data through comparison of the peak intensities. To do this, however, it is necessary to have several hundred diffraction patterns of laboratory prepared samples of known percentages of the minerals believed to be present. These percentages are based on the weathering scheme presented by Jackson (18). This scheme is shown in Fig. 26. The assumption made is that minerals weathered in place from parent materials will give a normal distribution of the percentages of the minerals in the material. As weathering

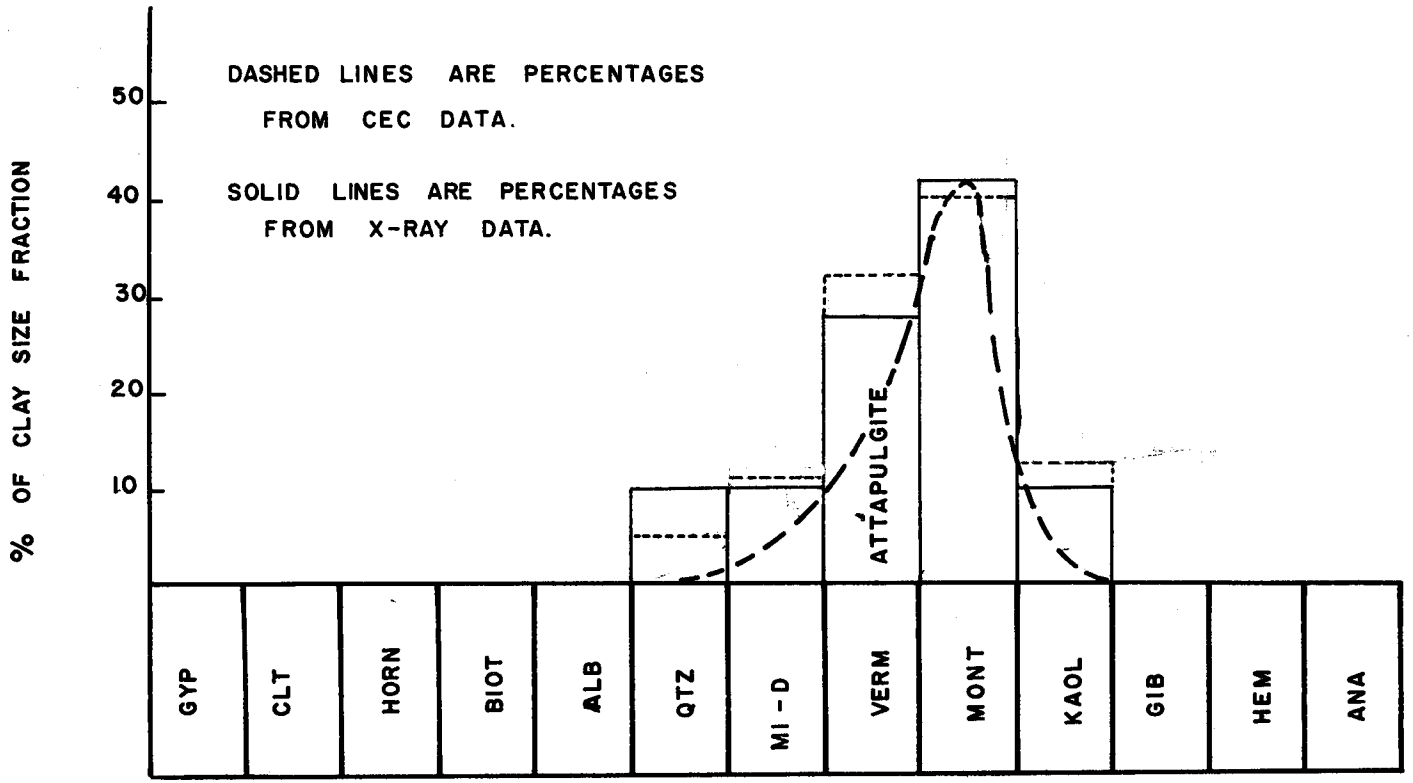

FIG. 26 - MINERAL ESTIMATES PLOTTED ON JACKSON'S WEATHERING SCHEME

proceeds, minerals that are higher in the scale (gypsum, chlorite, hornblende) will be gradually transformed by chemical weathering through biotite, albanite, quartz, mica, vermiculite (attapulgite included), montmorillonite, kaolinite, and gibbsite to the hardest and least soluble minerals hematite and anatase. The percentages of minerals obtained by the CEC analysis are plotted on Fig. 26 along with the results obtained by x-ray diffraction. It is apparent that a normal distribution is roughly approximated and for this reason it is felt that the mineral estimates are correct and that similar materials should yield similar results

The analysis of x-ray diffraction data was conducted on the slides prepared by magnesium saturation and glycerol solvation for all materials. The steps involved may be outlined as follows:

1. Obtain values for peak intensities of the major identification peaks.
2. Calculate percentages of total intensities.
3. Correct percentages based on the relative amount of each size fraction.
4. Plot estimated percentages of minerals on the weathering scheme to verify a normal distribution.

The percentages for material 4 from x-ray diffraction data are shown in Table 10.

Table 10. Mineral Estimates for Material 4 From X-ray Diffraction

Mineral	Intensity	Percentage	Size Fraction μm	Corrected % Total Clay Size
Montmorillonite	42 50	14 69	2-0.2 <0.2	38.8
Mica	6.9 12.7	33.5 8	2-0.2 <0.2	20.0

Table 10. Mineral Estimates for Material 4 From X-ray Diffraction. (con't)

Mineral	Intensity	Percentage	Size Fraction μm	Corrected % Total Clay Size
Attapulgite	5.6	27.5	2-0.2	20.7
	10.2	7.0	<0.2	
Kaolinite	3.2	15.0	2-0.2	10.5
	1.8	5.0	<0.2	
Quartz	10.0	10.0	2-0.2	10.0
	8.0	10.0	<0.2	

These percentages are only slightly different from those calculated from the cation exchange capacity data. These differences are within experimental error and within tolerances for the analysis to be done in this study. From these data it is felt that the x-ray diffraction data will yield values substantially accurate enough to allow the percentages to be indicative of the material. Since the materials in this study are composed of essentially the same minerals errors should be minimized.

Remaining Materials.--The remaining materials were prepared similarly to material 4. Both potassium and magnesium saturated samples were prepared in the event it became necessary to determine the presence of minerals such as chlorite or vermiculite which require the heating process. The diffraction patterns for these samples indicated that the separation of the sizes was more complete than that attained for the first separation of material 4. As an example, quartz did not appear in the <0.2μ fraction and montmorillonite did not appear in the 2-0.2μ fraction as much as it did in material 4. For this reason the percentage estimated from these diffraction patterns should be at least as good or better than those obtained for material 4. The x-ray diffraction

data for each material are presented in Appendix C.

Relation of Clay Mineralogy to Thermal Activity.--The next question which must be considered is how to relate the clay mineralogy just determined to the thermal activity, determined earlier. Throughout the analysis the quantities which demonstrated the closest relationship to the thermal behavior were the volumetric moisture content and the suction. These quantities are indicative of the clay mineralogy, the size of the particles and their arrangement (pore structure). Of the properties readily available for the clay minerals the only quantity which can be quantified and related logically to the thermal activity is the specific surface area for the clay minerals.

The laboratory determination of the specific surface area of clay minerals is extremely inconsistent and highly dependent on the technique used. One technique that has found wide acceptance is the Brunauer, Emmett, and Teller method (BET) (5). Typical values determined by this method are given in Table 11. These values will be used in the calculation

Table 11. Typical Values of Specific Surface Area (5)

Mineral	Specific Surface Area ($meter^2/gram$)
Attapulgite	140
Mica (Illite)	113
Kaolinite	22
Montmorillonite	82

of the specific surface area of each materials' clay fraction. These values represent laboratory test data and as such are very different from the theoretical values which have been calculated from the

dimensions of the crystalline structure. The major difference between theory and measurement arises with montmorillonite for which theoretical values of specific surface are a typically run 800 meters^2/gram. The much lower value in Table 11 means that the major part of the potential surface of the mineral could not be reached by the penetrating liquid or gas. Since the total surface cannot be reached in the laboratory it may be inferred that the surface of the montmorillonite will not be fully utilized by the moisture in compacted samples. For this reason it is felt that the laboratory determined values for the specific surface area would better represent field behavior than the theoretical values. The specific surface area for the quartz would be 29 m^2/gm to represent the larger size present in the size fraction.

The values of the specific surface area for the clay fraction in each material were calculated based on the amount of each mineral present. The values thus calculated are presented in Table 12.

Table 12. Specific Surface Areas of the Clay Fraction for Material Tested

Material	Specific Surface Area M^2/gm
4	92.5
5	86.2
6B	79.2
6JD	97.2
6FS	59.5
6BAR	83.1
7SA	79.4

The next problem that arises concerns how these data may be related to the thermal activity of the material. The clay fraction represents only a minor portion of the total material. Nearly fifty percent of the material was lost due to removal of the carbonates. The values given earlier for the percentage of clay are based on the amount recovered, thus, there are several possibilities for comparison which must be examined. These are as follows:

1. Thermal Activity vs. Percent Clay
    a. based on total amount
    b. based on recovered amount
2. Thermal Activity vs. Specific Surface Area
    a. no correction for percent clay
    b. corrected for varying amount of clay

Of these relationships only the specific surface area of the clay fraction with no correction whatsoever, demonstrated a consistent relationship. These data are shown in Fig. 27 with the corresponding values of the freeze coefficient.

This relationship indicates that the amount of -#200 material and likewise the amount of clay present, within the limits examined for the materials in this study, will not affect the freeze-thaw behavior of the base course. The type of clay minerals and the amount of each present do affect the thermal activity in a consistent manner which allows the maximum freeze coefficient to be predicted through a study of the clay mineralogy.

There was a very narrow range in percent fines (-#200) of all the base courses studied. It ranged from a high of 10% to a low of 9%. Greater thermal activity would be expected of base courses with a higher percentage of fines.

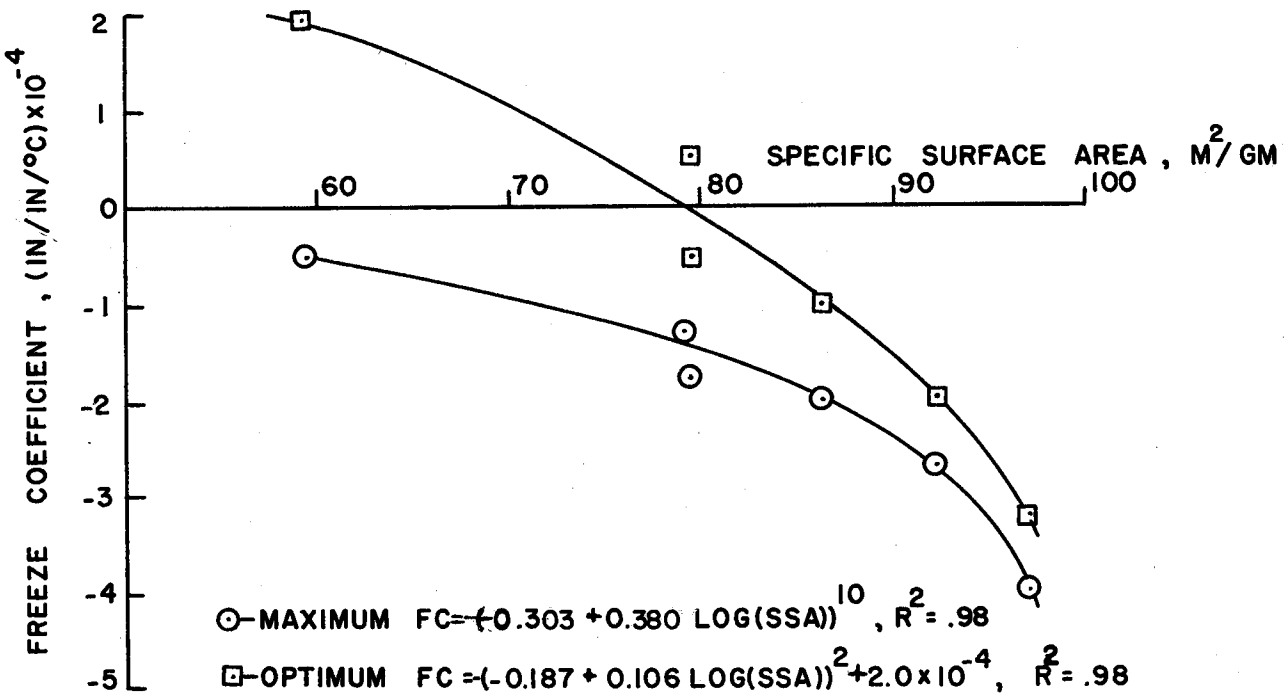

FIG. 27 -FREEZE COEFFICIENT AS A FUNCTION OF SPECIFIC SURFACE AREA FOR MAXIMUM VALUE AND OPTIMUM MOISTURE VALUE WITH REGRESSION EQUATION, [MODIFIED AASHO COMPACTION]

Importance of Mineralogy.--The basic makeup of the clay minerals in the samples of base course material appears to be large percentages of montmorillonite and attapulgite with lesser percentages of mica, kaolinite, and quartz. The properties of montmorillonite are well documented and nearly all highway engineers are aware of the consequences involved when montmorillonite is present, the most noticeable factor being the high volume change upon the addition of moisture. Another important factor in relation to freeze-thaw is the rate at which this water is absorbed. Although montmorillonite has a high potential for moisture it takes relatively longer for the particles to absorb this water due to their extremely small size which renders interior particles relatively inaccessible.

This phenomenon is illustrated in Fig. 38 for several clay minerals (26). These data show that sodium montmorillonite, which is indicated in the material tested, has the ability to attract a large amount of water; but the time necessary to reach comparable states of consistency, liquid limit or plastic limit, is nearly 20 to 1,000 times greater than attapulgite, the other major mineral. The speed and ease with which a mineral absorbs water is directly related to the structure. Attapulgite has a fibrous structure with channels running along the axis of the fiber as is shown in Fig. 29 which is a transmission electron micrograph of the clay fraction of material 4. Water is loosely held in these channels, tighter than free water, but not as tight as an adsorbed water layer.

Attapulgite will thus attract more water quicker and will hold this water tighter than free water. Thus, the montmorillonite will take even longer to attract moisture as the water added will be held by the fibrous

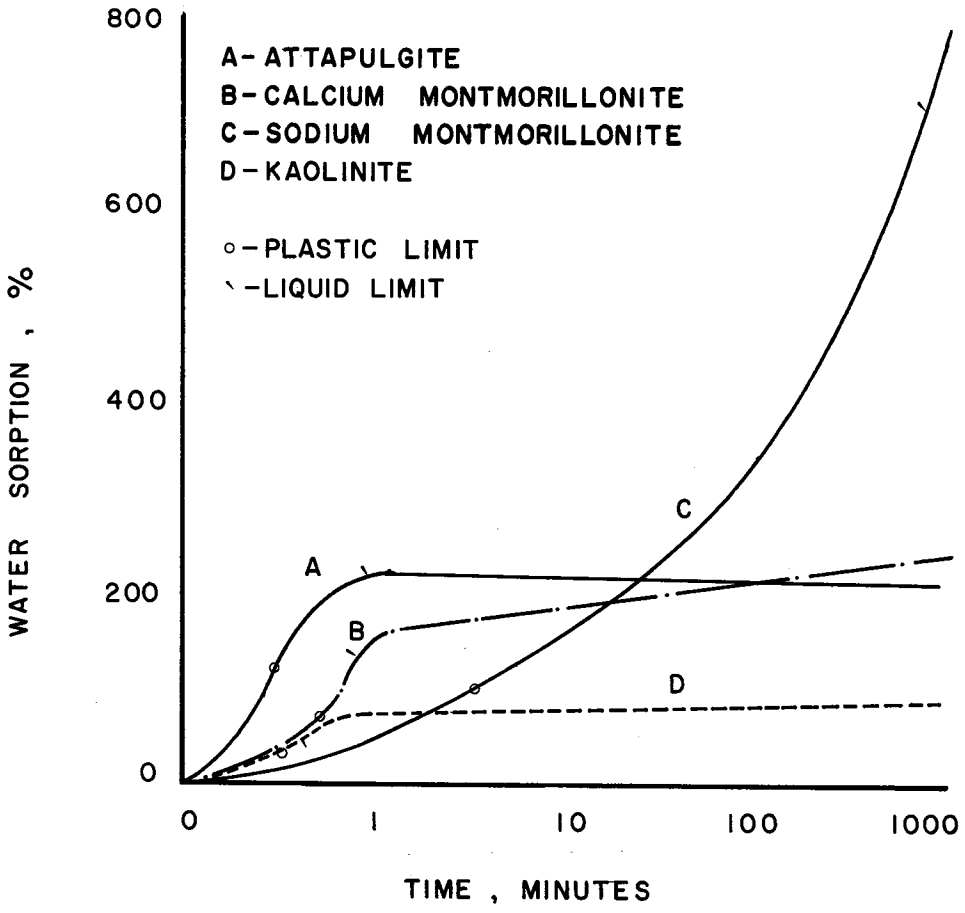

FIG. 28 — WATER SORPTION CURVES FOR SEVERAL CLAY MINERALS (26)

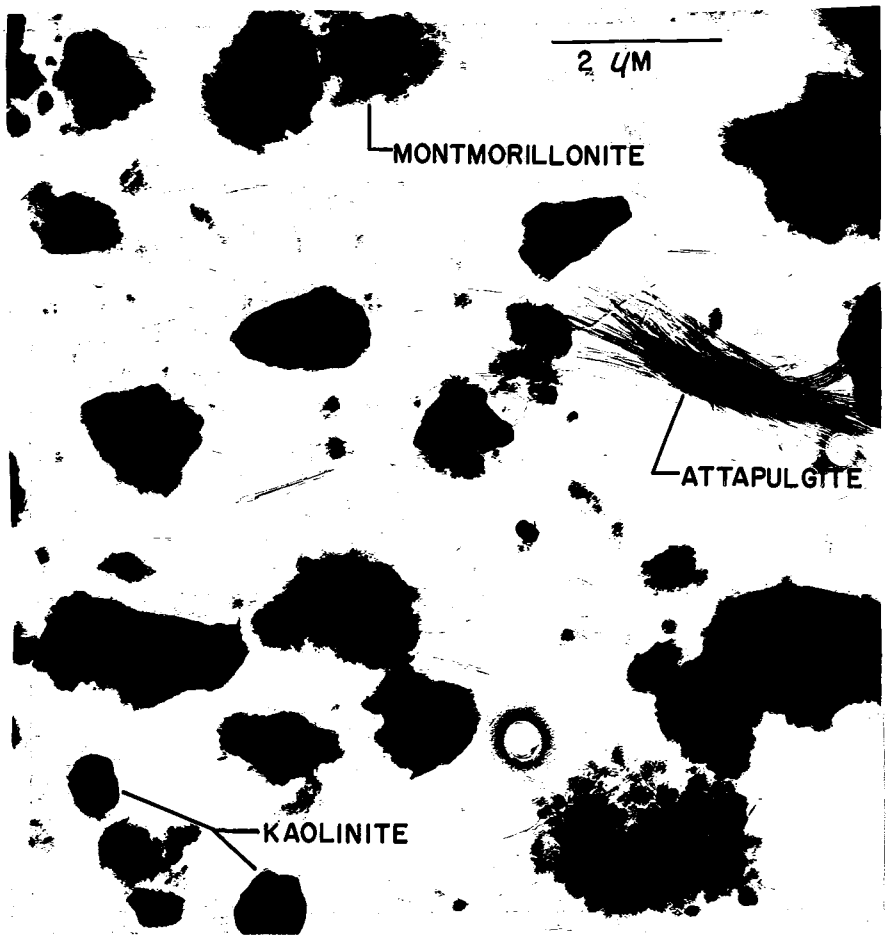

FIG. 29 - ELECTRON MICROGRAPH OF MATERIAL #4 SHOWING VARIOUS CLAY MINERALS PRESENT

metal plate

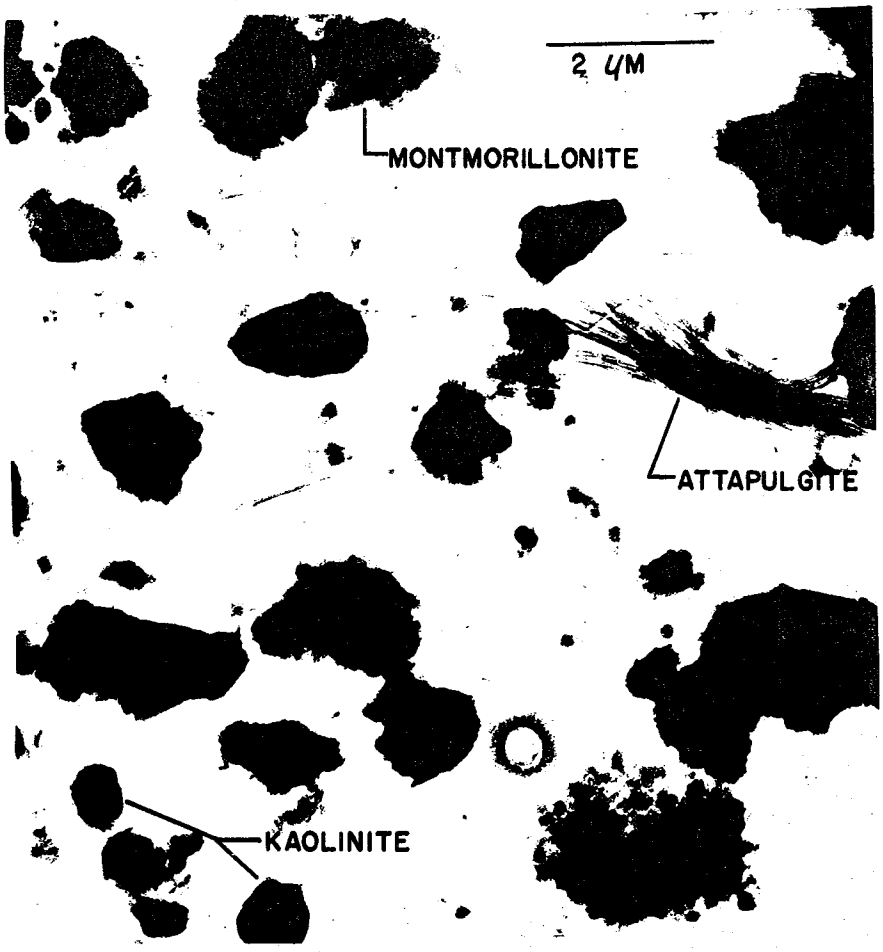

FIG. 29 - ELECTRON MICROGRAPH OF MATERIAL #4 SHOWING VARIOUS CLAY MINERALS PRESENT

attapulgite. Thus moisture influence on freeze-thaw activity will be directly influenced by the amount of attapulgite present more so than the amount of montmorillonite. This was borne out in the calculations of specific surface area which showed attapulgite to have a high and readily accessible surface area. Thus, a study of clay mineralogy, through x-ray diffraction as a simple expedient, and clay properties gives insight into the thermal behavior of a material. As such it presents a powerful tool currently not being used outside of research. It's use in a design procedure is warranted by the data in this report.

CHAPTER V

ANALYSIS OF DATA AND OBSERVED RELATIONSHIPS: CONCLUSIONS AND RECOMMENDATIONS

General.--The area of investigation, west Texas, contains extensive transverse cracking that cannot be explained through the normal considerations of low-temperature or thermal-fatigue cracking of the asphaltic concrete surface layer. The mechanism of shrinkage cracking of the base course resulting from suction gradients set up by the subgrade is a valid mechanism and may be acting in certain cases. Limited data collected, however, indicate that common construction procedures may produce a considerably drier base course, thus ruling out this mechanism in most pavement structures.

A dry base course of limited thickness and water content placed over a semi-infinite subgrade means that the subgrade will serve to control the level of suction in the base course. If the subgrade is clayey it will assume a relatively high suction. The base course will attempt to draw water from the subgrade as it is still at a higher suction potential. The water transfer will be small due to the high equilibrium suction level in the subgrade. A silty subgrade, which would have a lower suction level, would allow the base course easier access to the moisture, causing a relatively larger transfer of water. The subgrade can be seen to in effect 'tune' the base course by determining the amount of water the base course obtains to lower the suction level. As was noted previously, the suction level can be used to indicate the thermal activity of the base course material.

Thermal Activity.--The base course materials tested in this study demonstrated quite vividly that the base course in a pavement possesses thermal activity. This thermal activity varied with material and

compactive effort. The major relationships showed essentially that the drier a material, the greater the freeze strain and the less the residual strain. Increased compactive effort increased the freeze strain while decreasing the residual strain, when considering similar samples.

The lower compactive effort produced a relationship that was more unstable as slight changes in moisture would cause large changes in the thermal activity. This was not true for the samples compacted with the higher compactive effort. Thus, the effect of the subgrade would have a pronounced effect on the behavior of a base course produced with a light compactive effort. This effect, however, is such that the thermal activity is decreased as the base course absorbs water. Thus, for lighter compactive efforts the thermal activity is very unpredictable. For the heavier compactive effort the thermal activity is greater but it is more stable and predictable.

The importance of the clay mineralogy of the base course in influencing thermal activity was shown in the relationships obtained for the specific surface area. This relationship indicates that the finer the particle distribution, the larger the specific surface area, the greater the thermal activity; although the amount of clay did not relate to the thermal activity, the variation in clay content for the materials tested was not sufficient to form a relationship of these variables. Since most base course materials will have an amount of fines similar to the materials tested in this report the relationship for the specific surface area should be a valid predictive tool for most base course materials composed of untreated "caliche" and be indicative of the behavior of other granular materials.

The relationships formed with the suction further emphasize the importance of the particle size. Suction is highly influenced by the surface area exposed to the free water. For a given amount of water the higher the surface area the higher the suction since more of the water will become adsorbed water on the surface of the clay minerals. This decreases the amount of free water, which decreases the menisci radii, increasing the suction in the sample. These considerations are extremely important in formulating the mechanism to relate the data obtained.

Proposed Mechanism for Contraction Volume Change.--The importance of the moisture state and its relation to thermal activity has been established. The importance of the pore structure and size can be inferred from the clay mineralogy data. These quantities can be combined to formulate a mechanism to describe the observed behavior; and which manifest themselves in a loss of load carrying ability after freeze-thaw activity.

As the material freezes the suction increases due to the loss of free water as it becomes ice. The adsorbed water and the water held in extremely fine pores will not freeze. As more and more water freezes the menisci of the remaining water will become smaller while serving to increase the suction in the material. This action also serves to exert greater and greater tensile forces in the menisci. These forces will tend to pull the particles surrounded by the adsorbed water into closer contact which lessens the available surface area and makes more free water available for freezing. This action continues to the point where lowering the temperature further cannot freeze any adsorbed water or the water held in the extremely fine pore spaces. This action explains the behavior noted earlier where

the samples exhibited nearly all their thermal activity in the temperature range of $0^{o}C$ to $-6.8^{o}C$.

This freezing action leaves the clay particles pulled together with little more than their film of adsorbed water surrounding them. As this water layer is highly ordered, as previously discussed, the particle arrangement in this frozen state would be such that the parallel faces of the clay minerals would align. This configuration is likely, even though the preferred particle attraction is edge to face, since the surface tension forces increase on freezing and the particle attraction forces decrease (27).

As a material thaws the ice in the larger voids will thaw first and the smaller voids will thaw last. This results in a general redistribution of water away from the finer particles, the clay minerals. Once the material is thawed the clay minerals will attempt to assume the position they had originally with the preferred edge to face relationship. Although more free water has been made available it has been made available to the larger particles leaving the clay minerals in the compacted form held together by the adsorbed water film. The tensile forces exerted by this water film will not allow the particles to separate completely thus causing the non-recoverable strain. Some proof of this may be adduced from the fact that there is more non-recoverable strain in the wetter more dispersed soil structure than in the dispersed soils just dry of optimum. This produces larger packets of clay minerals with an increased distribution of larger voids produced by the rearrangement.

This open or honeycombed structure accounts for the noted decrease in load carrying ability following freeze-thaw activity. The decrease in the suction, upon thawing, to a value below that of

the original, as-compacted value is caused by the increase in free water resulting from the decrease in surface area as the clay particles rearranged themselves into tighter groups. This rearrangement of particles continues for each freeze-thaw cycle until an optimum state is attained where the clay particles do not undergo any further rearrangement. This is indicated in studies which measured the effect of freeze-thaw cylces on the viscoelastic characteristics of a clay material (22). Their results indicate that after nine freeze-thaw cycles there is negligible change in the viscoelastic properties. A typical result is shown in Fig. 30 for the creep modulus. This is important in relation to the proposed mechanism since moisture is the major variable influencing viscoelastic behavior of soils (7). It is apparent that the moisture state and particle orientation reach an equilbrium position with an overall volume decrease for both freeze and residual strain.

This mechanism explains the behavior of the samples tested which fall near optimum moisture. For samples extremely wet or dry the behavior changes drastically. For a dry sample the residual strain becomes expansive and for a wet sample the freeze strain becomes positive. This phenomenon relates directly to the moisture state and the pore structure as shown in Fig. 31. As these are already forced into a parallel orientation by compacting wet of optimum the resulting freeze contraction upon freezing will be masked by the expansive property of the water as the samples are very nearly saturated. The residual volume change, a decrease in this case, is apparent when the material thaws and the effect of the ice is removed.

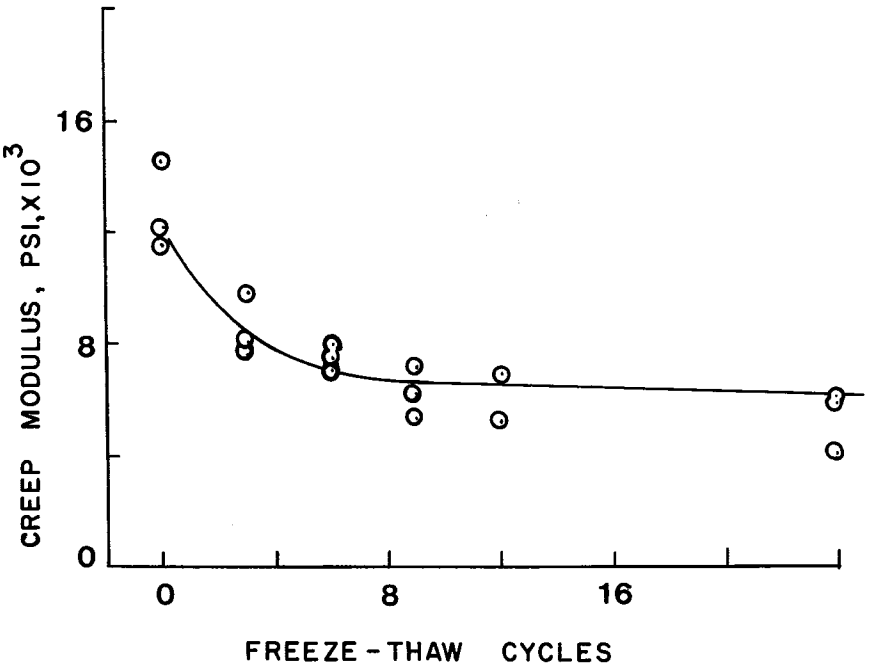

FIG. 30 - CREEP MODULUS VERSUS NUMBER OF FREEZE-THAW CYCLES (22)

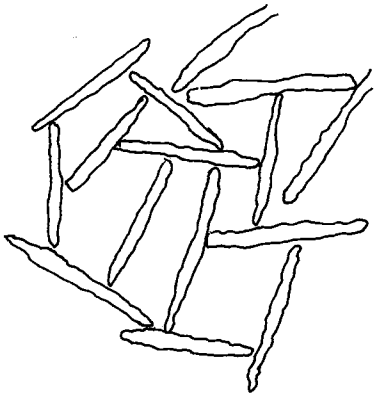

FLOCCULATED STRUCTURE

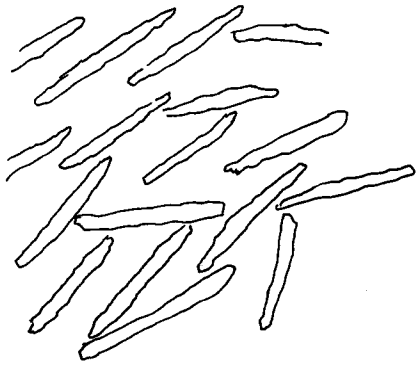

DISPERSED STRUCTURE

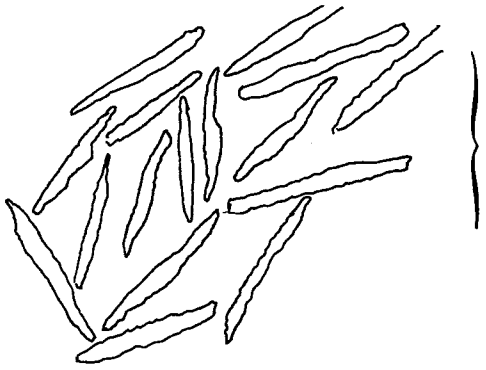

STRUCTURE PRODUCED BY FREEZING, SIMILAR FOR BOTH STRUCTURES, A MORE DISPERSED ORIENTATION.

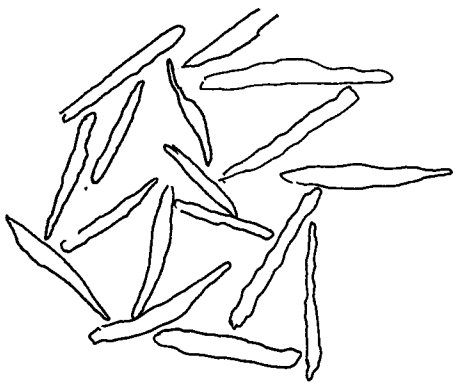

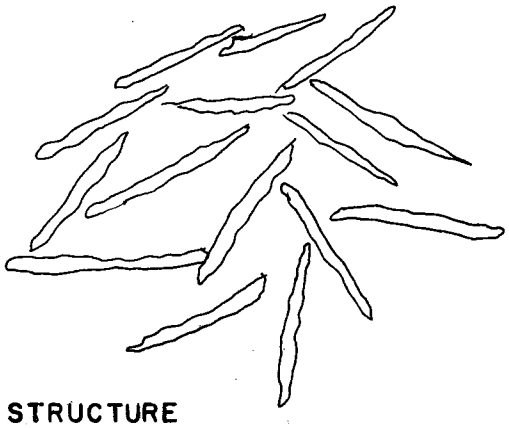

THAWED STRUCTURE

FIG. 31 - PARTICLE STRUCTURE FORMED DURING COMPACTION AND THE PROPOSED REORIENTATION DUE TO FREEZE-THAW

Compaction dry of optimum, however, produces a flocculated structure which is also shown in Fig. 31. As the material becomes drier the structure becomes more flocculated due to the decreasing amount of water available. With decreasing moisture, continuity of adsorbed water films is lost. This loss of continuity serves to explain the decrease and levelling off of freeze strain for the drier samples. With this lack of moisture continuity the particles will not be pulled irreversibly into parallel orientation and the edge to face orientation will persist, bringing about substantially reduced residual volume contraction. If the sample becomes dry enough this orientation may be enhanced during the smaller freeze contraction, causing a residual volume increase, as noted in the drier samples.

The mechanism derived from this study has as its basis a particle structure imparted by compaction and moisture content, and a particle reorientation. The interpretation of the data presented in this study is consistent with the mechanism proposed in this chapter.

Conclusions and Recommendations.--To summarize, the conclusions may be stated as follows:

1. Base course material in use in west Texas is thermally active and produces transverse cracking.
2. Two distinct types of thermal activity are found for freeze-thaw cycling of base course. These are:
    a. freeze strain, due to a freeze, and
    b. residual strain, due to freeze-thaw cylcing
3. The moisture state, suction, and pore structure (compaction and clay mineralogy) can describe the thermal behavior of

an untreated base course.

4. The clay mineralogy, in particular the specific surface area, can predict the maximum thermal activity of a material and the freeze coefficient at optimum moisture content.
5. The data collected and the proposed mechanism explain the loss of strength, decrease in suction, and change in viscoelasticity of a base course following a winter's activity.
6. The noted mechanism will continue to operate once the pavement is cracked and will allow moisture to infiltrate, resulting in further accelerated deterioration of the base due to the action of ice lensing brought about by the increased availability of moisture.
7. Under the influence of freeze-thaw activity, cracking of an untreated base and then reflection cracking through the asphaltic concrete surface layer appears to be unavoidable given the magnitude of activity noted in this study.

This study does confirm that base course materials possess properties capable of producing cracking under Texas environmental conditions. This study further confirms that shrinkage cracking of subgrade and base course are not likely in west Texas. The environmental conditions which activate the proposed freeze mechanism must be obtained and their influence studied to describe the degree of cracking which will be produced. Several recommendations for further work are as follows:

1. The actual environmental variables influencing pavement behavior must be calculated. This work is in progress and consists of cataloguing freeze-thaw parameters and temperature distributions for pavements in west Texas.

2. An elastic finite element and/or viscoelastic computer code should be modified to calculate thermal stresses in pavement systems under the influence of the calculated environmentally caused stress and displacements.
3. The proposed mechanism of particle reorientation should be validated by visual investigation. This work has begun using scanning electron microscope techniques. The validation of particle reorientation will allow proper selection of admixtures to properly reduce the thermal activity in an economical manner. Additives studied in connection with reducing frost heave damage, a very dissimilar problem, should be investigated to determine their effectiveness in reducing damage caused by the mechanism reported in this study. These additives should include the following:
    1. Metallic salts: to alter suction and clay structure.
    2. Lime and/or cement: in very low percentages to effect a moisture redistribution.
    3. Dispersants: to provide a dispersed clay structure and to isolate clay minerals by providing surface coatings on the clay minerals.
    4. Asphalt: in low percentages to study it's thermal behavior.
4. Provide a continuous moisture barrier within the asphalt or directly above the base course to prevent moisture from entering the base course once the pavement has cracked due to thermal activity, preventing accelerated deterioration due to the increased moisture and ice lensing.
5. Clay mineralogy shows a much stronger relationship to environmental behavior than more commonly used material properties (such as Atterberg limits) and as such should be determined on all granular

materials used in pavement construction. This can provide a design basis for determining proper amounts of additives to eliminate freeze-contraction.

REFERENCES

1. Aitchison, G.D., Editor, Moisture Equilibria and Moisture Changes in Soils Beneath Covered Areas., A Symposium in Print, Butterworths, 1965.

2. Bergan, A.T., and Monismith, C.L., "Characterization of Subgrade Soils in Cold Regions for Pavement Design Purposes," Highway Research Board Record No.431., Highway Research Board, Washington, D.C., 1973.

3. Bradley, W.F., "The Structural Scheme of Attapulgite," American Mineralogist, 25: 405-413, 1940.

4. Brown, R.W., "Measurement of Water Potential with Thermocouple Psychrometers: Construction and Applications," USDA Forest Service, Research Paper INT-80, 1970.

5. Brunauer, S., Emmett, P.H., Teller, E., "Adsorption of Gases in Multimolecular Layers," Journal of the American Chemical Society, 60 , 309-319, 1938.

6. Carothers, H.P., "Freeze Damage in Flexible Pavements," Highway Design Division, Texas Highway Department, 1948.

7. Carpenter, S.H., Thompson, L.J., Bryant, W.R., "Viscoelastic Properties of Marine Sediments," Offshore Technology Conference, Paper No., 1903 May 1973.

8. Carpenter, S.H., Lytton, R.L., Epps, J.A., "Environmental Factors Relevant to Pavement Cracking in West Texas," Technical Report 18-1, Texas Transportation Institute, 1974.

9. Dillon, H.B., and Andersland, O.B., "Predicting Unfrozen Water Contents in Frozen Soils," Canadian Geotechnical Journal, 111:2, 53-60,1966.

10. Dunlop, R.J., "Shrinkage Cracking of Soil-Cement," National Roads Boards, New Zealand, Road Research Unit Bulletin No. 12, 1972.

11. George, K.P., "Mechanism of Shrinkage Cracking Soil-Cement Base," Highway Research Record, No. 442., Highway Research Board, Washington D.C., 1973.

12. Grim, R.E., Clay Mineralogy, McGraw-Hill, 1968.

13. Hajek, J.J., and Haas, R.C.G., "Predicting Low-Temperature Cracking Frequency of Ashpalt Concrete Pavements," Research Record 407, Highway Research Board, Washington, D.C., 1972.

14. Haas, R.C.G., Chairman, ad-hoc Committee on Low-Temperature Behavior of Flexible Pavements, "Low-Temperature Pavement Cracking in Canada, The Problem and its Treatment," Proceedings, Canadian Good Roads Association, 1970.

15. Hamilton, A.B., "Freezing Shrinkage in Compacted Clays," Canadian Geotechnical Journal, 111:1, 1-17, 1966.

16. Hendricks, S.B., and Jefferson, M.E., "Structure of Kaolin and Talc-Pyrophyllite Hydrates and their Bearing on Water Sorption in Clays," American Minerologist, 23:863-875, 1938.

17. Jackson M.L., Soil Chemical Analysis-Advanced Course, Published by the author, Madison, Wisconsin, 1956, modified by J.B. Dixon, 1973.

18. Jackson, M.L., Willis, A.L., Pennington, R.P., "Standards for Quantitative X-Ray Diffraction Analysis of Soil Clays: I. Abridgement of Component Percentages Based on Weathering Sequence," Proceedings Soil Science Society of America, Vol. 12, pp. 400-406, 1947.

19. Jackson, M.L., et al., "Weathering Sequence of Clay Size Minerals in Soils and Sediments I.," Journal of Physical and Colloid Chemistry, Vol. 52, pp. 1237-1260, 1948.

20. Koopmans, R.W.R., and Miller, R.D., "Soil Freezing and Soil Water Characteristic Curves," Soil Science, 30:680-685, 1966.

21. Low, P.F., and Lovell, C.W., "The Factor of Moisture in Frost Action," Highway Research Board No. 225, Highway Research Baord, Washington, D.C., 19.

22. Pagen, C.A., and Khosla, V.K., "Effect of Freeze-Thaw on Rheological Parameters of a Compacted Clay," Transportation Research Record No. 497, Transportation Research Board Washington, D.C., 1974.

23. McLeod, N.W., "Influence of Hardness of Asphalt Cement on Low Temperature Transverse Pavement Cracking," Canadian Good Roads Assoication, Montreal, 1970.

24. Richards, B.G., Murphy, H.W., Chan, C.Y.L., and Gordon, R., "Preliminary Observations on Soil Moisture and Dry Compaction in Pavement Design on the Darling Downs, Queensland," Proceedings, Australian Road Research Board, Bol. 5, Part 5, pp. 116-146, 1970.

25. Shahin, M.Y., and McCullough, B.F., "Prediction of Low-Temperature and Thermal Fatigue Cracking in Flexible Pavements," Research Report No. 123-14, Center for Highway Research, Austin, Texas, August, 1972.

26. White, A.W., and Pichler, E., Water Sorption Characteristics of Clay Minerals," Illinois State Geological Survey, Circular #266, 1959.

27. Yong, R.N., "Soil Suction Effects on Partial Soil Freezing," Highway Research Record No. 68, Highway Research Board, Washington, D.C., 1964.

28. General Soils Map of Texas, Published by Texas Agricultural Experiment Station, in Cooperation with the Soil Conservation Service, 1973.

APPENDIX A

MOISTURE SUCTION MEASUREMENT TECHNIQUES

There are various methods available to measure the soil moisture suction. The method used in this study combines the highest repeatability and accuracy for both field and laboratory testing. This method utilizes the thermocouple psychrometer as was shown in Fig. 8. This device consists of a very fine thermocouple tip which is a welded bead of two dissimilar metals, copper and constantan. A junction of this type produces an emf (electro-motive force) on the order of several microvolts which is proportional to the temperature of the junction. By reading the induced emf the temperature of the junction may be inferred. The junction is protected by a ceramic tip which is porous to moisture in its vapor form only. This protects the junction from contaminants in the soil and moisture.

The moisture in the soil is utilized differently depending on the type of soil and the structure. As moisture is added to, or taken away, work must be done as compared to a common datum usually taken as a pool of pure water at the same elevation, given a value of zero. Thus, as the soil is dried out, or moisture removed, energy is expended. This gives the remaining moisture energy a negative value; and as more moisture is removed the soil moisture suction, which is a measure of this energy level, increases in magnitude. Thus, suction is a negative quantity.

As mentioned in the text, the soil moisture suction is related to the relative humidity of the soil. The thermocouple psychrometer accomplishes this in the following manner:

1. A zero reading is taken of the sample by recording the emf of the thermocouple. This is the dry bulb reading.

2. A current is passed through the thermocouple to produce cooling of the junction tip. This cooling produces a condensation of moisture on the tip when the temperature of the tip falls below the dew point temperature.
3. When the cooling current is switched off the tip will stabilize at the dew point temperature prior to the evaporation of the moisture. This emf is recorded and is the wet bulb temperature.
4. The difference in the wet bulb and dry bulb temperatures is proportional to the relative humidity which is in turn proportional to the soil moisture suction.

To avoid the mathematics involved what is done is to calibrate the thermocouple psychrometers in salt solution of a known osmotic suction. There are two components of suction in a soil. These are:

1. Osmotic, or solute,
2. Matrix or capillary.

Total suction is equal to the sum of the osmotic and matrix suction. Thus measurements in a solution of salt which will be only osmotic suction, will be the same as measurements in soil having only matrix or soil moisture suction, or a combination of the two.

Suction values for solution concentrations are shown in Table 13. These solutions were used to construct the calibration curve shown in Fig. 32. This curve shows the linearity of the psychometric technique over 40 bars (580 psi). With individual calibration the thermocouple psychrometers are accurate ± 5 percent of the reading.

A more advanced measuring technique is termed the dew point method. In this method, the thermocouple junction tip is maintained

Table 13. Relative Activities (Aw) and Water Potentials of KCl solutions at 25°C (4)

Molality* (m)	Aw	lnAw	Potential Bars	Potential Psi
.1	0.996668	-0.0033375	-4.59	-66.57
.3	.99025	-.0097978	-13.48	-195.51
.5	.98394	-.016190	-22.28	-323.15
.7	.97763	-.022624	-31.13	-451.51
1.0	.96818	-.032337	-44.49	-645.28
1.2	.9619	-.038845	-53.45	-775.24
1.4	.9556	-.045416	-62.49	-906.35
1.6	.9492	-.052136	-71.74	-1040.52

*Molality = # of molecular weights/1.0ℓ H_2O at 25°C

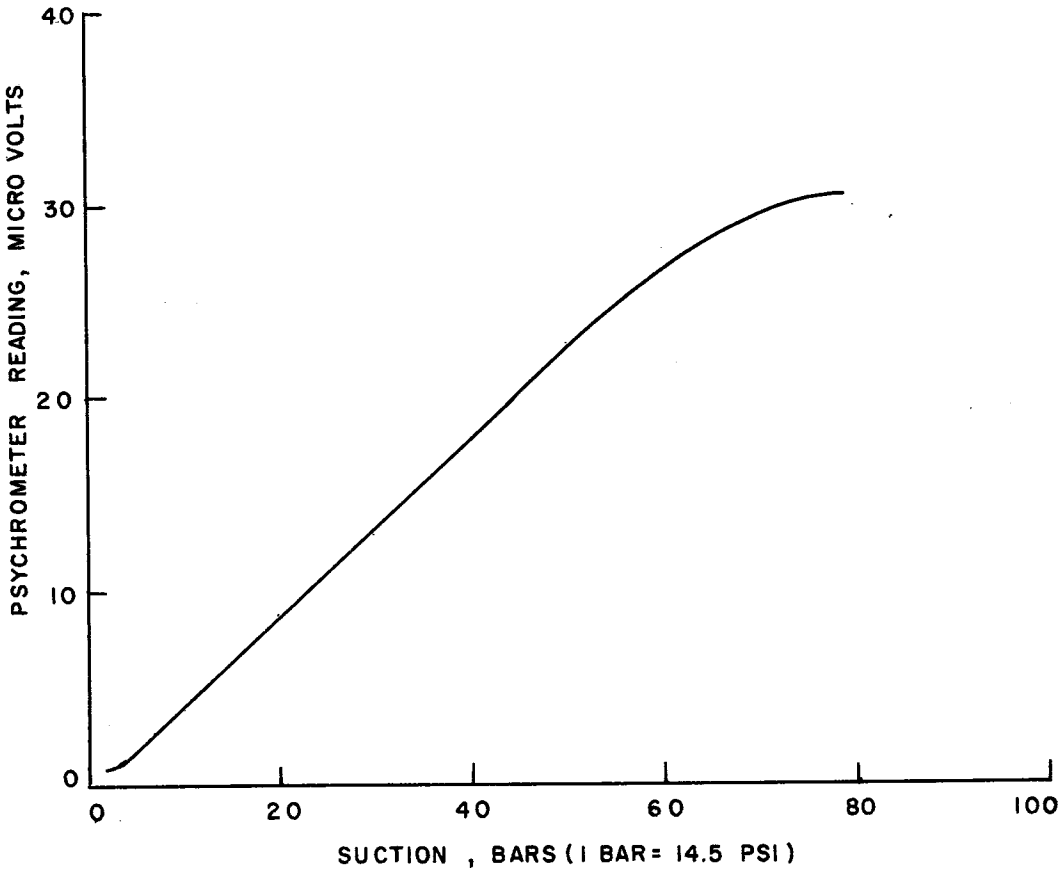

FIG. 32 -THERMOCOUPLE PSYCHROMETER CALIBRATION CURVE

at the dew point temperature by a proper flow of cooling current. The measurements are obtained as follows.

1. A cooling coefficient, which is a function of the tip geometry determined when the psyschrometer is constructed is set on the measurement box.
2. The microvoltmeter is zeroed and a cooling current passed through the tip to condense a bead of water.
3. The function switch is rotated to dew point. The cooling current then is maintaned at a level such that heat is removed from the tip at the same rate it flows in from the surroundings. This process continues until the temperature of the tip is at the dew point where evaporation ceases and the device maintains the tip at the dew point temperature.

The current necessary to maintain the dew point temperature is proportional to the relative humidity. This method of operation produces a larger range of linear operation than the psychrometric technique and yields more reproducible results.

Both methods are highly susceptible to temperature change during measurements and to temperature gradients. The dew point technique allows temperature correction to be made electronically during the measurement while the psychrometric technique requires several correction calculations after the uncorrected measurement is taken. For these reasons the dewpoint technique was utilized extensively in this study.

Suction, shown to be a negative quantity was shown as a positive magnitude throughout this report to simplify its discussion.

APPENDIX B
CLAY FRACTIONATION AND DISPERSION PROCEDURES

General Information

Samples (<2 mm) will be washed with pH 5 buffer, H_2O_2 treated, Fe removed and fractionated into 2 mm-50 μm, 50-20 μm, 20-5 μm, 5-2 μm, 2-0.2 <m, and <0.2 μm. Samples of greater than 5 μm diameter material will be stored dry in vials in file cases provided. Fractions 5 μm diameter will be stored in suspension at a pH between 5 and 7 free of salts. All samples will be clearly labeled with profile number, soil name (or number keyed to the name), depth, size fraction, date and initials of student with a pen or secure gummed label.

Laboratory Procedure

A. Removal of Divalent Cations and Binding Materials.

1a. Destruction of carbonates and removal of exchangeable divalent cations. Weigh each sample (size dependent on texture) of <2 mm air dry soil to give 20 gm. per 250 ml. labeled centrifuge tube (10 gm. for clays and clay loams). A moist material may be used and allowance for moisture content must be made.

1b. In every case, moisture loss at 105-110°C is determined on a representative sample. A sample of about 5 g is weighed to the nearest mg in a tared 50 ml beaker, dried over night at 105 to 110°C, cooled 20 min. in a desiccator and reweighed. This determination will permit calculation of particle size data at the conclusion of the fractionation.

2. Add 10 ml. of pH 5 N NaOAc buffer per gram of soil and bring soil into suspension by stirring with a policeman. Heat the

sample in a near-boiling water bath for 10 minutes, set it on the bench and observe immediately for bubbles indicative of the presence of carbonates. A few bubbles may arise from HOAc and a continuous flow of bubbles indicates carbonates. If carbonates are present, return the sample to the water bath and heat for 20 minutes longer.

3. Wash the sample by mixing with a policeman and centrifuging at about 2000 r.p.m. for 5 minutes or longer as necessary to make the supernatant clear. Repeat the heating in fresh buffer solutions as needed to destroy carbonates. If carbonates were completely dissolved or none were present police down the sides of the container and wash two additional times with pH 5 N NaOAc. Extra acid addition is required for efficient processing of highly calcareous samples.

4. Removal of organic matter and H_2O_2. First add 10 ml. of pH 5.0 N NaOAc and then slowly add 10 ml. of 30% H_2O_2 to the sample, which is in the form of a centrifuge cake. Cover the sample with a watchglass and allow it to stand overnight without heating. Surface soils may froth over and therefore, should be observed until foaming ceases. If it is not convenient to leave the sample overnight, proceed directly to the heating step but the probability of frothing over is greater. Add another 10 ml. of 30% H_2O_2 and place the bottle in a water bath controlled at about 100°C. Keep the container covered with a tightly fitting cover glass during H_2O_2 treatment when the sample is not being stirred. Watch the sample and stir vigorously or cool in a water bath as necessary to prevent frothing over.

CAUTION: Avoid contact of 30% H_2O_2 with the skin or eyes. Never stopper a container containing even a small amount of H_2O_2.

5. When the reaction has subsided remove the sample from the water bath, police down the sides of the bottle with a minimum of water, centrifuge and discard the clear supernatant. If the sample contained a large amount of organic matter and is still dark or has an organic "scum" on top, add 10 ml. of pH 5 N NaOAc and 10 ml. of 30% H_2O_2 and mix thoroughly as before. When the reaction subsides, place the sample in the water bath and observe until the reaction reaches its peak and subsides. Centrifuge and decant the clear supernatant.
6. Repeat step 5 above until the black or dark brown color is destroyed or until no further reduction of dark color is detected. NOTE: About 2 ml. of 30% H_2O_2 per gram of surface soil may be adequate.
7. The sample is then diluted to about 200 ml. with pH 5 N NaOAc and washed two times with the pH 5 solution.
8. The sample is then washed two times with absolute methanol or a mixture of 25% water and 75% acetone. Keep the volume to 2/3 of tube capacity as deflocculation may occur. NOTE: Flocculate as necessary by mixing 1 g. NaCl or 5 ml. saturated NaCl solution with the sample and warming in a hot water bath.
9. Free Fe Removal. (optional step) About 20 gm. of sample (10 gm. for red clays and clay loams) per tube is treated for iron removal at 80°C in a water bath. 80 ml. of 0.3 M Na citrate solution and 10 ml. of 1 M $NaHCO_3$ solution are added to a sample and mixed.

The mixture is heated in the water bath for 5 to 10 minutes to bring the solution to 80°C.

10. Add 2 gm. of sodium dithionite powder with a spoon. Stir vigorously for a minute to mix the reagent thoroughly with the sample and prevent frothing over. A red sample should turn grey immediately. Mixing is continued at intervals of 2 or 3 minutes throughout the 15-minute treatment.
11. Centrifuge and decant the clear supernatant into a 1 l. volumetric flask.
12. The treatment (steps 9 and 10) is repeated two times. Use NaCl as needed to flocculate clay as described above. The decantate after each treatment is combined into the 1 l. volumetric flask and saved for analysis.
13. After the three treatments wash the sample 3 times with Na citrate and combine the washings in the same 1 l. volumetric flask.
    NOTE: Do not leave the sample in the citrate for a long period of time. The three treatments to remove iron oxides should be done consecutively, preferably without delay, to avoid oxidation of Fe. If it is necessary to stop during iron removal or citrate washing, leave the sample tightly stoppered as a centrifuge cake after decantation of the citrate solution.
14. Determine the Fe extracted by a KSCN or atomic absorption method.
15. Mix the sample in 100 ml. of pH 10.0 Na_2CO_3 solution for 5 minutes with a "milk-shake" type blendor.

B. Separation of Sand at the 50 μm Lower Limit with a 300 Mesh Sieve.

1. The well-mixed sample is allowed to stand for about 20 sec. to allow all sand to settle.

2. The supernatant is decanted onto a 50 μm sieve resting on a large funnel which drains into a 600 ml. beaker. A jet of pH 10.0 Na_2CO_3 is used to aid the passage of the solution through the sieve where necessary.
3. The sample remaining in the tube is mixed with another 100 ml. of pH 10.0 solution and is decanted onto one side of the sieve. This step is repeated until most of the sample has been transferred to the sieve. Using a fine jet wash bottle, wash the remaining particles of soil down to the bottom side of the tube held in a horizontal position, then wash all of the particles onto the sieve.
4. Wash the particles on the sieve by tilting it to one side and playing a stream of pH 10.0 solution back and forth across the sample until all of the particles have accumulated at the lower side of the sieve. Tilt the sieve in the opposite direction and repeat the process until the solution passing through is clear.
5. Wash the material on the sieve with acetone dispensed from a wash bottle to remove most of the water.
6. Dry the sample a few minutes until visibly dry on glazed paper on a 100°C plate or in the oven. Place the top and bottom on the sieve and shake it for about 5 minutes until no more particles pass through the sieve. Transfer the material from the bottom of the sieve into the beaker which contains the silt and clay.
7. Transfer all the sand particles from the sieve to a tared Al. dish and dry them for an hour in the oven at 110°C. Cool them in a desiccator and weigh them on the analytical balance. Record the weight of the sand for later use and store the sand in a storage vial provided.

C. Preliminary Separation of Silt and Clay.

1. Pour the silt and clay suspension into a 250 ml. centrifuge tube. Fill the tube to the line 10 cm. above the inside bottom and centrifuge for 5 minutes at 2000 r.p.m. Pour the supernatant suspension into a 3 l. flask labeled <2 μm.
2. Repeat step C.1 until all of the suspension has been centrifuged. Do not mix the material in the bottom of the tube prior to these centrifugations.
3. Add pH 10.0 Na_2CO_3 solution to fill it to the 10 cm. mark. Mix the sample thoroughly with a policeman or by shaking. Centrifuge for 5 min. at 1500 r.p.m.
4. Fill the tube one-half full with pH 10.0 Na_2CO_3 and mix the sample 5 min. with the electric stirrer.
5. Add pH 10.0 Na_2CO_3 solution to the 10 cm. mark, mix the sample, and centrifuge the prescribed time and speed to make the 2 μm separation at 25°C. Decant the supernatant suspension into the flask labeled <2 μm.
6. Repeat step C.5 until the supernatant is almost clear. About 6 washings are commonly required.

D. Separation of Silt Fractions.

1. The fine silt 5-2 μm is now removed by filling to the 10 cm. mark with pH 10.0 Na_2CO_3 solution, mixing the sample, and centrifuging the prescribed time for 5 μm separation and for 25°C suspension. Decant the supernatant into a beaker marked 5-2 μm.
2. Repeat the previous step until the supernatant solution is nearly clear. Allow the suspension in the beaker marked 5-2 μm to settle 3.5 hours per 5 cm. of suspension depth and decant the supernatant into the container marked <2 μm if it is not completely clear. If it is clear discard it.

3. Wash the 5-2 μm fraction two times with distilled water and store it in a solution of 50:50 ethanol and water. Obtain the 5-2 μm fraction weight as for the 2-0.2 μm fraction. (E.2).
4. The silt remaining in the tubes is transferred to a 500 ml. tallform beaker for separation at 20 μm by sedimentation. The silt is sedimented in pH 10.0 Na_2CO_3 solution for 2 min. 5 sec. per 5 cm. sedimentation depth. The supernatant is decanted into a beaker labeled 20-5 μm.
5. Step D.4 is repeated until the supernatant becomes almost clear. Then 2 more washings are made with distilled water to remove the sodium carbonate and the sample in the beaker is dried at 110°C, weighed and stored in a vial labeled 50-20 μm.
6. The 20-5 μm fraction is transferred to 250 ml. centrifuge tubes with distilled water, centrifuged for 5 minutes at 2000 r.p.m. and the clear supernatant is discarded. The sample is consolidated into one 250 ml. centrifuge tube, washed with distilled water two times and dried. The sample is transferred to a tared 100 ml. beaker with a minimum of water, dried over night at 110°C, weighed, and transferred to a vial labeled 20-5 μm.

E. Fractionation of the Clay.

1. The suspension of <2 μm material is transferred to 250 ml. centrifuge tubes if there is less than 2.4 l. volume. Where more than 2.4 l. volume is involved a preliminary supercentrifuge separation is desirable to reduce volume before fractionation of the clay at 0.2 μm. Where the volume is less than 2.4 l. the suspension is centrifuged for about 30 minutes at 2400 r.p.m. to fractionate at 0.2 μm depending on the average suspension temperature, centrifuge tube and centrifuge trunnion cup employed. The average

of the suspension temperatures before and after centrifugation is employed. The supernatant is decanted into a 2 or 3 l. flask labeled <0.2 μm.

2. Fractionation at 0.2 μm as described in E.1 is repeated after combining the sample into one tube with pH 10.0 Na_2CO_3 solution as transferring solution. Removal of the 0.2 μm material is continued by repeated centrifuge washings with pH 10.0 Na_2CO_3 solution as described in E.1 until the supernatant is almost clear following centrifugation. The 2-0.2 μm clay in the centrifuge cake is washed two times with distilled water and the supernatant is combined with the 0.2 μm suspension. The 2-0.2 μm material is transferred to a volumetric 200 ml. flask with distilled water and made to volume so that the final mixture is 50:50 ethanol and water. Mix the sample thoroughly and immediately pipette a 20 ml. aliquot into a tared 50 ml. beaker or weighing bottle to determine the amount of the fraction. The aliquot is dried on the 100°C plate and finally two hours in the oven at 110°C before final weighing.

3. Where the clay is fractionated only at 0.2 μm the clay in the beaker labeled 0.2 μm is flocculated by dropwise addition of 1N HCl until the clay flocculates or until pH 4.5 is reached. Do not acidity more than to pH 4.5. Heat the sample on the hot plate to accelerate flocculation. Allow the sample to stand overnight and siphon or decant off the clear supernatant. Wash the sample chloride free with methanol or ethanol. Transfer the <0.2 μm clay to a 200 ml. volumetric flask with water and ethanol to make the final volume exactly 200 ml. in a 50:50 mixture

ethanol and water. Mix the sample thoroughly and immediately pipette a 20 ml. aliquot into a tared 50 ml. beaker or weighing bottle. Dry the aliquot and weigh as for the 2-0.2 μm sample (E.2).

4a. Optional Prodedure for Volume Reduction or Montmorillonite Purification. Separation of the 0.03 μm clay with steam turbine supercentrifuge. Operation of the supercentrifuge will first be demonstrated by the instructor. The suspension of <2 μm clay from E.1 or the 0.2 μm clay from E.3 is poured into the feed reservoir for the supercentrifuge. The reservior is filled to the level which will deliver 180 ml. per min. The rate of flow is checked by measuring the flow of distilled water from the feed nozzle held at the level of the bottom of the centrifuge bowl.

b. The water in the steam line is carefully bled out into a waste container. The oil flow is started, the cooling water is turned on, and the steam valve is slowly opened until the steam pressure is raised to 20 p.s.i. The bowl speed is checked after the sound indicates it has reached a uniform speed. It should be running at 45,000 r.p.m. If this speed is not obtained adjust the pressure regulator and check the centrifuge. Check the rate of oil flow. It should be 6 drops per minute.

c. The feed nozzle is installed and the flow into the centrifuge bowl is started. After the suspension has begun to flow from the outlet spout, the rate of flow and the speed of the super-centrifuge are checked again.

d. Suspension is added every few minutes to maintain the desired level in the reservoir and hence the desired rate of flow. When almost all of the sample has drained from the reservoir

its walls are washed with pH 10.0 water and the washing solution is permitted to drain into the centrifuge.

e. A 300 ml. volume of 1% Na_2CO_3 replacing solution is added to the reservoir and allowed to drain into the centrifuge. The hose clamp is put in place to prevent air from getting in the hose and obstructing flow of the next suspension.

f. The oil flow, steam, and cooling water are turned off.

g. The feed nozzle is removed and the drain cup put in place. The bowl is allowed to coast to a stop. The clear Na_2CO_3 solution which drains from the centrifuge bowl is discarded.

h. The centrifuge is disassembled immediately by removing the drag assembly, the spindle guard and then carefully uncouple the bowl while supporting it with the fingers so that it will not drop into the frame.

i. The bowl protecting cap is installed.

j. The centrifuge bowl is taken to a laboratory bench and the bottom is removed from it with the wrench provided.

k. The liner is removed by grasping the corner with forceps and slowly pulling it away from the wall of the bowl by rolling it into a small roll.

l. The clay is washed into a 800 ml. beaker from the bowl bottom, the bowl and the liner with a policeman and a medium-tipped wash bottle which contains water. Scrubbing the liner and centrifuge parts with a rubber policeman aids greatly in removing the clay.

m. The clay suspension is then dispersed by mixing two minutes with the mixer provided if further removal of 0.08 μm clay is needed. The beaker is held with the mixer near one side to obtain adequate

mixing action. Then observe for the presence of aggregates after a minute of sedimentation. Three or more supercentrifuge separations are usually necessary to remove the <0.08 μm clay if appreciable montmorillonite is present. When the effluent is almost clear separation at 0.08 μm is considered complete.

n. During the last centrifugation to remove <0.08 μm particles, a replacing solution of 0.5% (0.1N) NaCl is used instead of the 1% Na_2CO_3. This clear solution which drains from the centrifuge bowl is discarded.

o. For continued separation of the <0.08 μm fraction, the resuspended sample is made to 500 ml. volume with water, mixed, and centrifuged as described earlier under Step 4.

p. Where the removal of <0.08 μm clay is complete, the sample of 0.2-0.08 μm clay removed from the liner and centrifuge parts in a minimum of water is made to a known volume usually of 200 ml. with a final concentration of about 50% ethanol. A 10% aliquot is taken, washed three times with 0.05 N HCl and dried in a tared container as described in E.2 to get the weight of the <0.03 μm clay.

q. The 0.08 μm clay is flocculated, sampled to determine the amount, and prepared for storage as described for <0.2 μm clay in E.3.

Identifying Minerals in Clay Samples by an X-ray Diffraction Technique

OBJECTIVES:

1. To determine the major clay mineral in a mixed clay sample.
2. To study x-ray diffraction criteria employed in identifying clay minerals.

PROCEDURE:

1. Employing the conversion table write the spacings for each peak on the x-ray curve or curves. The nearest 0.01 angstrom ($\mathring{A}$) is the maximum that is merited by the data.
2. Compare the x-ray spacings (d/n values) for your material with those given in the information provided and identify the major minerals present in your material.

Where less than three x-ray peaks are employed for mineral identification the identification should be considered tentative. Where a complex mixture or a larger population of samples is involved, more data are generally necessary for positive mineral identification.

X-ray Diffraction Criteria for Identifying Clay Minerals in Relatively Pure Samples

1. Smectite Group - Minerals in this group have long been called montmorillonites in general discussions. The group term smectite seems to be gaining acceptance.

   Smectite minerals expand and contract depending on hydration, solvation and the cations that occupy the exchange sites. Smectites are identified by their d/n values of about 17.8A when they are Mg^{2+} or Ca^{2+} saturated and glycerol or glycol solvated. Low intensity higher orders may occur where n = 2, 3, 4, etc. giving spacing of $8.9\mathring{A}$, $5.9\mathring{A}$, $4.45\mathring{A}$, etc. On heating at $500^{o}C$ or above, montmorillonite

collapses and has a d/n of 10Å and weak higher orders may be shown.

2. Vermiculite gives d/n values of 14.2Å and higher orders when Mg^{2+} Saturated and solvated with glycerol or glycol. When vermiculite is K^{+} saturated and heated at 300°C or above, it collapses to give a d/n vlaue of 10Å and some higher orders. K^{+} saturation without subsequent heating will often collapse vermiculite to 10Å.
3. K-Mica gives a d/n value at 10Å with higher orders.
4. Kaolinite gives 7.2Å d/n value with higher orders. The kaolinite structure is destroyed on heating at 525°C for two hours
5. Tabular halloysite gives a 7.4Å d/n value and higher orders. The x-ray peak is broad and may require other criteria for positive identification.
6. Tubular halloysite when fully hydrated gives a 10Å d/n value and a 4.45Å peak at least half the height of the 10Å peak. Most tubular halloysite has dehydrated to some extent and gives a 7.2Å or lightly higher d/n value. Tubular halloysite gives a poor x-ray pattern owing to the tubular morphology of the crystals.
7. Chlorite gives d/n values of 14.2Å and higher orders. Chlorite spacings do not change with cation saturation or solvation. Poorly crystalline chlorites may collapse slightly on heating.
8. Quartz gives sharp peaks at 3.35Å and 4.26Å. Quartz is not a platy structured mineral, therefore, it does not give a sequence of higher orders like the platy minerals mentioned earlier.
9. Gibbsite gives d/n values of 4.85Å, 4.37Å and 4.31Å. The structure of gibbsite is destroyed on heating at 300°C for two hours.

10. Attapulgite gives a strong 10.5Å peak that is not changed by cation saturation or solvation. The 10.5Å peak is stable on heating to about 300°C.

11. Sepiolite gives a strong x-ray peak at about 12.1Å. The 12.1Å peak is stable regardless of cation saturation and solvation but may be altered by heating at 300°C.

Preparation of Clay and Fine Silt Samples for DTA, XRD and CEC Analysis

Mg-Saturation of clay for DTA, XRD, and CEC

350 mg sample of clay is transferred to a glass 50 ml centrifuge tube.

1. Wash sample once with pH 5 N NaOAc buffer.
2. Treat the centrifuge cake in 1 ml of pH 5.0 NaOAc with 2 ml H_2O_2. Heat in beaker of boiling water until reaction subsides. Avoid frothing over of sample. Wash sample 3 times with pH 5.0 NaOAc. Discard supernatant.
3. Wash sample 3 times with pH 7 MgOAc.
4. Wash sample 2 times with N $MgCl_2$.
5. Wash sample free of salts by using:
    a. Two washings or more with 70% alcohol and water mixture.
    b. Wash with alcohol until free of chloride by $AgNO_3$ test. Do not add $AgNO_3$ to sample. Make the test in a 50 ml beaker. Remove aliquot for x-ray analysis (1/7 of total sample).
6. Make a final wash of sample remaining in the tube with acetone and centrifuge a minimum to get rid of the supernatant. Allow the loose centrifuge cake to air-dry at room temperature.
7. Lightly grind 100 mg DTA sample with mortar and pestle to pass 70 mesh screen and transfer to weighing bottles provided. Label the bottle with your initials, sample name, and particle size.
8. Equilibrate the sample over saturated $Mg(NO_3)_2 \cdot 6\ H_2O$ solution in a vacuum desiccator for 4 days or longer. (about 56% RH).
9. Use the greatest possible precautions to keep a uniform procedure for loading and packing the sample in the sample holder.

10. The remaining 200 mg sample in the centrifuge tube will be used for CEC determination according to the procedure provided.

Saturation of Clays and Silts for X-ray Analysis

K and Mg saturation are done on duplicate 50 mg samples for x-ray analysis. Saturate with each cation separately.

1. Steps 1 through 5 are the same as above except the K salts are used for K saturation and the H_2O_2 treatment may be omitted.
2. Add glycerol to the sample as 10% solution in water as follows: 5-2μ 0.1 ml, 2-0.2μ 0.2 ml, <0.2μ 0.3 ml of the 10% solution. The sample should appear moist after water has evaporated.
3. Add sufficient water to make the sample volume to about 1 ml or more for montmorillonitic fine clays.
4. Mix throughly and decant the sample onto a labeled slide placed on a level surface.
5. Cover samples with a raised glass on large stoppers to prevent contamination or disturbance while they are drying. Sample should dry to a smooth uniform film.

Cation Exchange Determination
For Clay Samples, 2-0.2 μm and <0.2 μm

Objective: To determine the cation exchange capacity of two clay samples in duplicate by saturating the clay with Ca^{++}, determining the interstitial salt solution, and replacing the exchangeable Ca^{++} (plus the interstitial solution) with Mg^{++}.

About 100 mg of clay is required for each determination and the exact weight must be determined. Half the 200 mg sample (use a spatula) from the combined DTA and XRD saturation procedure and place each 100 mg sample in a separate tared 50 ml glass centrifuge tube. Dry the sample overnight or until constant weight at 100°C, cool it 20 minutes in a desiccator and weigh the sample in the tube quickly to enable calculating clay weight to the nearest 0.1 mg by difference.

Ca^{++} Saturation and Ca^{++}/Mg^{++} Exchange:

1. The Mg^{++} saturated clay is first dispersed by trituration with a rubber policeman in a few drops of pH 4.0 N NaOAc.

2. The samples are washed three times with 7.0 N NaOAc (20 ml per wash) and the clear supernatant is discarded. This step (2) adjusts the sample pH to 7.0.

3. The sample is then washed two times with N $CaCl_2$ (10 ml/wash).

4. The sample is then washed three times with 0.01 N $CaCl_2$ to complete saturation of the cation exchange sites with Ca^{++} (10 ml/wash). The sample is washed last with 0.01 N salt to permit weighing interstitial solution to determine its volume.

5. Wipe each tube clean and weigh the clay and interstitial solution in the tube. Calculate the solution volume by difference assuming a solution density of one g per ml.

6. The Ca-clay plus interstitial solution is washed five times with $\underline{N}$ $MgCl_2$ and the clear supernatant is saved in 100 ml volumetric flask (10 ml/wash for 100 mg clay) for atomic absorption analysis and CaEC calculation.

7. The CaEC will aid in quantitative clay mineral estimation.

8. Formula for calculating CaEC:

$$\frac{\text{CaECmeq}}{100\text{g}} = \frac{\left[(\text{Ca } \mu\text{g/ml} \times 100 \text{ ml})_r - (\text{Ca } \mu\text{g})_i\right]}{(\text{s mg})} \frac{(10^{-3}\text{mg}/\mu\text{g})}{(20.0 \text{ mg/meq})} \frac{(10^5\text{mg})}{(100)}$$

$( )_r$ = Ca^{++} replaced from sample

$( )_i$ = Interstitial Ca^{++} determined by multiplying volume determined gravimetrically (Step 5) times the concentration determined

s = sample weight

APPENDIX C

X-RAY DIFFRACTION MINERALOGY STUDY

Material 5.-- The x-ray diffraction pattern for material 5 is shown in Fig. 33. The clay minerals noted in the figure are: montmorillonite, attapulgite, mica, kaolinite, and quartz. There is no quartz in the <0.2μ fraction and essentially no montmorillonite in the 2-0.2μ fraction. The percentages calculated for each mineral are listed in Table 15 and plotted on the weathering sequence in Fig. 34. The plot of the percentages looks very similar to that obtained for material 4 as should be expected.

Table 15. Percentages for Material 5

Mineral	Percentage
Montmorillonite	35.5
Attapulgite	25.9
Mica	15.8
Kaolinite	11.0
Quartz	11.8

Material 6B.-- The x-ray diffraction pattern for material 6B is shown in Fig. 35. The clay minerals present include montmorillonite, mica, kaolinite, and quartz with a small amount of attapulgite. The peaks for this material were somewhat broad and not as well defined as some of the other samples and for this reason the potassium slide was x-rayed. The quality is comparable to that of the slides for material 4 and the accuracy of the percentages should be comparable. The percentage are given in Table 16.

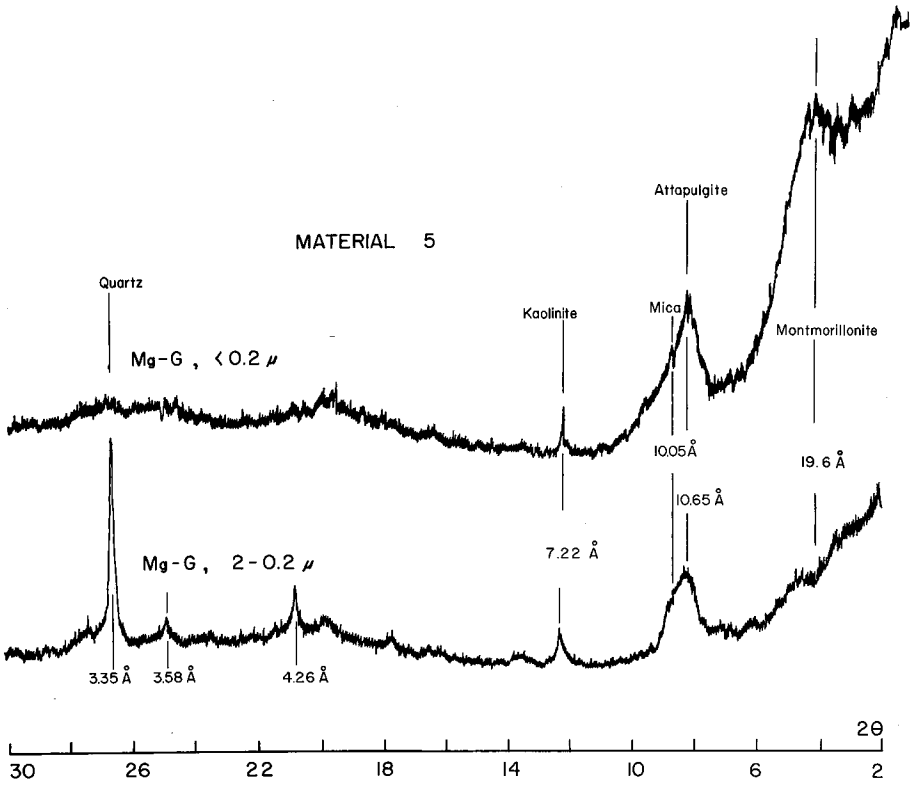

FIG. 33 - X-RAY DIFFRACTION PATTERNS, MATERIAL 5

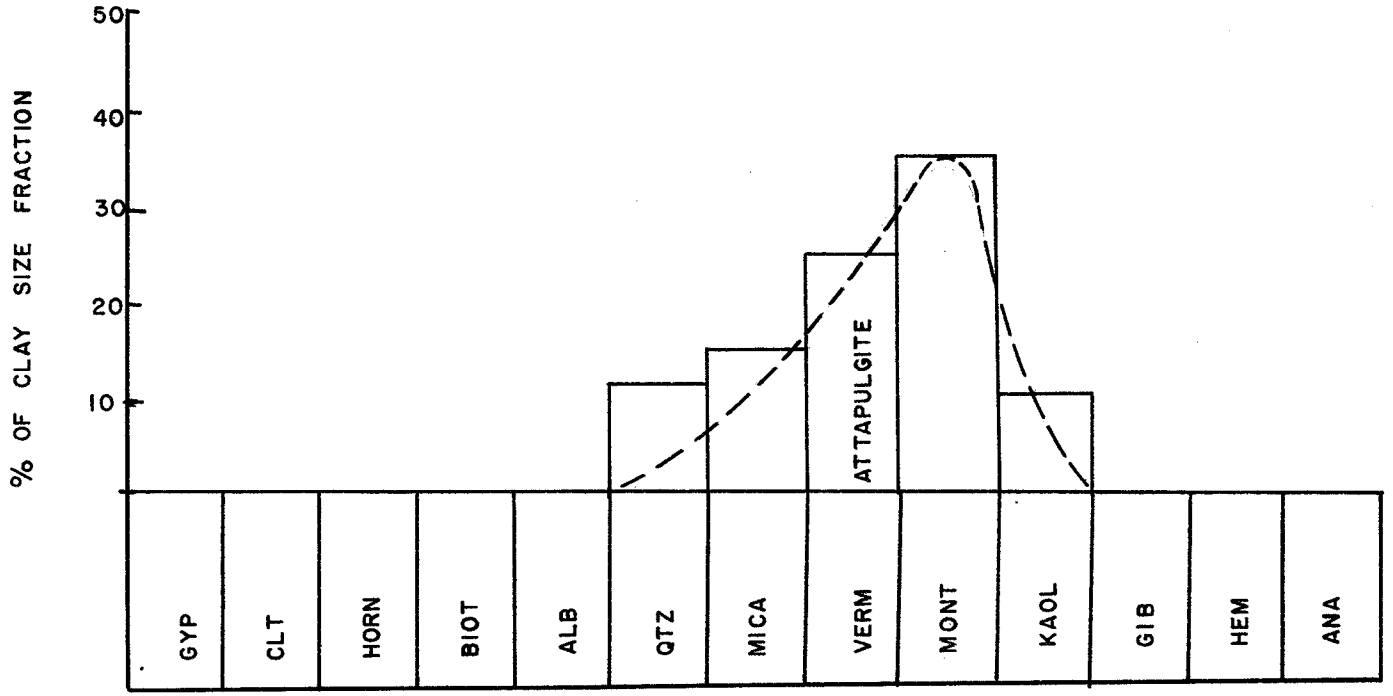

FIG. 34 - MATERIAL ESTIMATES FROM X-RAY ANALYSIS PLOTTED ON JACKSON'S WEATHERING SCHEME

MATERIAL 5

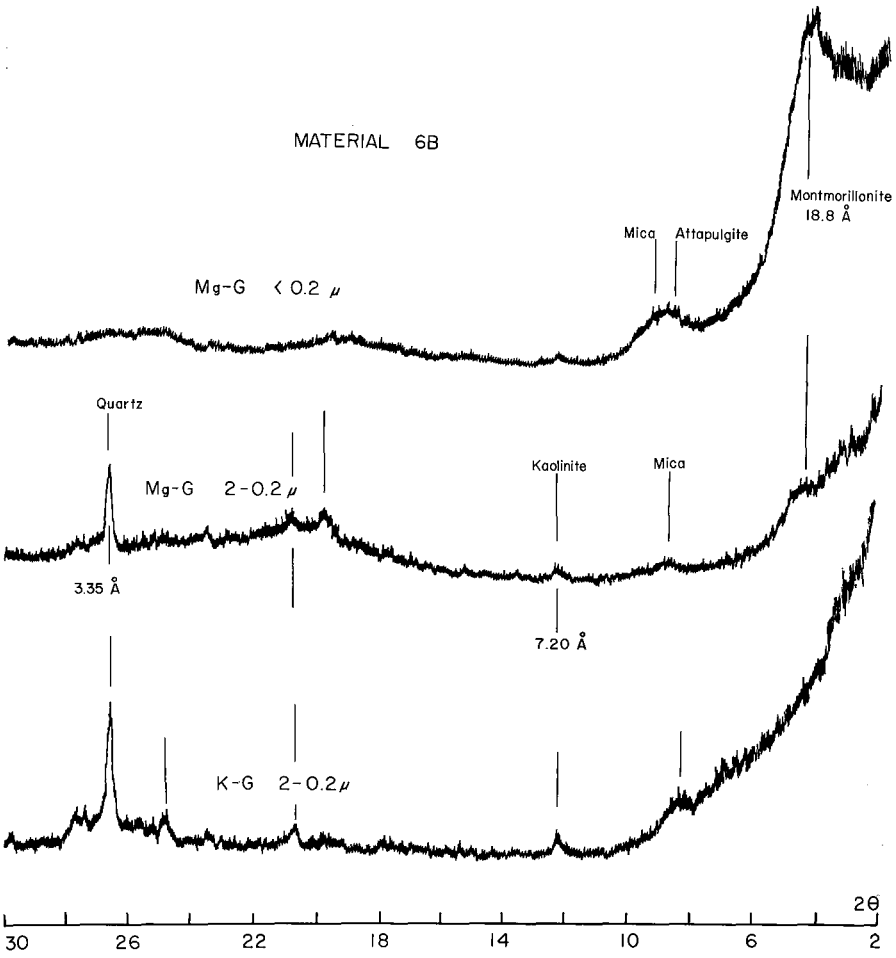

FIG. 35 - X-RAY DIFFRACTION PATTERNS, MATERIAL 6B

Table 15. Percentages for Material 6B

Mineral	Percentage
Montmorillonite	41.8
Attapulgite	13.7
Mica	7.0
Kaolinite	7.9
Quartz	29.6

Material 6JD.-- The x-ray diffraction patterns for material 6JD are shown in Fig. 36. The minerals present include montmorillonite, attapulgite, quartz and kaolinite. There is a definite absence of mica in this material. The calculated percentages are given in Table 17. The $<0.2\mu$ fraction can be seen to be composed entirely of montmorillonite and attapulgite. This would indicate this material to be more active than the others, but perhaps not in a thermal manner. The diffraction peaks were quite strong and well defined. The several intermediate peaks between attapugite and montmorillonite in the $<0.2\mu$ fraction represent sodium montmorillonite not fully expanded (10) as the peaks do not match values for minerals giving peaks in this area. This was verified with heat treatment which collapsed the montmorillonite to 10Å.

Table 16. Percentages for Mateial 6JD

Mineral	Percentage
Montmorillonite	38.9
Attapulgite	45.3
Quartz	12.9
Kaolinite	2.9

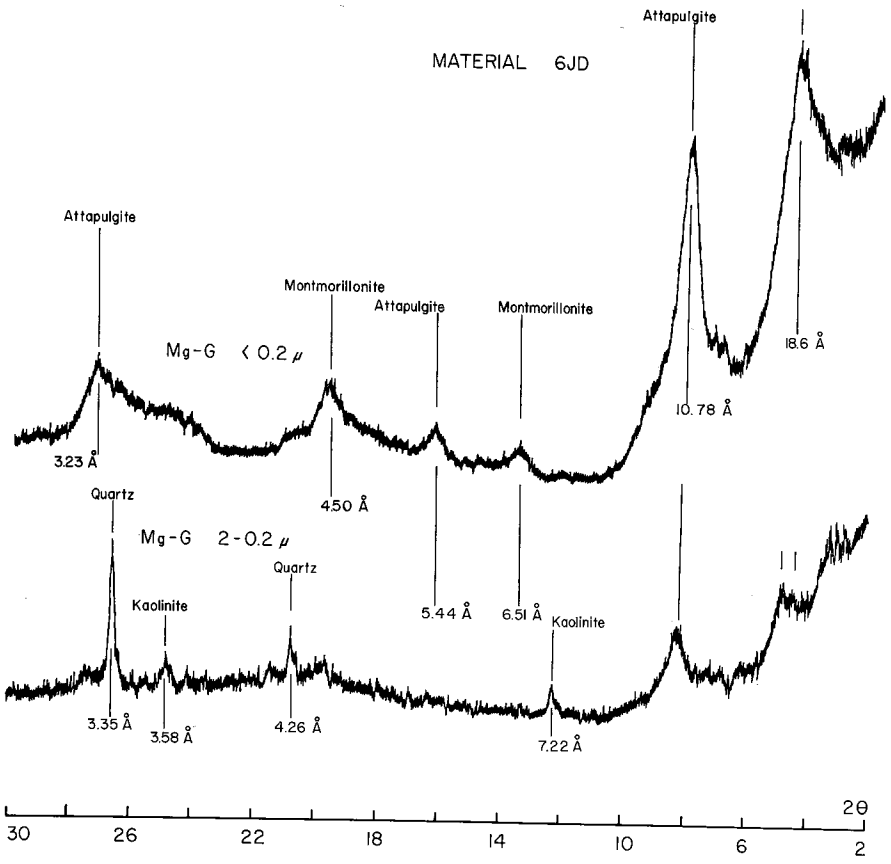

FIG. 36 - X-RAY DIFFRACTION PATTERNS, MATERIAL 6JD

Material 6FS.-- The x-ray diffraction pattern for material 6FS is shown in Fig. 37. The minerals present include montmorillonite, mica, kaolinite and quartz. The percentages of each are listed in Table 18. These values are the most questionable values of those obtained. The reason for this can be seen by examining the x-ray diffraction pattern for the <0.2μ fraction. The peaks for mica and montmorillonite are broad and weak. This could be due to a misalignment of the x-ray diffractometer; but this is not likely as calibration was checked halfway through testing and found to be in order. The reason for the pattern becomes apparrent when the manner in which this material was obtained is investigated.

Table 18. Percentages for Material 6FS

Mineral	Percentage	Corrected Percentage
Montmorillonite	68.7	51.5
Mica	17.3	12.9
Kaolinite	11.2	8.4
Quartz	2.8	2.2

This material was obtained from crushing material that was blasted from rock formations. Crushing action will destroy any crystalline structure present after a certain period of grinding (12). It is felt that excessive crushing action has produced this amorphous material with no crystalline structure which concentrated in the <0.2μ fraction size. A cation exchange capacity determination would be necessary to substantiate this assumption. For the analysis presented here the corrected percentages as calculated for Table 18 will be used. These values assume the material to be 25 percent amorphous.

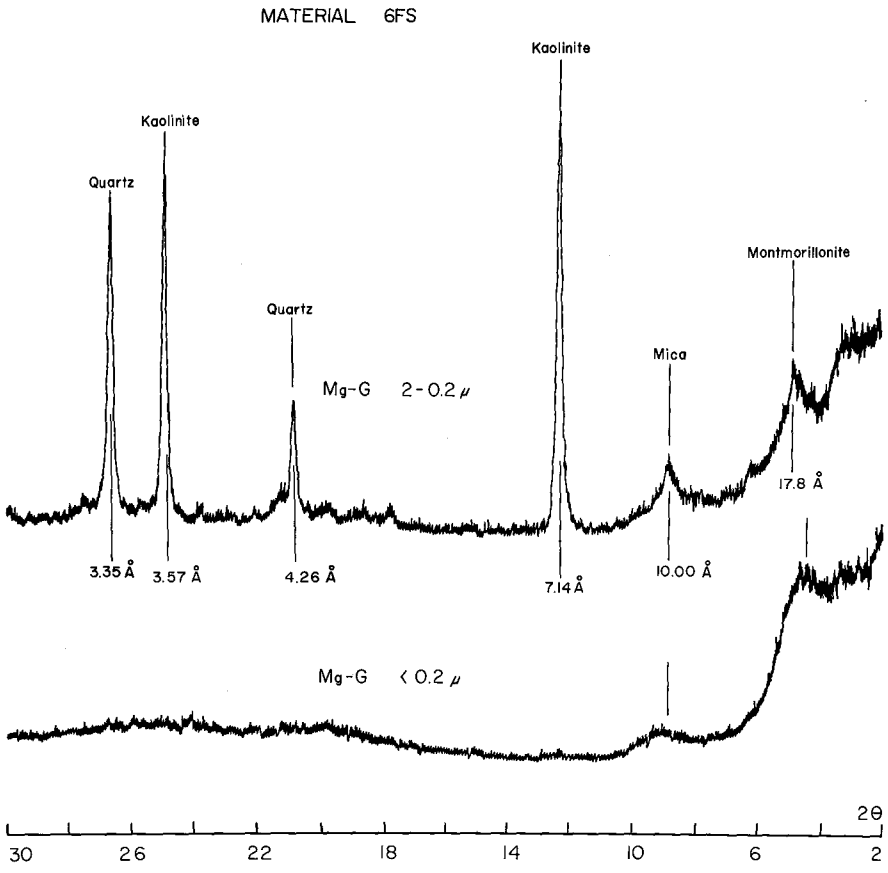

FIG. 37 - X-RAY DIFFRACTION PATTERNS, MATERIAL 6FS

Material 7SA.-- The x-ray diffraction patterns are given in Fig. 38. The minerals present include montmorillonite, mica, kaolinite, and quartz. The percentages calculated from the x-ray diffraction patterns are given in Table 19.

Table 19. Percentages for Material 7SA

Mineral	Percentage
Montmorillonite	58.0
Mica	18.2
Kaolinite	6.2
Quartz	16.2

Material 6BAR.-- The x-ray diffraction patterns for material 6BAR are given in Fig. 39. The minerals present include montmorillonite, attapulgite, kaolinite and quartz. The potassium saturated slide was run to check the magnesium saturated sample when difficulty was encountered in running the magnesium slide. The percentages are given in Table 20.

Table 20. Percentages for Material 6BAR

Mineral	Percentage
Montmorillonite	39.8
Attapulgite	33.0
Kaolinite	13.3
Quartz	13.9

The thermal data for this material were not presented in this report. The specific surface area of this material indicates that it will possess a

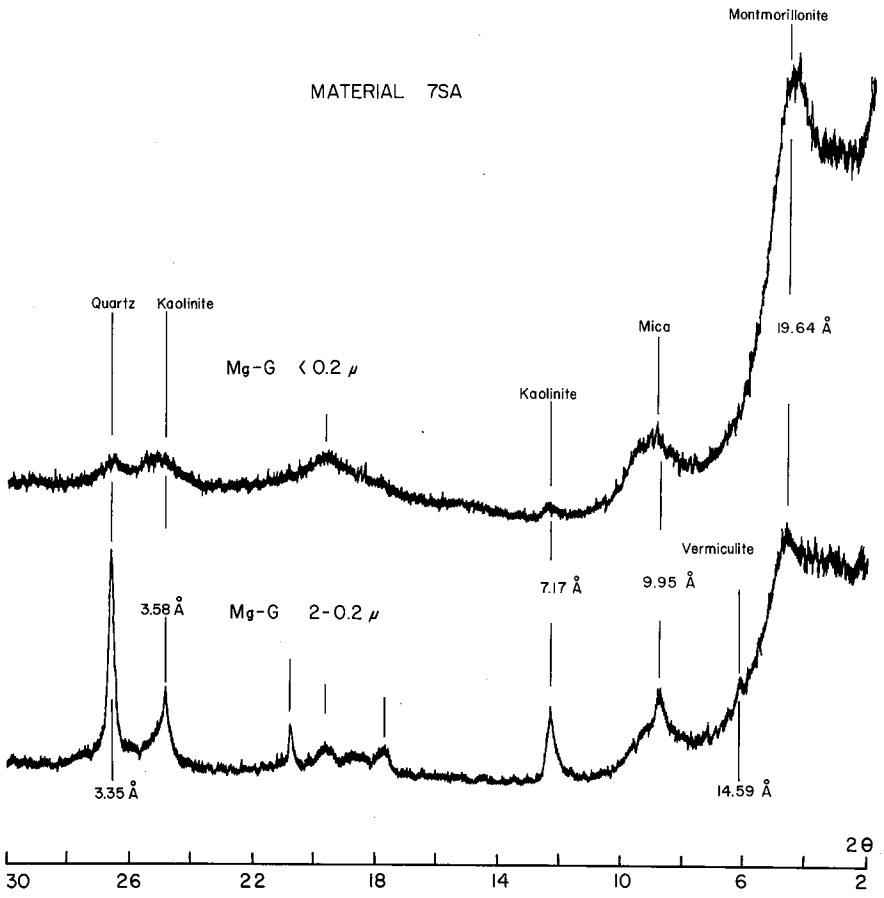

FIG. 38 - X-RAY DIFFRACTION PATTERNS, MATERIAL 7SA

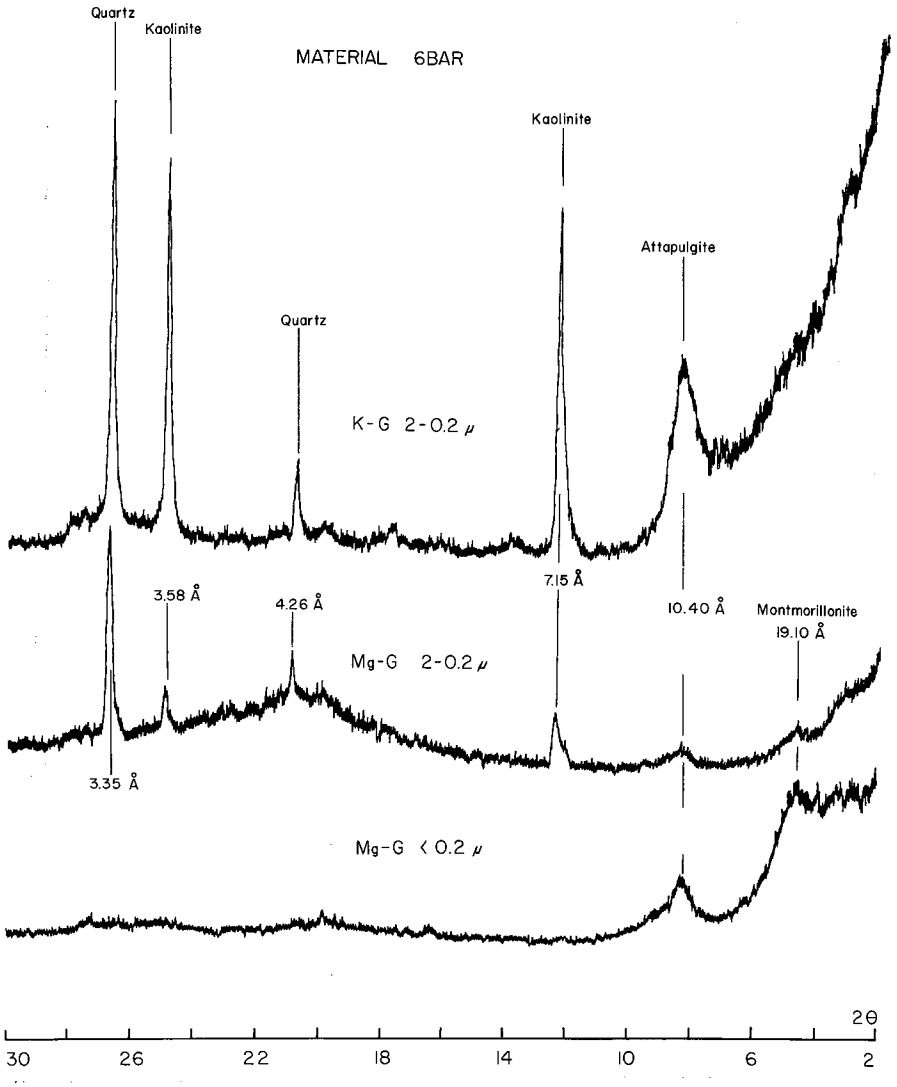

FIG. 39 - X-RAY DIFFRACTION PATTERNS, MATERIAL 6BAR

medium amount of activity; and because of this, this material will be used to study the affects of additives in reducing the thermal activity which will be detailed in a subsequent report.